NSTX Upgrade

PF 1 Flex Bus Analysis

NSTXU-CALC-55-03-00

June 17, 2016

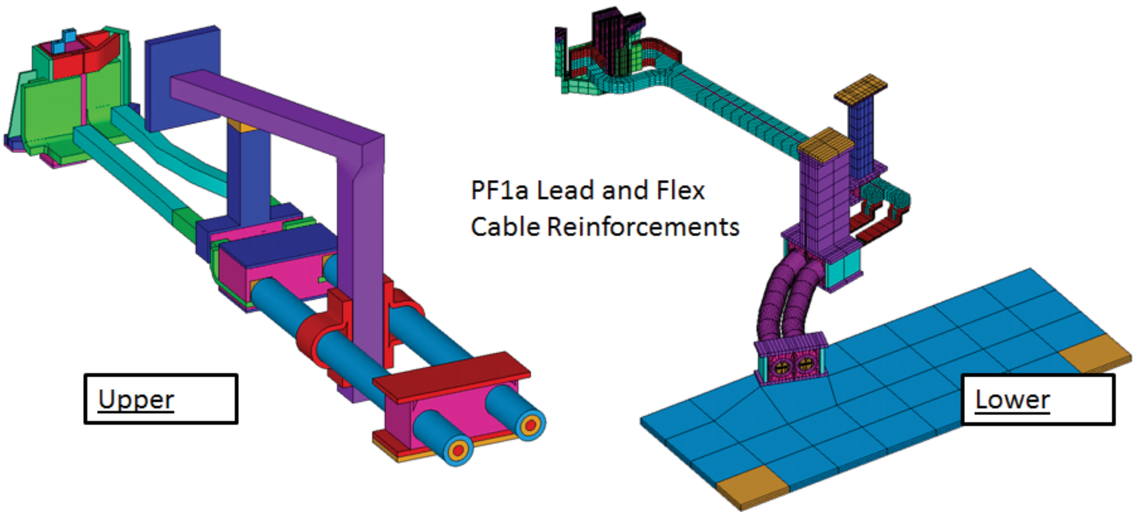

(PF1 Upper Mid Cable Support (Left) and Lower PF1a Bus and Cable Support (Right))

Prepared By:

Peter Titus, Peter H. Titus Digitally signed by Peter H. Titus DN: cn=Peter H. Titus, o, ou=Princeton Plasma Physics Laboratory, email=ptitus@pppl.gov, c=US Date: 2016.06.17 17:40:17 -04'00'

Reviewed By:

Reviewer	Sections	Signature
Andrei Khodak	**All**	Andrei Khodak Digitally signed by Andrei Khodak Date: 2016.06.17 14:56:34 -04'00'
Irving Zatz	**All**	Irving J. Zatz Digitally signed by Irving J. Zatz DN: cn=Irving J. Zatz, o, ou=PPPL, email=zatz@pppl.gov, c=US Date: 2016.06.17 14:18:27 -04'00'
Mike Mardenfeld	**4.0,10.0**	Michael Mardenfeld Digitally signed by Michael Mardenfeld DN: cn=Michael Mardenfeld, o=PPPL, ou=Mechanical Engineering, email=mmarden@pppl.gov, c=US Date: 2016.06.17 14:28:35 -04'00'
Ali Zolfaghari	**4.0,11.0**	Ali M. Zolfaghari Digitally signed by Ali M. Zolfaghari DN: cn=Ali M. Zolfaghari, o=PPPL, ou=Engineering, email=azolfagh@pppl.gov, c=US Date: 2016.06.17 16:04:06 -04'00'

PPPL Calculation Form

Calculation # **NSTXU-CALC-12-3-** Revision # **00** ____ WP #, **1903**
(ENG-032)

Purpose of Calculation: (Define why the calculation is being performed.)

The purpose of this calculation is to provide guidance on the initial design of the PF1 Upper and Lower flex bus and connections for the upgrade loads, and to provide qualification of the final design as reinforced as of June 14, and 15, 2016. Excessive motion of the flex cable connected to the PF1a upper bus was observed on videos of the machine during operation, and this calculation seeks to understand why and evaluate additional supports for the flex cable.

References (List any source of design information including computer program titles and revision levels.)

These are included in the body of the calculation, in section 6.3

Assumptions (Identify all assumptions made as part of this calculation.)

Stiffness and strength of the flex cables are assumed to be minimal. Support in the bus tower is assumed adequate – as per qualifications in Reference [9]. This calculation is not intended as the qualification of the inner terminal connections. These were qualified in calculation NSTXU CALC 133-01-2 [9]

Calculation (Calculation is either documented here or attached)

These are included in the body of the following document

Conclusion (Specify whether or not the purpose of the calculation was accomplished.)

Flex Cables have been modeled and are adequate to take the local full performance loads with some qualifiers discussed here. The flex cable supports are qualified as designed and installed June 14-16, 2016. Analysis is based on field sketches and is consistent with final drawings [20]. The complexity of the as-built conditions made detailed modeling of flex cabling difficult An analysis of the loading from the early operation of NSTX-U confirms the nature and magnitude of the bending of the solid bus bat lug that was observed. Possibilities of adverse field fit-up of the bus bar flags to the inner coil terminal connections was assessed and found acceptable, but confirmation of as-builts is still desirable.

As a part of the recovery plan, the lugs were liquid penetrant inspected to ensure that the plastic deformation did not initiate cracks and reduce fatigue life. Appendix D includes an assessment of this.

Operation with full centerstack heat-up is allowed. The added supports of PF1a Upper have been designed to allow adequate vertical growth without unacceptable stresses at the inner terminal connections or the flex bus connections.

Lug stresses have some sensitivity to PF1a current reversal. Allowed reversed currents will be qualified later.

Flex cable supports are either the same or similar to the ones used for NSTX and the service of the original flex cables and supports serves as qualification as to the basic load carrying capacity of the flex cables themselves. The supports for PF1a Lower may need to be modified to provide some strain relief for operation in which the lower bus bar heats substantially.

Cognizant Engineer's printed name, signature, and date

Neway Atnafu Neway Atnafu

Digitally signed by Neway Atnafu
DN: cn=Neway Atnafu, o=Princeton Plasma Physics Lab, ou=PPPL, email=natnafu@pppl.gov, c=US
Date: 2016.06.17 16:57:16 -04'00'

Coil Systems Engineer's printed name, signature, and date

Steve Raftopoulos Steve Raftopoulos Digitally signed by Steve Raftopoulos DN: cn=Steve Raftopoulos, o=Princeton Plasma Physics Laboratory, ou=Engineering, email=sraftopo@pppl.gov, c=US Date: 2016.06.17 17:01:29 -04'00'

I have reviewed this calculation and, to my professional satisfaction, it is properly performed and correct.

Checker's printed name, signature, and date

Reviewed By:

Reviewer	**Sections**	**Signature**
Andrei Khodak	**All**	Andrei Khodak Digitally signed by Andrei Khodak Date: 2016.06.17 14:57:04 -04'00'
Irving Zatz	**All**	Irving J. Zatz Digitally signed by Irving J. Zatz DN: cn=Irving J. Zatz, o, ou=PPPL, email=zatz@pppl.gov, c=US Date: 2016.06.17 14:18:54 -04'00'
Mike Mardenfeld	**4.0,10.0**	Michael Mardenfeld Digitally signed by Michael Mardenfeld DN: cn=Michael Mardenfeld, o=PPPL, ou=Mechanical Engineering, email=mmarden@pppl.gov, c=US Date: 2016.06.17 14:28:58 -04'00'
Ali Zolfaghari	**4.0,11.0**	Ali M. Zolfaghari Digitally signed by Ali M. Zolfaghari DN: cn=Ali M. Zolfaghari, o=PPPL, ou=Engineering, email=azolfagh@pppl.gov, c=US Date: 2016.06.17 18:49:56 -04'00'

2.0 Table of Contents

3.0 Revision Status Table

Rev	Date	Description
0	6-17-2016	Original Issue

4.0 Executive Summary

Connections to the PF coils and bus connections are addressed in the calculations listed below.

NSTXU Structural Analysis of PF1, TF and OH Bus Bars NSTXU-CALC--55-01-02 [12]
Stress Analysis of the Inner PF Coils (1a,1b &1c), Center Stack Upgrade NSTXU CALC 133-01-2 [9]
NSTXU Analysis of Existing and Upgrade PF4/5 Coils and Supports . NSTXU-CALC-12-05-01 [13]
NSTXU CHI Bus Bar Analysis NSTXU-CALC-54-01-1 Rev 0 [5]
NSTX Upgrade PF 2/3 Terminal and Flex Bus Analysis NSTXU-CALC-55-02-01 [17]
NSTX Upgrade PF 1 Flex Bus Analysis NSTXU-CALC-55-03-00 (This Calculation)

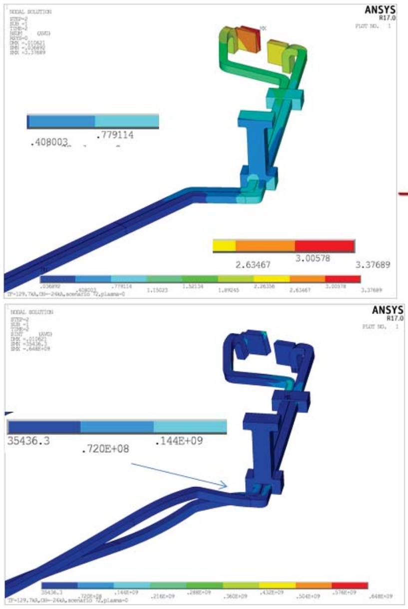

Calculations were performed and filed that cover the PF 1a bus. Andrei's is shown, Also Ali Zolfaghari addressed the bus and inner terminal connection in the PF1 coil calculation

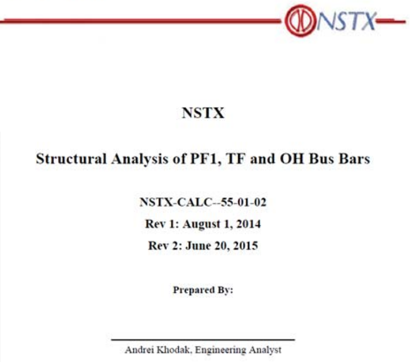

NSTX

Structural Analysis of PF1, TF and OH Bus Bars

NSTX-CALC--55-01-02
Rev 1: August 1, 2014
Rev 2: June 20, 2015

Prepared By:

Andrei Khodak, Engineering Analyst

Figure 4.0-1 Early Bus Analysis Results from[12] that Included the Flex Bus runs

The recent PF1a flex cable support issue resulted from a construction/field change in the solid bus for PF1a upper. It was shortened to provide needed clearance. The field change was not included in updated drawings or calculations. An ECN was initiated but never finished. The consequence of the shorter solid bus was a longer flex bus for which no additional support was provided. The plot of the PF1 a, b, and c, below (Figure 4.0-2), is based on the original qualified inner PF bus design, not the as built design. PF1a is the middle bar. The other two, PF1b, and c, are not yet installed. The intent was to have solid bus traverse the TF field and then begin the flex bus.

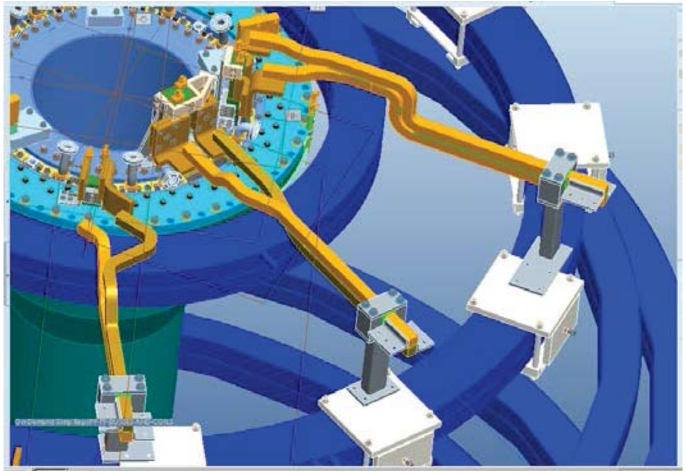

Figure 4.0-2 Original Upgrade Solid Bus Configuration

PF1a solid bar now ends at the umbrella structure with around 20 inches of flex cable within the TF field.

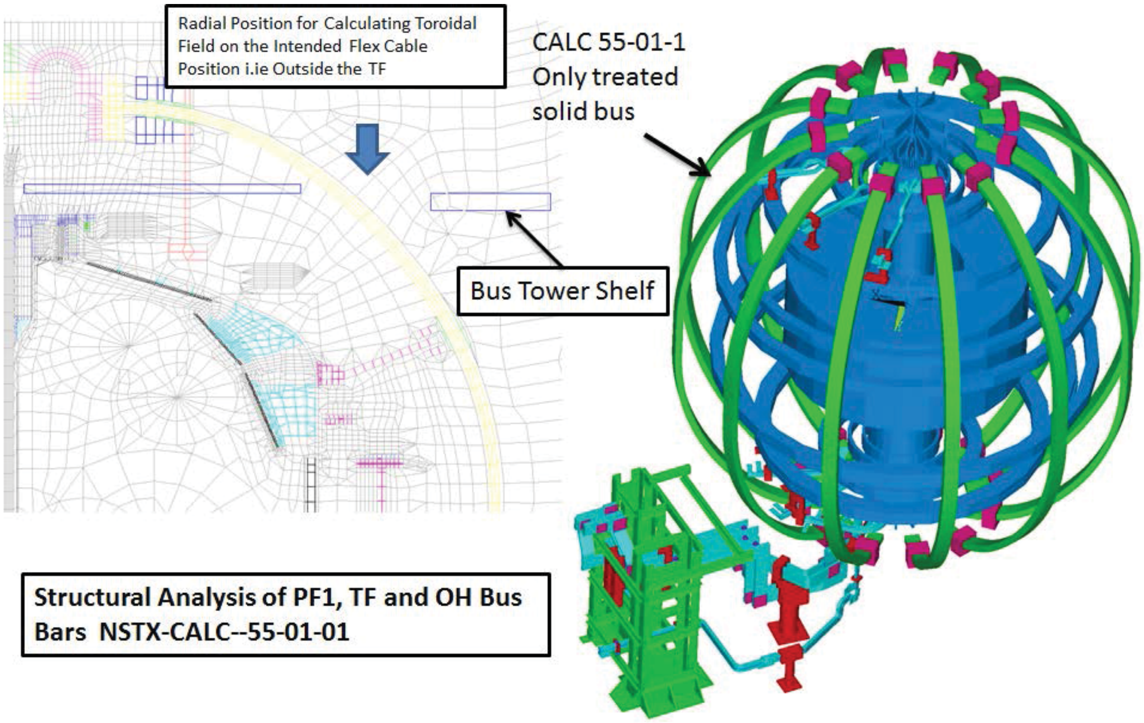

Figure 4.0-3 Original Intended Location of the Flex Bus – Outside the TF along with the Bus Model in the Bus Bar Qualification Calculation [12]

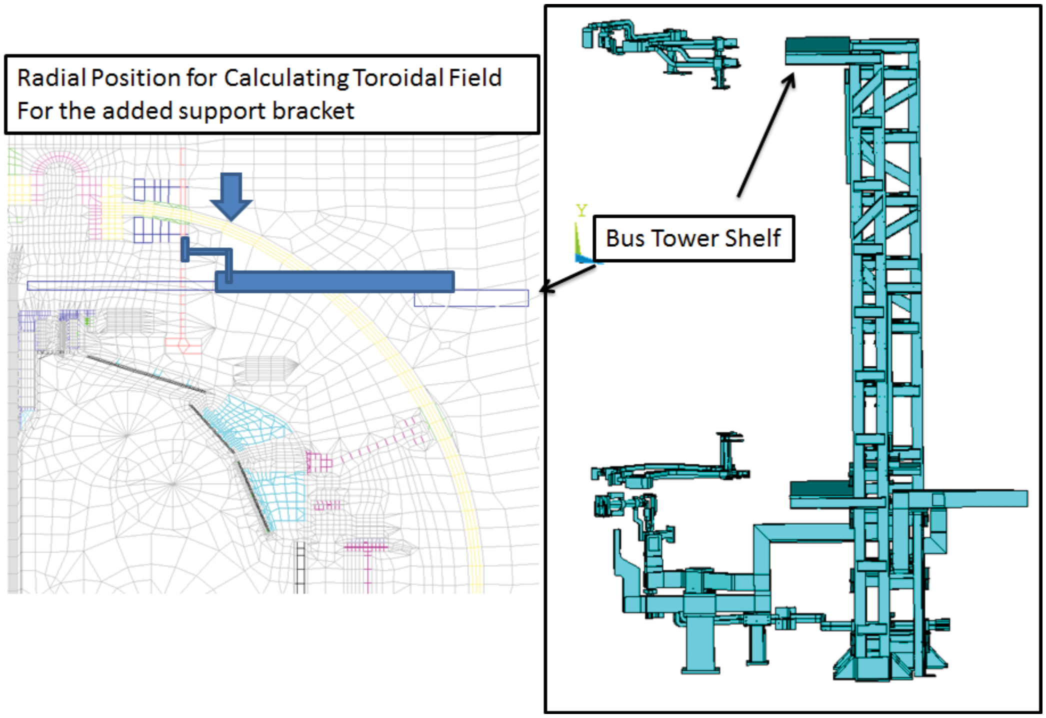

Figure 4.0-4 Actual Location of the Flex Bus –Inside the TF along with the Bus Model in the Bus Bar Qualification Calculation [12]

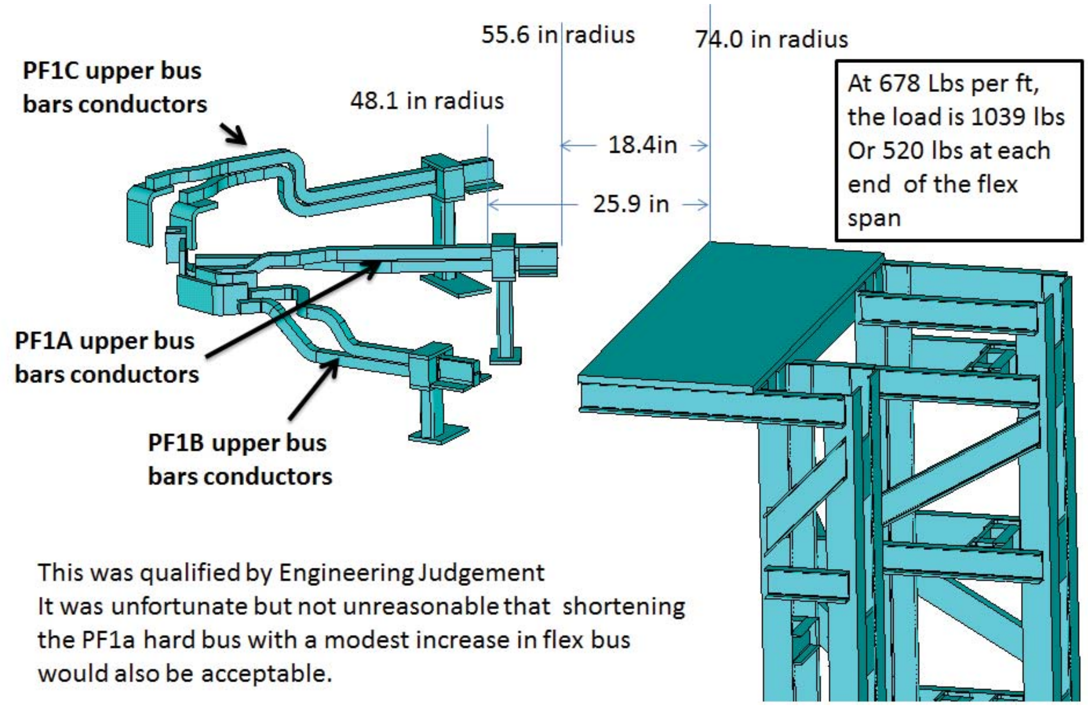

At 678 Lbs per ft, the load is 1039 lbs Or 520 lbs at each end of the flex span

This was qualified by Engineering Judgement
It was unfortunate but not unreasonable that shortening the PF1a hard bus with a modest increase in flex bus would also be acceptable.

Figure 4.0-5 Dimensions from the hard Bus Ends to the Bus Tower Shelf

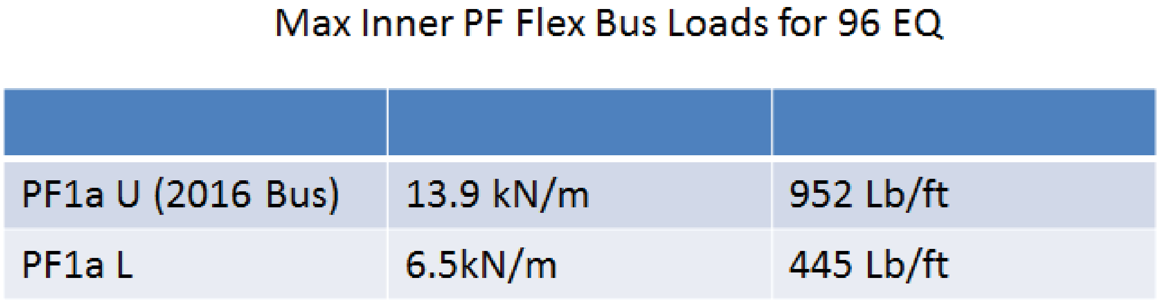

Max Inner PF Flex Bus Loads for 96 EQ

PF1a U (2016 Bus)	13.9 kN/m	952 Lb/ft
PF1a L	6.5kN/m	445 Lb/ft

Table 4.0-1 Design Loads (Computed Assuming Radial Bus Runs)

Design loads were calculated by both the author and Stefan Gerhard. This is presented in more detail in section 9.3. There is good agreement with loads on PF1a Upper. Note that the PF1a Lower loading is 445/952 = 47 % of the PF1a Upper loading. This is largely the consequence of the larger TF field at the end of the solid bus. The lower flex cables were missing a support at the bus tower shelf and during inspections flex bus motion had abraided the paint of the nearby TF coil. Had the support been installed, the lower loading of the lower flex might not have been needed. That alignment of much of the flex is toroidal.

Additional support for the flex cable feeding PF1a upper has been provided. As a consequence of the problem with the upper flex, the lower flex connections have been inspected and it has been concluded that a support is needed there too. Neway Atnafu has developed designs for both and these have been modified by technicians in the field to fit. Wooden mock-ups were used to ensure fit and proper access to nearby diagnostics. Updated, latest (June 16, 2016) models of these are included in this calculation.

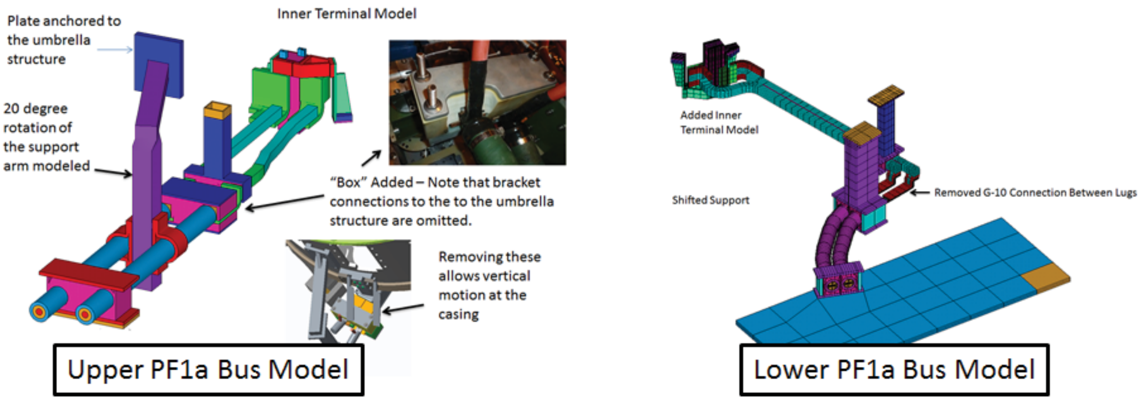

4.0-6 Models of the Upper (Left) and Lower (Right) Solid and Flex Bus

The analysis models include the PF1a and b connection to the inner coil terminal tower and the bent copper flag at the ends of the solid bus out to the support on the bus tower shelf. Added supports are also modeled. Analysis and reinforcement progressed in steps.

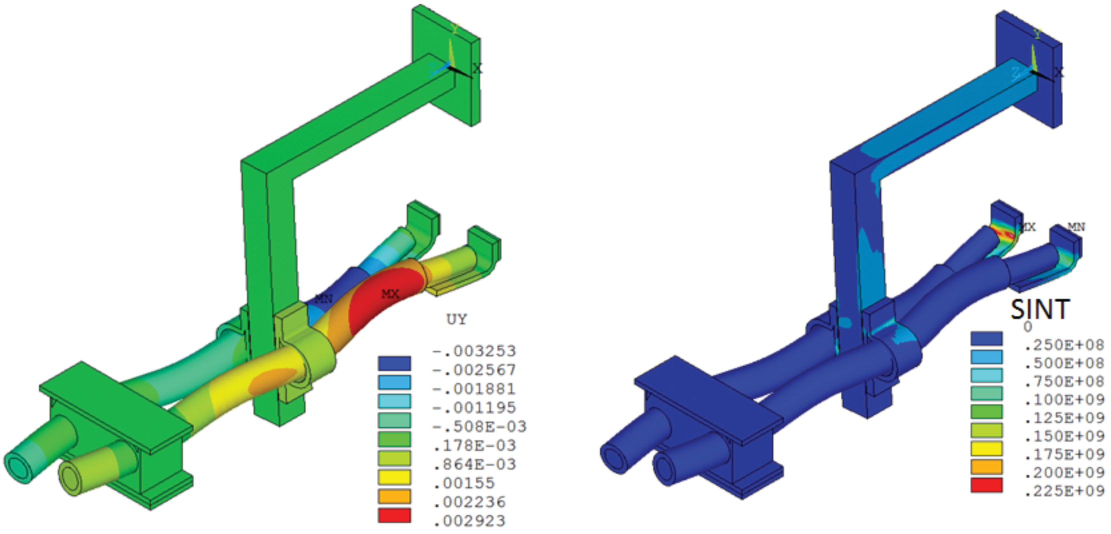

Figure 4.0-7 Early analysis of the flex cable mid span support.

Initial elastic stresses in the flag were high even for a case where there was a mid span support of the flex bus. The lugs are expected to be partially annealed copper near the braze to the solid copper with yields around 8 ksi (55 MPa) or lower. G-10 clamps with potted epoxy supports were added to surround the flags. These analysis results led to the use of elastic plastic copper properties (Section 6.4.1) and the use of large displacement solution to simulate the "arching" of the flexible cable using the ANSYS NLGEO option. Because the new solid bar support causes more bending at the inner connection to the coil flags, an analysis was performed with the 7mm Centerstack expansion. The model needed the addition of the inner terminal "tower" on the coil and the shortened solid bus.

A first step in benchmarking the analyses of the supports is to evaluate the cause of the observed behavior of the bent lugs and flex bus motion. As the model of the added supports was developed, analyses of the bus without the reinforcements were completed.

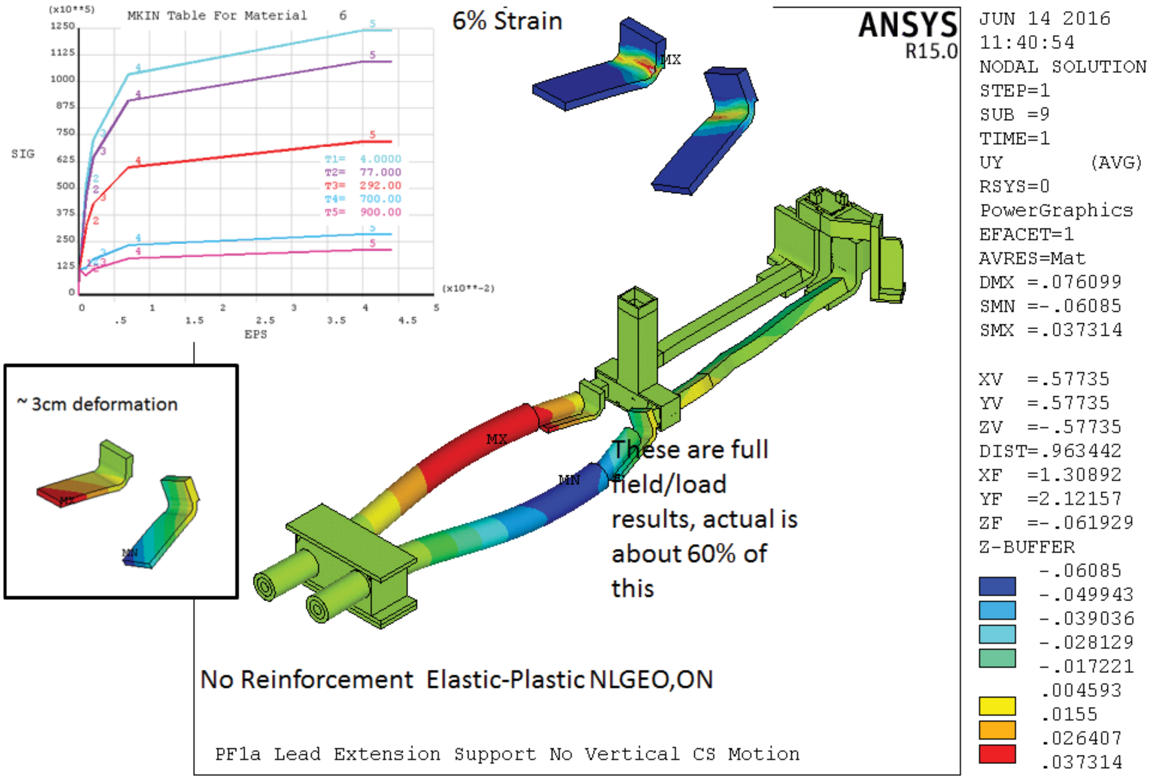

```
JUN 14 2016
11:40:54
NODAL SOLUTION
STEP=1
SUB =9
TIME=1
UY        (AVG)
RSYS=0
PowerGraphics
EFACET=1
AVRES=Mat
DMX =.076099
SMN =-.06085
SMX =.037314

XV  =.57735
YV  =.57735
ZV  =-.57735
DIST=.963442
XF  =1.30892
YF  =2.12157
ZF  =-.061929
Z-BUFFER
     -.06085
     -.049943
     -.039036
     -.028129
     -.017221
     .004593
     .0155
     .026407
     .037314
```

Figure 4.0-8 PF1a Upper Analysis of the Bus Behavior without the added supports and based on the shortened solid bus.

The lug deformations and the large ~3cm permanent set of the lug are consistent with the actual deformed shape. The motions of the flex bus are consistent with the deformed shape in figure 4.0-8.

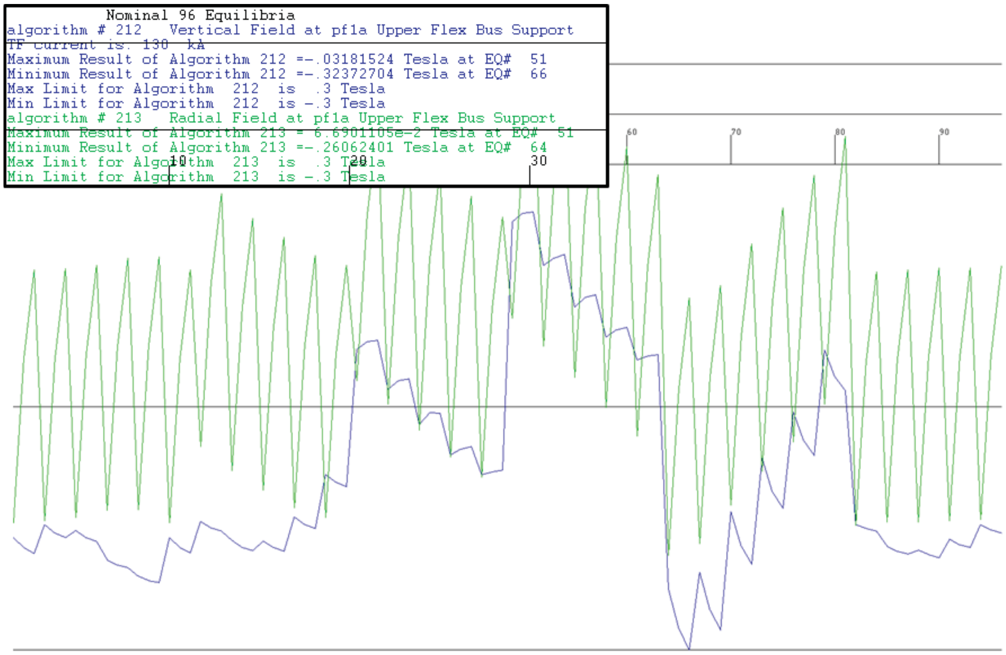

```
              Nominal 96 Equilibria
algorithm # 212   Vertical Field at pf1a Upper Flex Bus Support
TF current is. 130  kA
Maximum Result of Algorithm 212 =-.03181524 Tesla at EQ#  51
Minimum Result of Algorithm 212 =-.32372704 Tesla at EQ#  66
Max Limit for Algorithm  212  is  .3 Tesla
Min Limit for Algorithm  212  is -.3 Tesla
algorithm # 213   Radial Field at pf1a Upper Flex Bus Support
Maximum Result of Algorithm 213 = 6.6901105e-2 Tesla at EQ#  51
Minimum Result of Algorithm 213 =-.26062401 Tesla at EQ#  64
Max Limit for Algorithm  213  is  .3 Tesla
Min Limit for Algorithm  213  is -.3 Tesla
```

Figure 4.0-9 “DCPS” Algorithm Assessment of the Max Field on the PF1a Flex Bus

A couple of approaches have been used to quantify the Lorentz loads on the terminals and flex bus. A "DCPS" algorithm was written that computes the local vertical field at the terminals of PF1a, U&L and PF3 U&L, and multiplies this times the appropriate current for the same EQ for which the field was calculated. The toroidal field is combined using SRSS. For the finite element models, the background fields and peak PF1a currents (19 kA) are used to quantify the loads on the coil terminations.

The "DCPS" Algorithm results shown in figure 4.0-9 refer to a code used to check the implementation of the DCPS algorithms. This has correlated well with Stefan Gerhardt's calculations. Load calculations are also included in section 9.0 that agree reasonably well with Gerhardt's estimates of loads.

Field alterations of the outer connection to the flex bus and the fact that the bus drawings were not updated raised the concern that it was possible that the inner connections were altered as well.

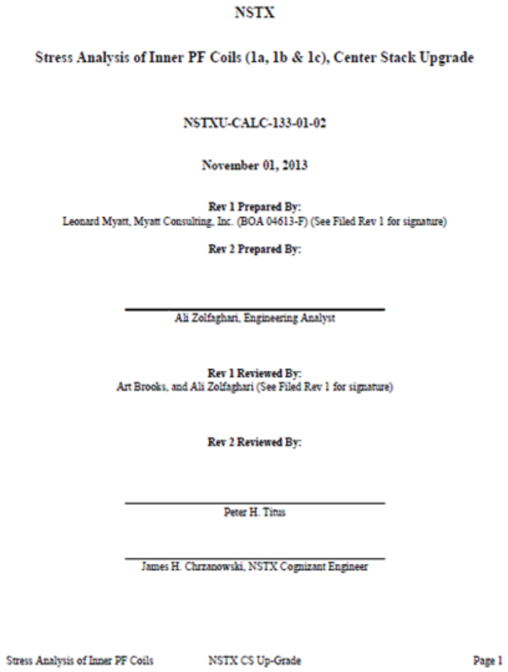

NSTX

Stress Analysis of Inner PF Coils (1a, 1b & 1c), Center Stack Upgrade

NSTXU-CALC-133-01-02

November 01, 2013

Rev 1 Prepared By:
Leonard Myatt, Myatt Consulting, Inc. (BOA 04613-F) (See Filed Rev 1 for signature)

Rev 2 Prepared By:

Ali Zolfaghari, Engineering Analyst

Rev 1 Reviewed By:
Art Brooks, and Ali Zolfaghari (See Filed Rev 1 for signature)

Rev 2 Reviewed By:

Peter H. Titus

James H. Chrzanowski, NSTX Cognizant Engineer

Stress Analysis of Inner PF Coils   NSTX CS Up-Grade   Page 1

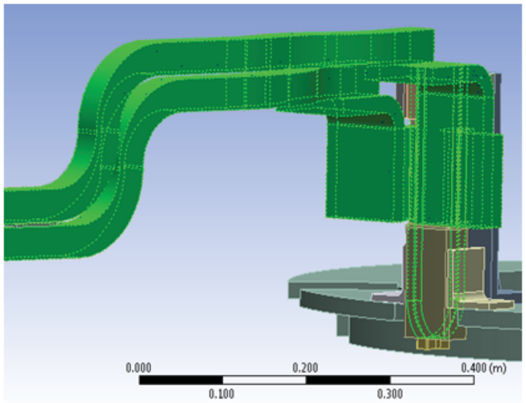

Figure 4.6-3 Geometry highlighting parts on which the EM force density from Maxwell is mapped.

Figure 4.0-10 Excerpt from Reference [9]

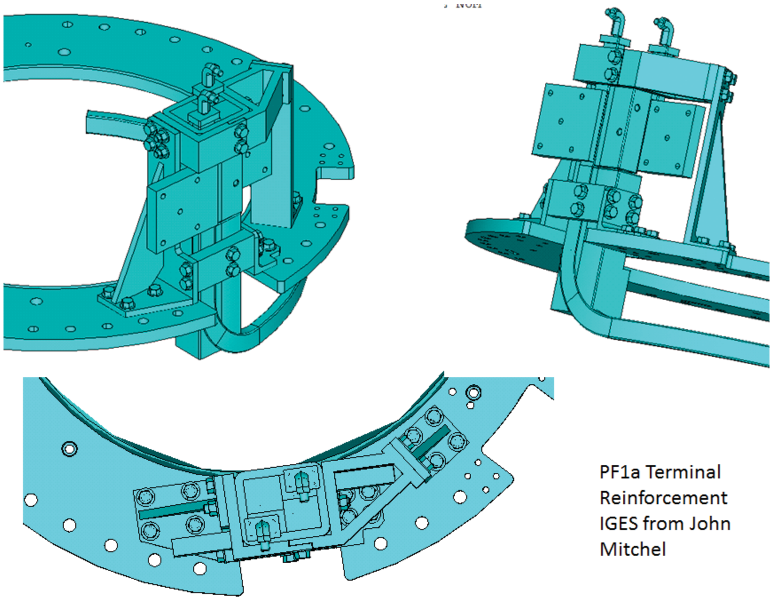

PF1a Terminal Reinforcement IGES from John Mitchel

Figure 4.0-11 IGES Models of the Inner Terminal Tower Showing the terminal reinforcements.

Inspections were done and it was very difficult to get a clear view of the inner terminals. In addition, they were covered with an insulating rubber. However, the bus bars could be seen and nothing looked disturbed.

The coil terminal reinforcements were constructed per the drawings and were not part of the field fit-up of the bus connections. The terminal reinforcements are as required by the calculations and are qualified. There was a concern that field modifications may have been made to the inner bus flags. Minimal changes to the connection to the coil would be possible and adverse assembly is unlikely. Confirmation of as-builts is still desirable. The modeling used in this calculation is intended to provide an appropriate boundary condition for the bus connections and evaluate centerstack casing expansion and not to substitute for the qualification provided by [9]. Solid Bus connections to the PF1a inner terminal are re-evaluated in this calculation to assess the acceptability of the modified bus and flex cable supports for the full 7 mm vertical expansion of the centerstack casing during high power long pulse shots (See section 12.2).

With all the reinforcements in the model, the stresses are acceptable. The model was mainly built from sketches, but the detailed drawing [20] shows good correspondence with the finite element model.

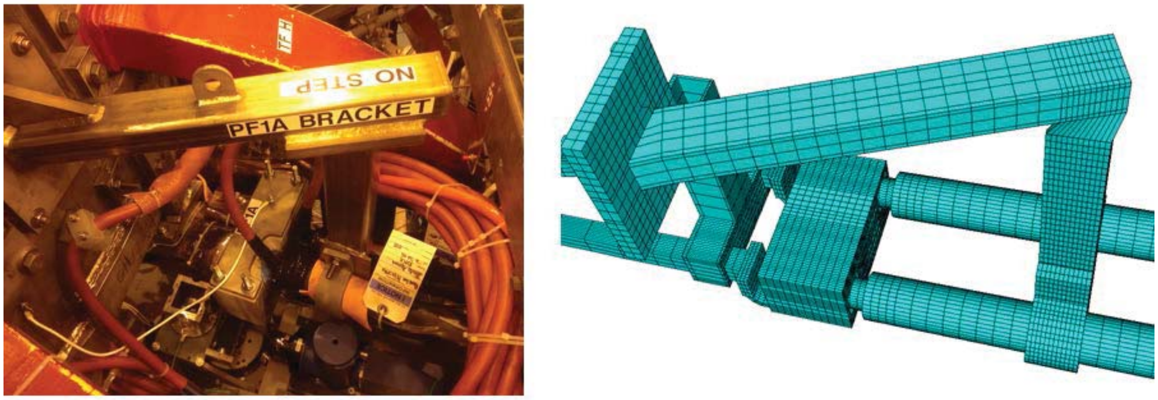

Figure 4.0-12 PF1aU Flex Cable Support and Analysis Model Oriented as in the Photo

The correspondence between the as-built conditions and the model also look reasonable.

There are still some stresses at the bend in the lug that produce some plastic strain. This is expected to yield, then cycle elastically after the initial loading. As currently being run, NSTX does not reverse the current in PF1a Upper and Lower – See Figure 9.1-2. The 96 Equilibria do have some current sets that are reversed. These are smaller than the positive currents – See the plot in Figure 9.1.1. The current reversal will have to be qualified at a future date and possibly a different current level established.

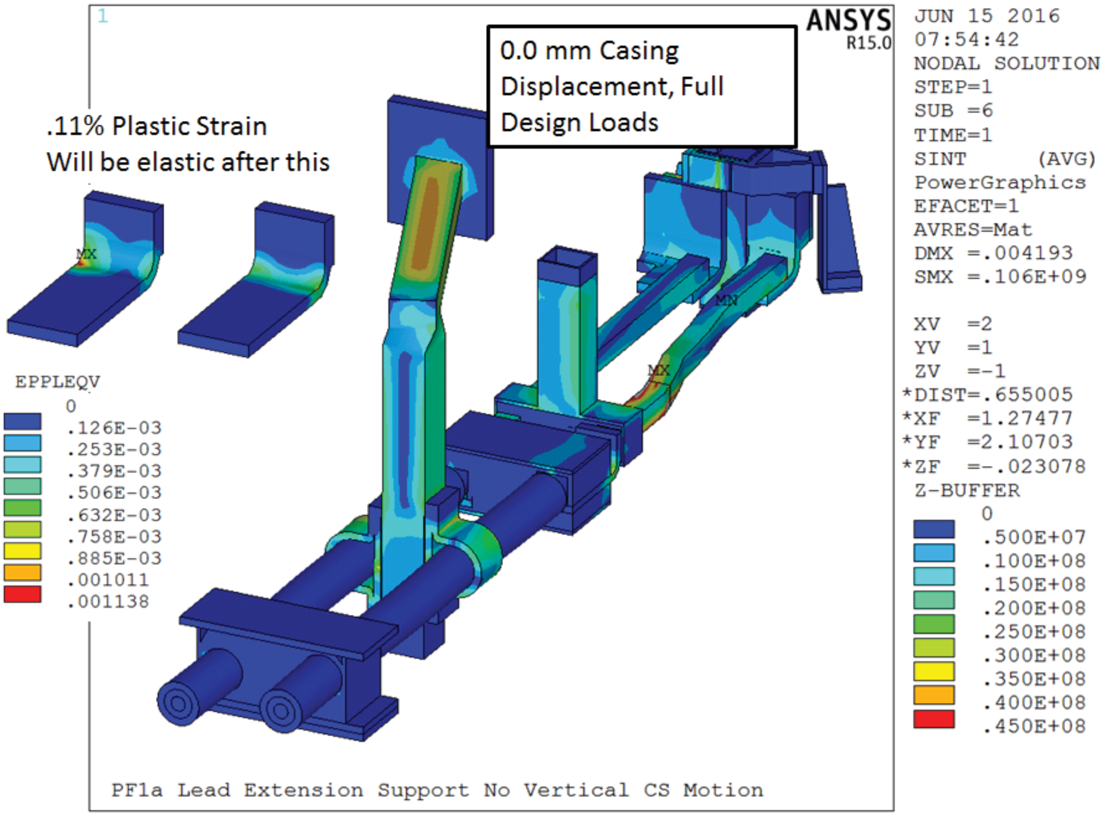

Figure 4.0-13 Stress Results for the Upper PF1a With Added Supports an No Centerstack Expansion

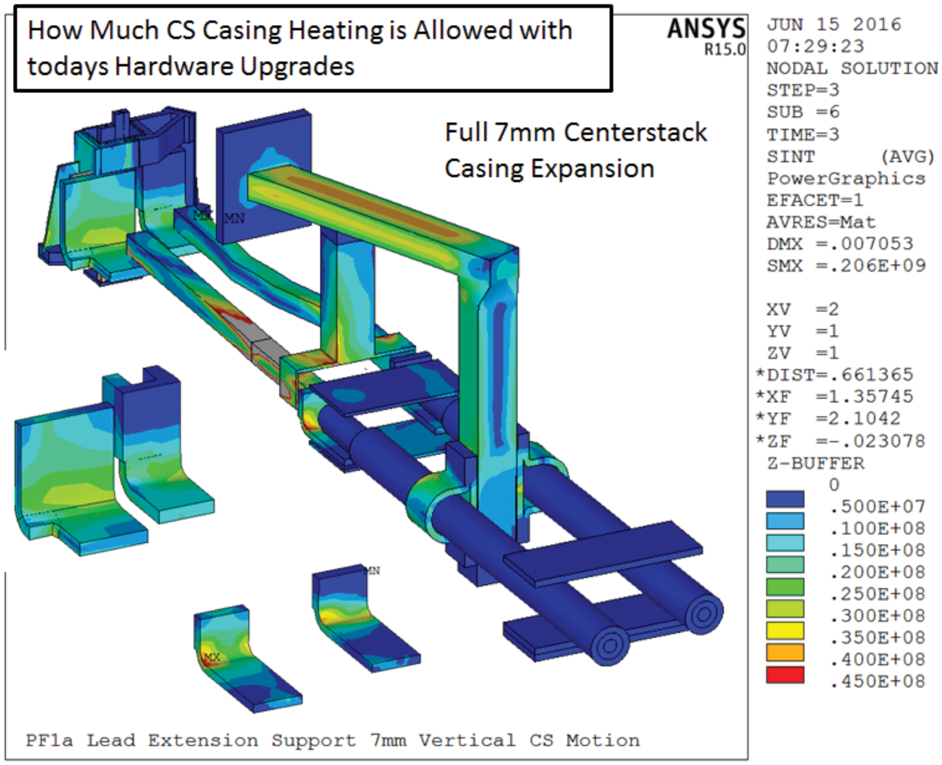

Figure 4.0-14 Stress Results for the Upper PF1a With Added Supports and 7mm Centerstack Expansion

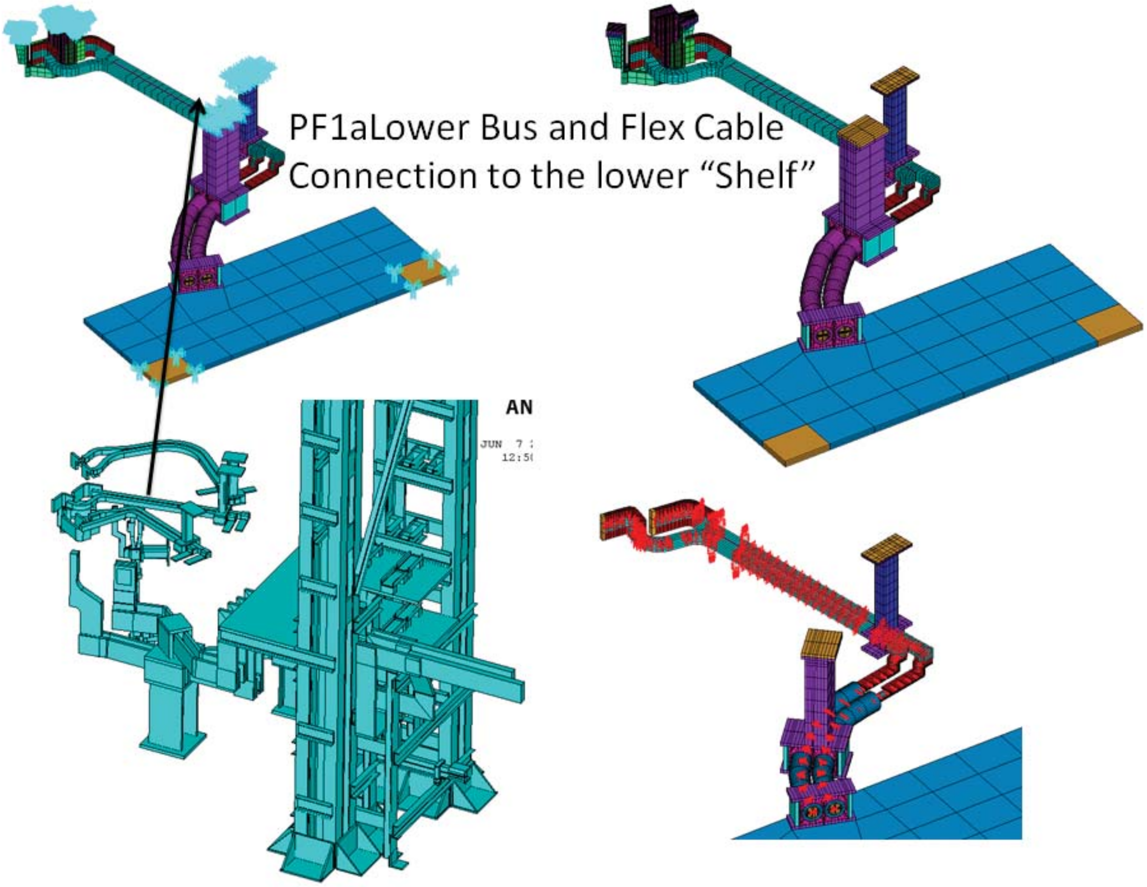

Figure 4.0-15 Lower PF1a Bus Bar Analysis Model

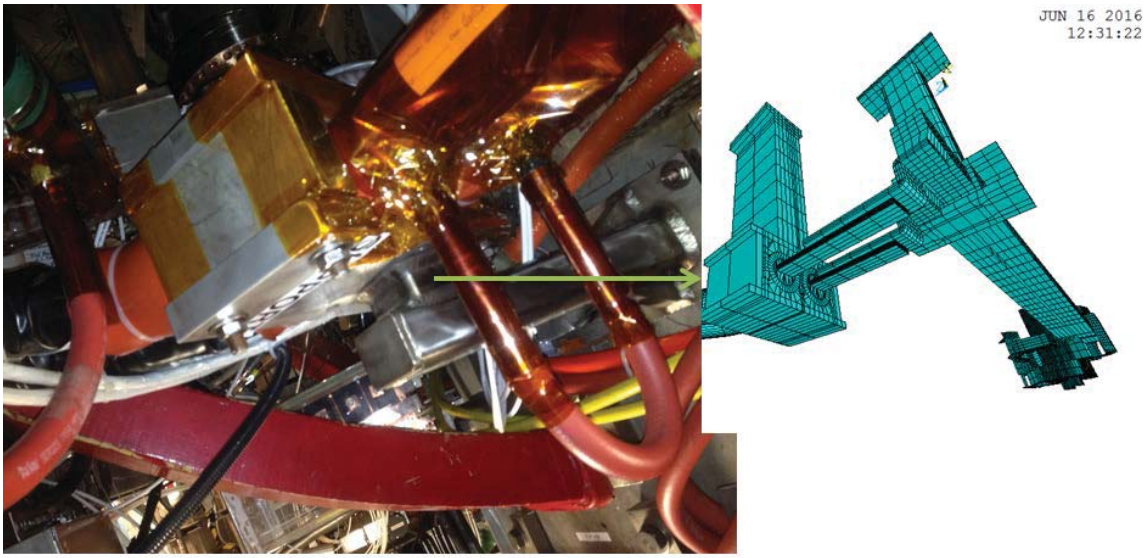

Figure 4.0-16 As-Built Photo of the Lower PF1a Flex Cable Support, and the Model Oriented Similarly to the Photo

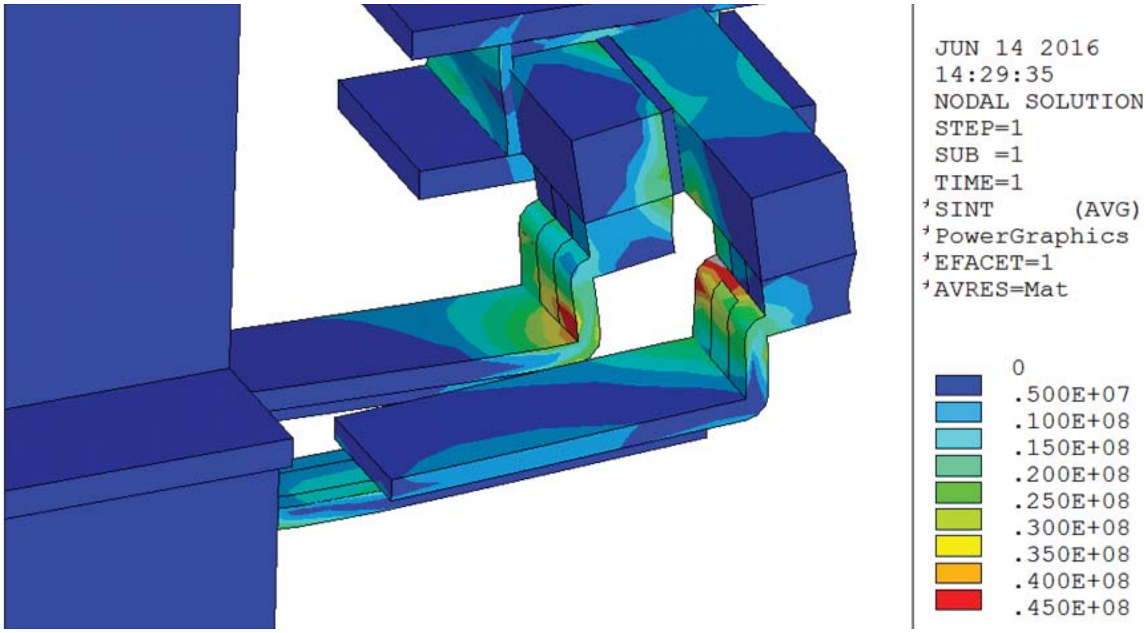

Figure 4.0-17 Stress in the Bus end Lug for full loading – Final June 16 Installed Condition

The stresses on the bus lugs are acceptable but a bit higher than they were before the G-10 plate connecting the two was removed (or it was decided that it was too difficult to install). This local area will also have some "shake-down" characteristics that will need to be respected – i.e. reversal of currents.

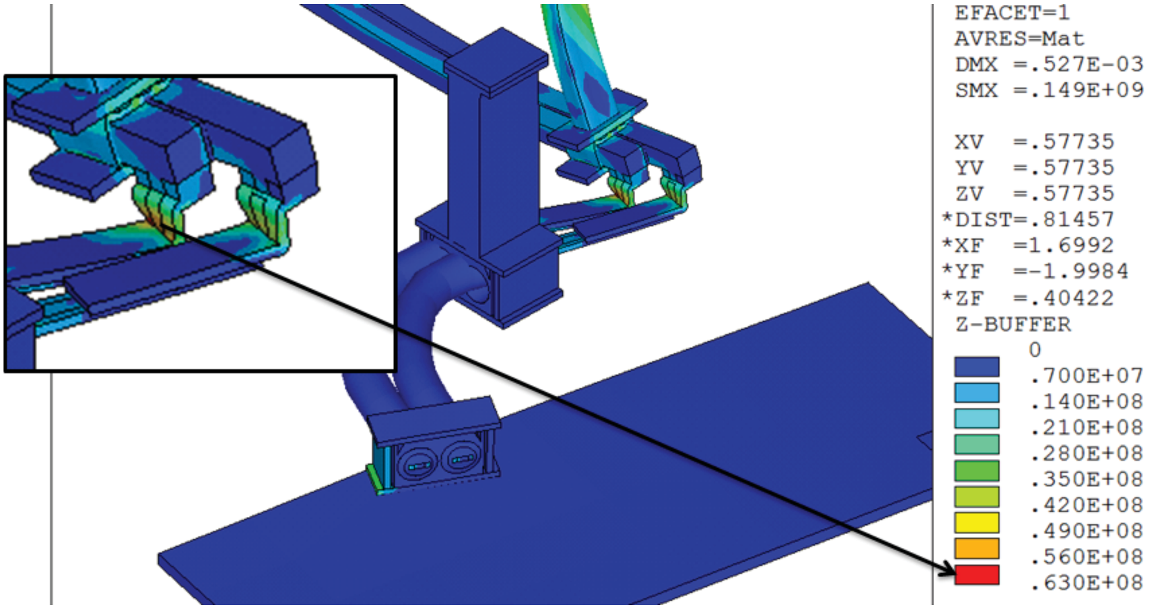

Figure 4.0-18 Stress in the Log due to the Radial Expansion of the Air Cooled Solid Bus Bar

The supports for the PF1a upper and lower flex clamps are acceptable as installed (June 17). The supports for PF1a Lower may need to be modified to provide some strain relief for operation in which the lower bus bar heats substantially. In Section 8.0, a temperature plot from [12] is shown which shows about 50C average heat up for multiple full power shots.

The results of the calculations indicate that the PF1a Bus and supports are stressed within the capacity of the members selected. The lugs on the ends of the hard bus are being considered as fully annealed and the amount the lugs bent due to the early operation is an indication that the lugs are in fact annealed. The addition of supporting struts and local clamps of the lugs has limited the stress in the lugs to levels that are within the expected cyclic stress allowable of 45 MPa of the annealed copper. The "one-sided" nature of the loading is cited as reason to expect an elastic response for load cycles after the initial plastic bending of the lugs. For elastic cyclic loading, the allowable fatigue stress for copper used in NSTX is 125 MPa. As a part of the recovery plan, the lugs were liquid penetrant inspected to ensure that the plastic deformation did not initiate cracks and reduce fatigue life. Appendix D includes an assessment of this.

The altered, shortened length of the solid bus changed the angle imposed by the hard bus connection to the terminal tower as the centerstack casing grows. PF1aU moves with the upper end of the casing. PF1a Lower does not move in this way. This was simulated and supports that would have held the lug clamp rigidly with respect to the umbrella structure were omitted and the needed vertical degree of freedom was allowed without excessive loading at the terminal. The terminal was modeled in sufficient detail to confirm that the stress in the conductors and flags in the terminal tower were within the 125 MPa fatigue allowable. PF1a Lower does have some thermal stress concerns. The movement of the flex cable support close to the lugs means that the radial growth of the solid bus from Joule Heat is restrained. This will bend the lugs. A stress of 60 MPa was calculated for the thermal stress based on multiple high power 5 second shots. This will require some re-evaluation or hardware changes as operations approach full performance.

5.0 Digital Coil Protection System.

At this point, the protection all coil bus runs is not included in the DCPS. This is largely due to the fact that the bus runs cross the TF field and must be qualified with a large component of loading that is not dependent on the PF coil currents. The bus runs have been qualified for the full TF field and the 96 equilibria. It might be worth further investigation but it is not expected to be needed.

6.0 Design Input

6.1 Criteria

Stress Criteria are found in the NSTX Structural Criteria Document[11]. The stress criteria has been simplified into one tensile stress limit for copper conductors based on an assessment of the fatigue life capabilities of the OH conductor [10]. Maintaining the tensile stress below 125 MPa will satisfy the fatigue limit of all the copper except copper that has been annealed by the brazing operation. It should be pointed out that brazed conductor was included in the assessments in reference [10]. For components that may be fully annealed, low cycle fatigue and elastic-plastic shake-down are considered. As a part of the recovery plan, the lugs were liquid penetrant inspected to ensure that the plastic deformation did not initiate cracks and reduce fatigue life. Appendix D includes an assessment of this. Disruption loads should be minimal for these terminal connections. The field and current changes outside the vessel are small compared with the normal operating loads.

6.2 References

[1] NSTX Upgrade General Requirements Document, NSTX_CSU-RQMTS-GRD Revision 5, C. Neumeyer, June 14 2012
[2] NSTX-U Design Point Spreadsheet, **NSTXU-CALC-10-03-00** C. Neumeyer, http://w3.pppl.gov/~neumeyer/NSTX_CSU/Design_Point.html
[3] Drawing E-DC1501 PF-2 and PF-3 Coils Lead Reinforcement Bracket Assembly
[4] Drawing E-DC1500 PF-2 and PF-3 Coils Lead Reinforcement Bracket Details
[5] NSTX Upgrade CHI Bus Bar Analysis NSTXU-CALC-54-01-1 Rev 0 November 21, 2013 by P. Titus, Reviewed by A. Khodak
[6] Power Supply Cables PF and TF flag adapter plate details, Drawing E-DC1201
[7] 1EDC1742.pdf CENTERSTACK UPGRADE PF COIL SYSTEMS PF-1A UPPER COIL LEAD SUPPORT BRACKET ASSEMBLY
[8] PF Coil Feed Changes, Design Basis for Umbrella Bus Loads, S. Ramakrishnan, August 31, 2012

[9] "Stress Analysis of the Inner PF Coils (1a,1b &1c), Center Stack Upgrade" NSTXU CALC 133-01-2 L. Myatt and A Zolfaghari
[10] P. TITUS OH Conductor Fatigue Analysis NSTXU-CALC-133-09-00 Rev 0 Jan 7 2011, PPPL
[11] NSTX Structural Design Criteria Document, NSTX_DesCrit_IZ_080103.doc I. Zatz
[12] NSTX Structural Analysis of PF1, TF and OH Bus Bars NSTX-CALC--55-01-02 February 15, 2011 , Rev 2 June 2015, Andrei Khodak
[13] NSTX Upgrade Analysis of Existing and Upgrade PF4/5 Coils and Supports – With Alternating Columns. NSTXU-CALC-12-05-01 Rev 0 December 2011 Rev 1 April 2016, P. Titus, checked by I. Zatz
[14] PF-2&3 Lead Clamps Design Review 04/02/2015 By Neway Atnafu
[15] Email from Scott Gifford Apr 27 to Neway, and P. Titus: Gentlemen the pictures for the PF 2-3 Supports are in the photo drop.P:\Photo Drop\PF 2-3 Supports
[16] Flex Cable Catalog, Northern Connectivity Systems Inc Commodore Machine Company 1749 Northwood Drive, Troy Michigan
[17] NSTX Upgrade PF 2/3 Terminal and Flex Bus Analysis NSTXU-CALC-55-02-01
[18] Centerstack Upgrade PF Coil System Upper PF1a Bus Assembly, Drawing #E-DC1804
[19] PF-1aU Bus Bending FDR Slides S.P. Gerhart, Last Updated 5/26/2016
[20] drawing #DC11003 Centerstack Upgrade PF Coil System PF1a Upper Bus Support

6.3 Photos and Drawing Excerpts

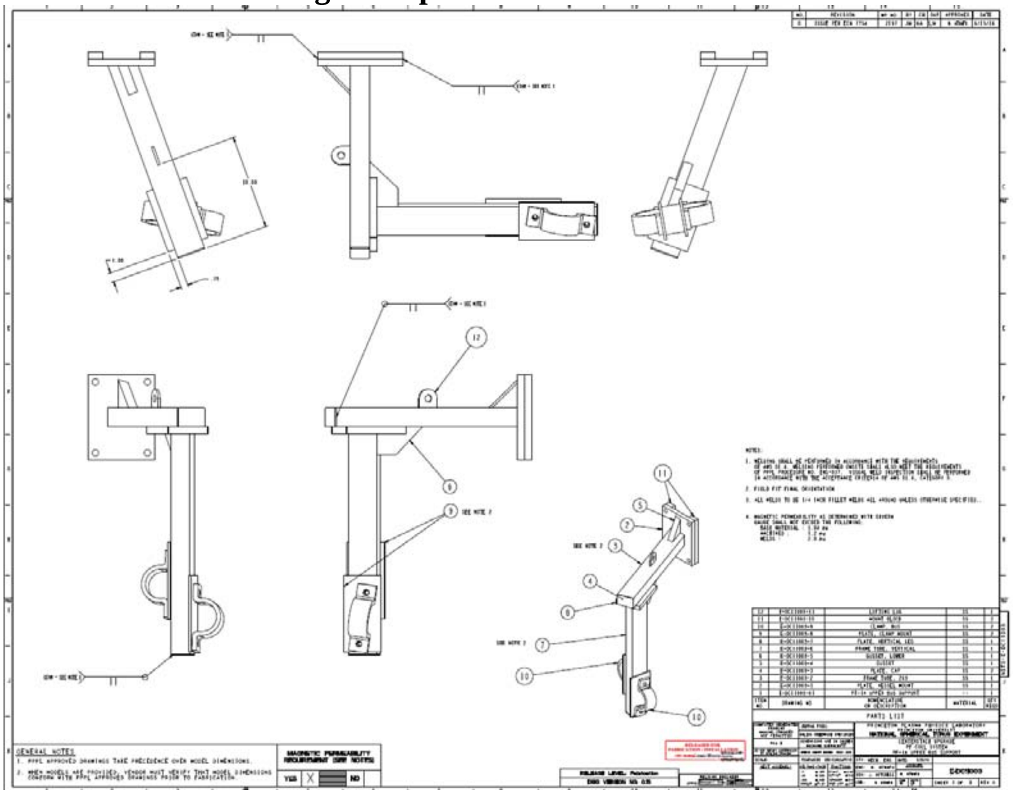

Figure 6.3-1 Reinforcement Configuration Drawing [20]

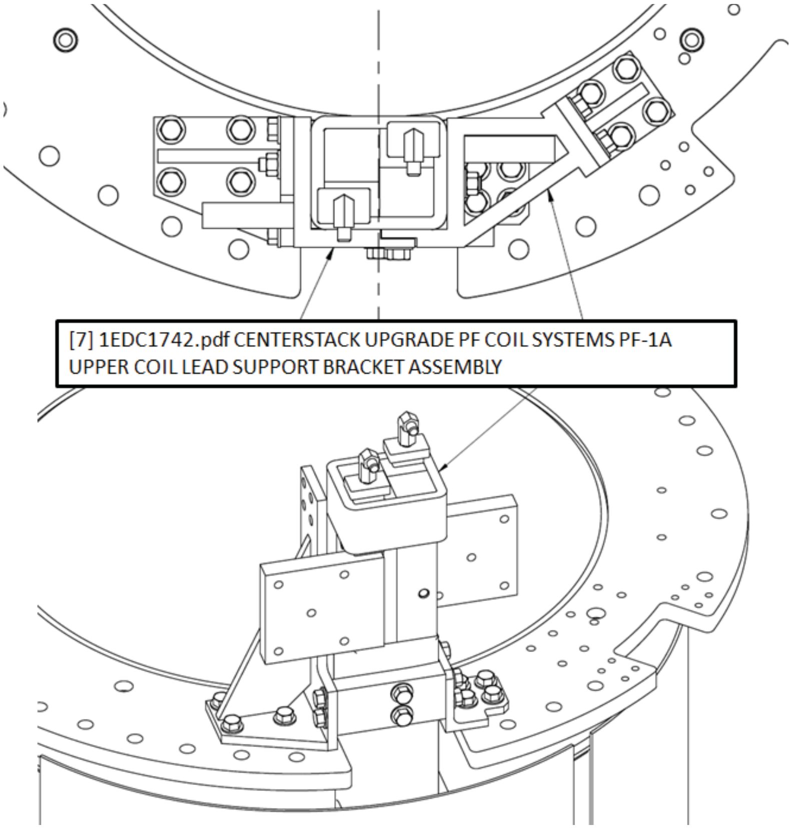

[7] 1EDC1742.pdf CENTERSTACK UPGRADE PF COIL SYSTEMS PF-1A UPPER COIL LEAD SUPPORT BRACKET ASSEMBLY

Figure 6.3-2 PF1a Upper and Lower Terminal Tower Assembly and Partial Assembly

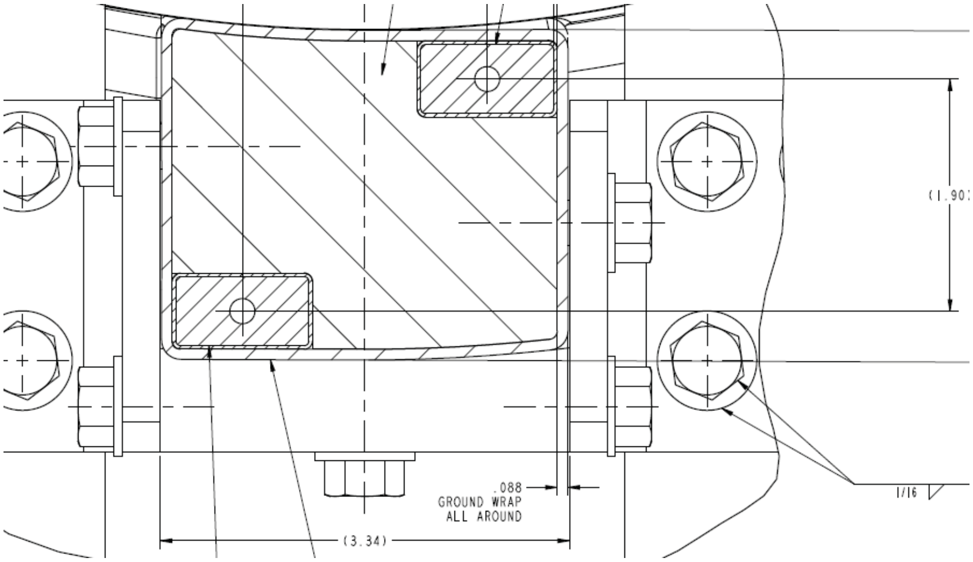

Figure 6.3-3 Cross Section of PF1a, and Terminal “Tower”

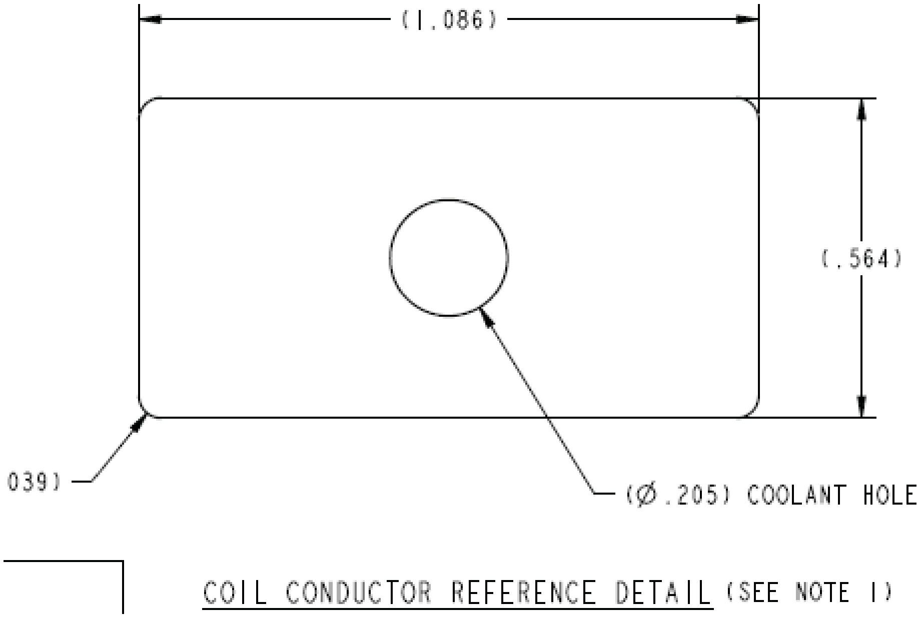

Figure 6.3-4 PF1a Coil Conductor Cross Section

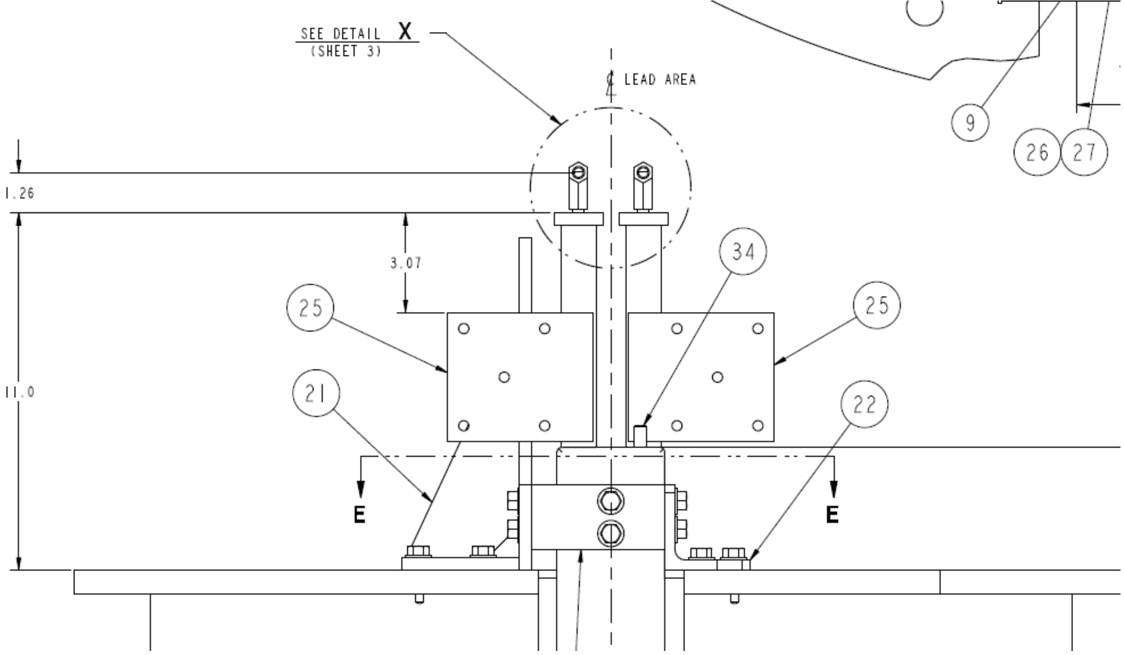

Figure 6.3-5 PF1a Terminal Layout - Elevation

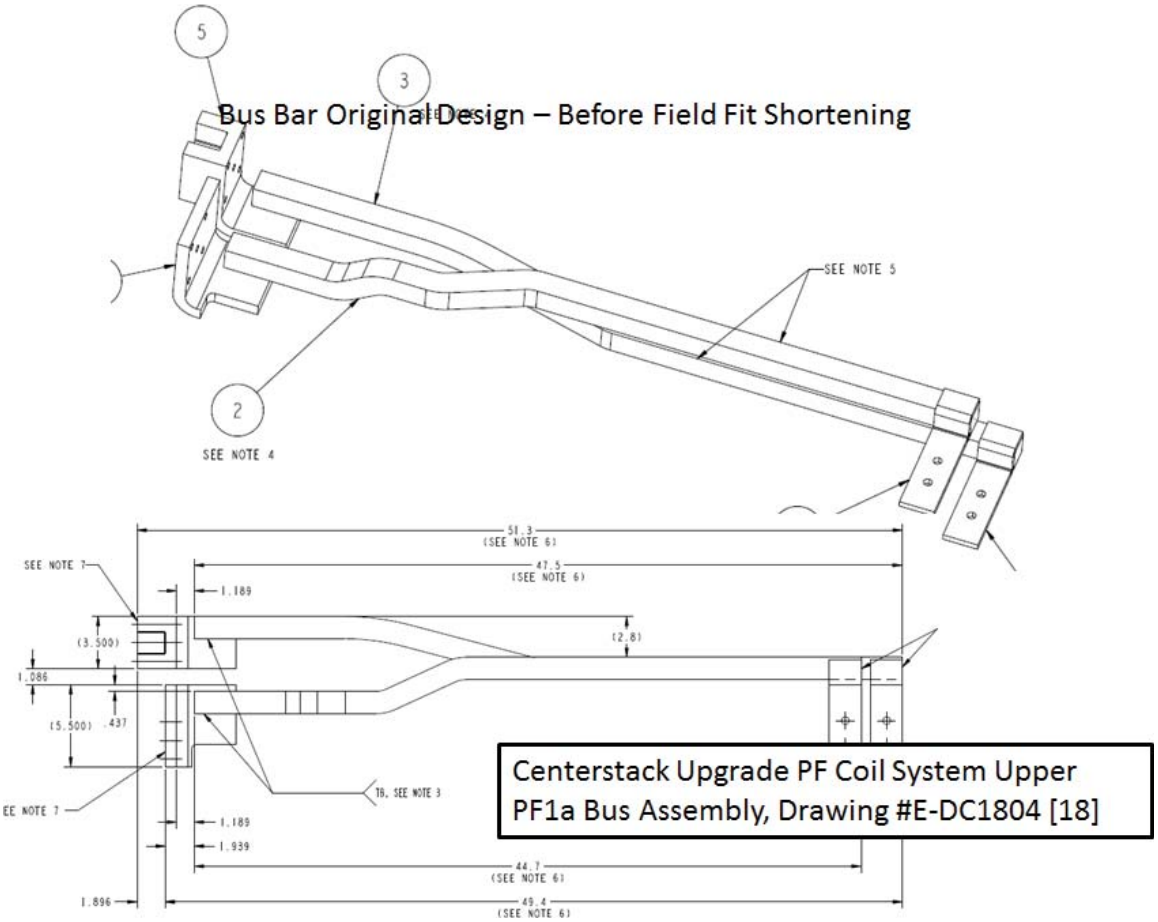

Figure 6.3-6 Original PF1a Upper Bus Design – Before Field Fit-Up

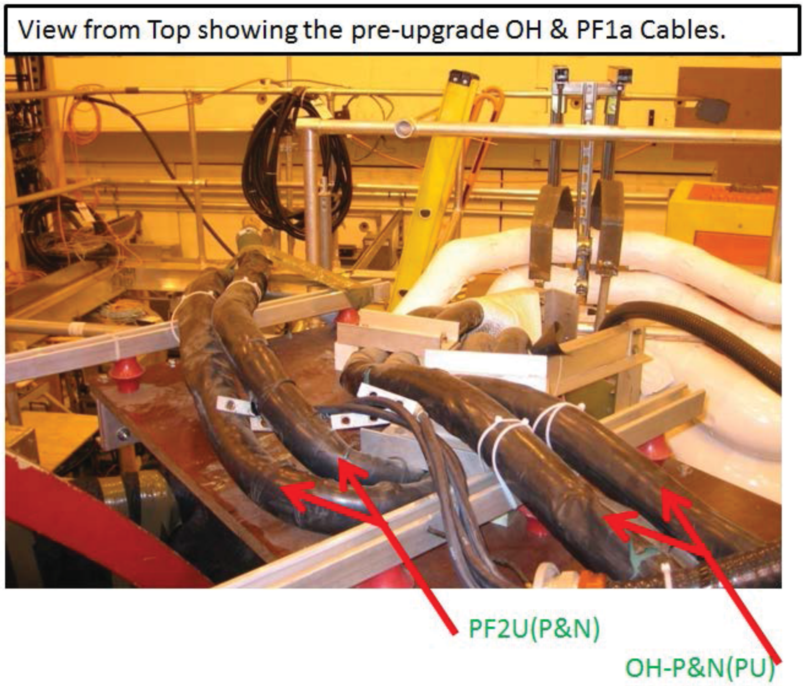

Figure 6.3-7 Cable Supports from Pre-Upgrade Configurations

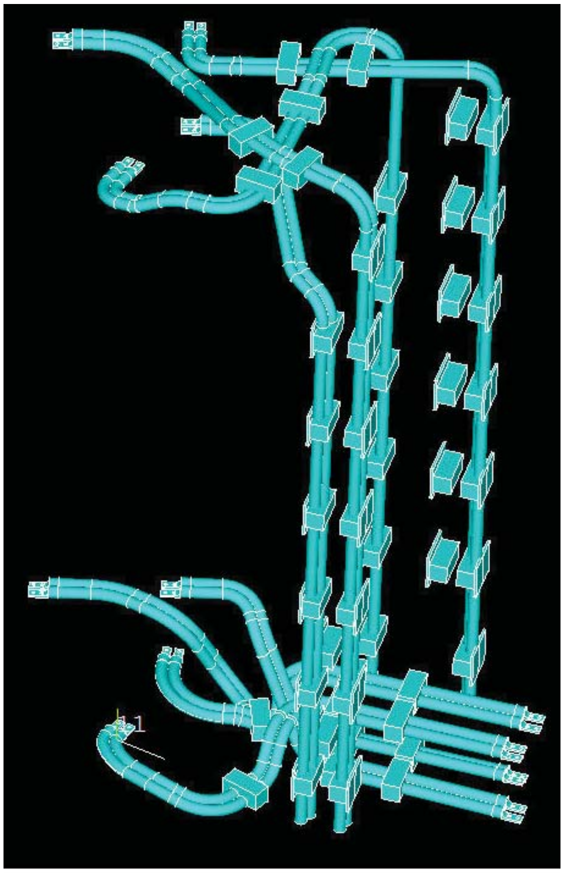

Figure 6.3-8 IGES Model from Jean Pierre Fra – This did not include PF1a b or c, but was used for qualification of PF 2 and 3

6.4 Materials and Allowables

6.4.1 Properties for Analysis

Annealed Copper Stress-Strain Used in This Calculation

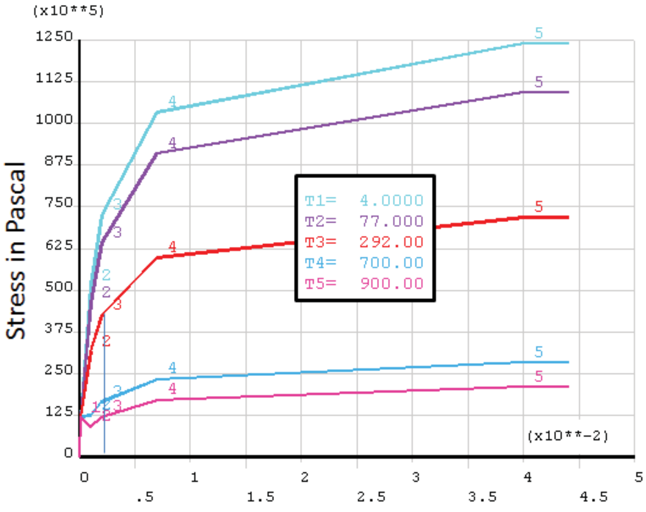

.2 % Yield ~40 Mpa = 5800psi

Annealed Copper Stress-Strain Used by M. Mardenfeld – See Appendix D

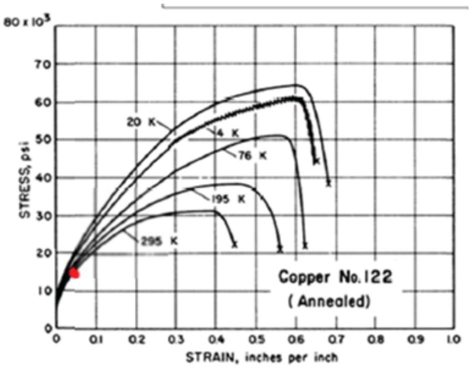

.2 % Yield ~8000psi

6.4.2 Static Allowables for Copper Stresses

The TF conductor properties are taken as representative of the PF1 bus physicals. The TF copper ultimate is 39,000 psi or 270 MPa. The yield is 38ksi (262 MPa). Sm is 2/3 yield or 25.3ksi or 173 MPa – for adequate ductility, which is the case with this copper which has a minimum of 24% elongation. Note that the ½ ultimate is not invoked for the conductor (it is for other structural materials). These stresses should be further reduced to consider the effects of operation at 100C. This effect is estimated to be 10%, so the Sm value is 156 MPa and the bending allowable is 233 MPa.

- From: 2.4.1.1 Design Tresca Stress Values (Sm), NSTX_DesCrit_IZ_080103.doc [11]
- • (a) For conventional (i.e., non-superconducting) conductor materials, the design Tresca stress values (Sm) shall be 2/3 of the specified minimum yield strength at temperature, for materials where sufficient ductility is demonstrated (see Section 2.4.1.2). [3]

The solid bus bars are not challenged by these limits.

6.4.3 Fatigue Limits for Copper Bus Bar

The normal operating fatigue based bus bar conductor allowable is taken to be 125 MPa based on the assessment of OH conductor fatigue based allowable in Ref [10].

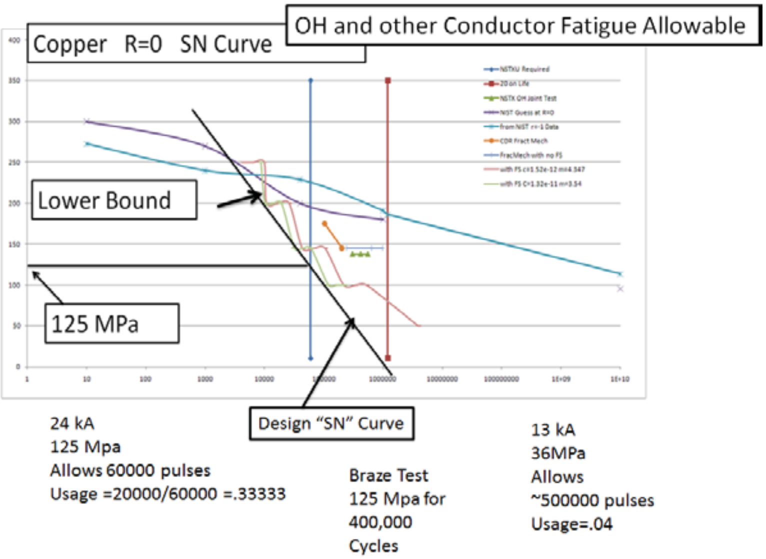

24 kA
125 Mpa
Allows 60000 pulses
Usage =20000/60000 =.33333

Braze Test
125 Mpa for
400,000
Cycles

13 kA
36MPa
Allows
~500000 pulses
Usage=.04

Figure 6.4.3-1 Copper Fatigue Allowable Adopted for NSTX-U Conductors [10]

The lugs at the ends of the solid bus are probably in some state of anneal. For load controlled plastic stain cycling the fatigue life is much less than the elastic fatigue performance. During the first year of operation, the currents in PF1a have not been reversed. The behavior of the lug under such a load is to initially yield and then cycle elastically. Load reversals or large changes in the poloidal field direction could alter this. A low cycle fatigue assessment of the brazed components will give a lower bound on the fatigue life.

As a part of the recovery plan, the lugs were liquid penetrant inspected to ensure that the plastic deformation did not initiate cracks and reduce fatigue life. Appendix D includes an assessment of this.

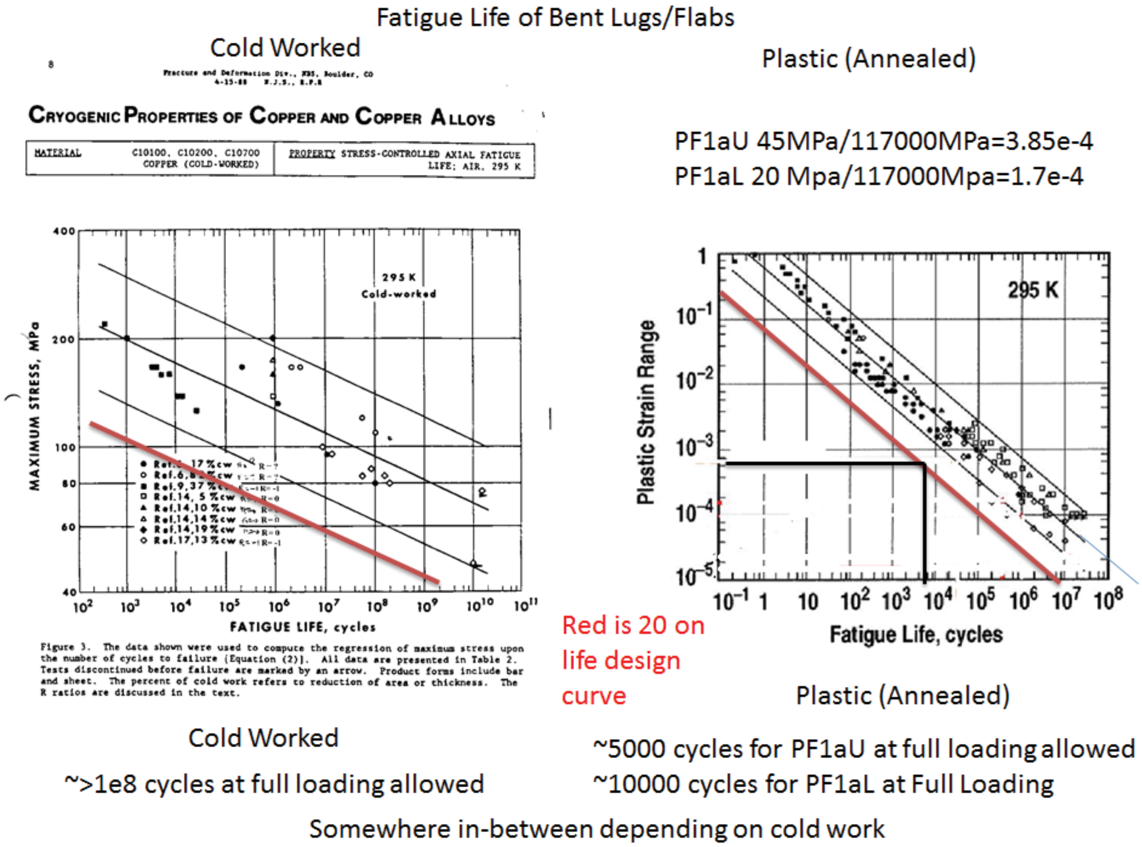

Fatigue Life of Bent Lugs/Flabs

Cold Worked

Plastic (Annealed)

8

Fracture and Deformation Div., NBS, Boulder, CO
4-15-88 N.J.S., R.P.R

CRYOGENIC PROPERTIES OF COPPER AND COPPER ALLOYS

MATERIAL C10100, C10200, C10700 COPPER (COLD-WORKED)	PROPERTY STRESS-CONTROLLED AXIAL FATIGUE LIFE; AIR, 295 K

Figure 3. The data shown were used to compute the regression of maximum stress upon the number of cycles to failure [Equation (2)]. All data are presented in Table 2. Tests discontinued before failure are marked by an arrow. Product forms include bar and sheet. The percent of cold work refers to reduction of area or thickness. The R ratios are discussed in the text.

PF1aU 45MPa/117000MPa=3.85e-4
PF1aL 20 Mpa/117000Mpa=1.7e-4

Red is 20 on life design curve

Cold Worked

~>1e8 cycles at full loading allowed

Plastic (Annealed)

~5000 cycles for PF1aU at full loading allowed
~10000 cycles for PF1aL at Full Loading

Somewhere in-between depending on cold work

Figure 6.4.3-2 Copper Fatigue Allowable for Elastic High Cycle vs. Plastic Low Cycle Fatigue

Disruption loading has minimal effect on the PF1 bus bars. Severe disruption loads and bake-out loads are assumed to occur only a few cycles and do not require a fatigue assessment. Stresses for these cases should meet static allowables.

6.5 Maximum PF 1a U, L Currents

These are as specified in the design point spreadsheet:

Coil	Min Curr*	Max Curr*
	(kA)	(kA)
OH (half-plane)	-24	24
PF1a	-8	19
PF1b	-6	13
PF1c	-5	16
PF2a	-11	15
PF2b	-11	15
PF3a	-16	12
PF3b	-16	12
PF4b	-16	6
PF4c	-16	6
PF5a	-34	0

These are the maximum currents possible for the individual coils. In Section 9, the max currents expected for the 96 Equilibrium are specified and the min and max currents for actual operation in the last year are provided by Stefan Gerhardt [19].

7.0 Models

7.1 PF1a Upper Model

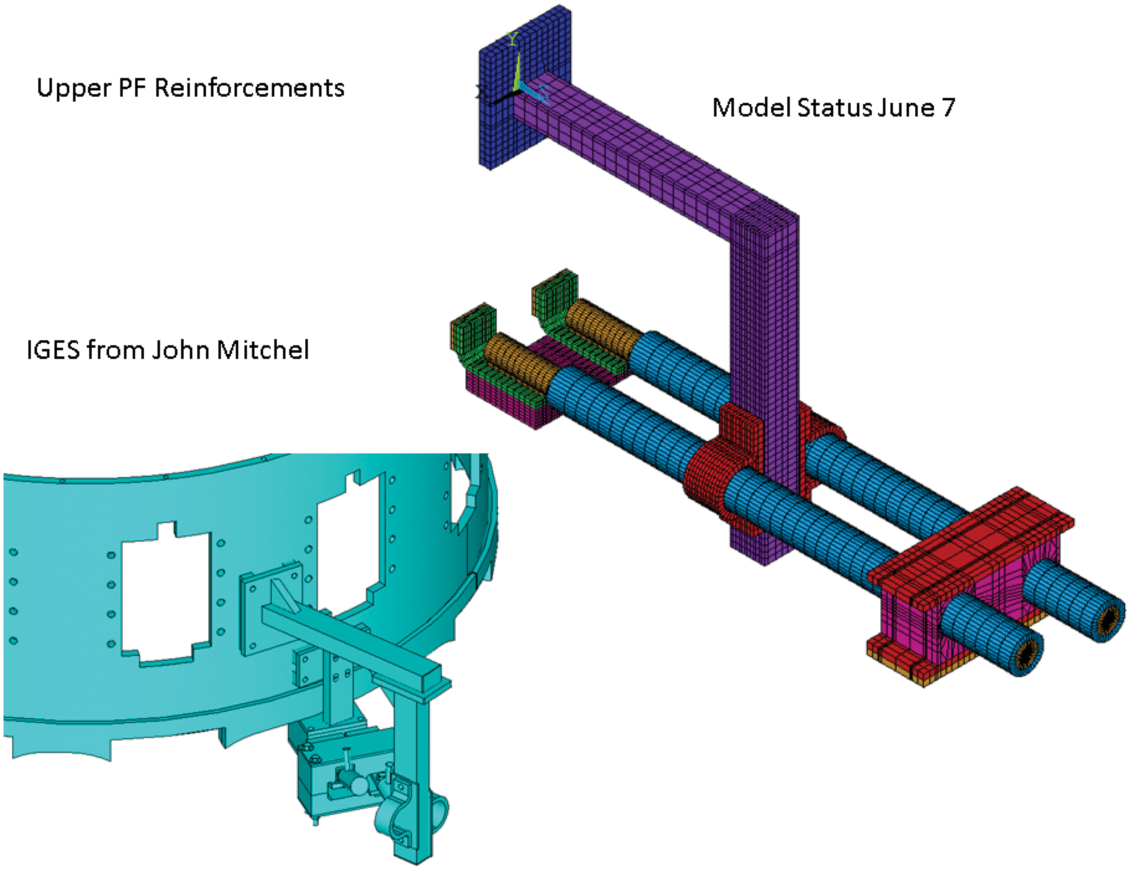

Figure 7.1-1 Model of NSTX PF 2, 3, 4, 5 Break-Out and Cables Up to the First Support

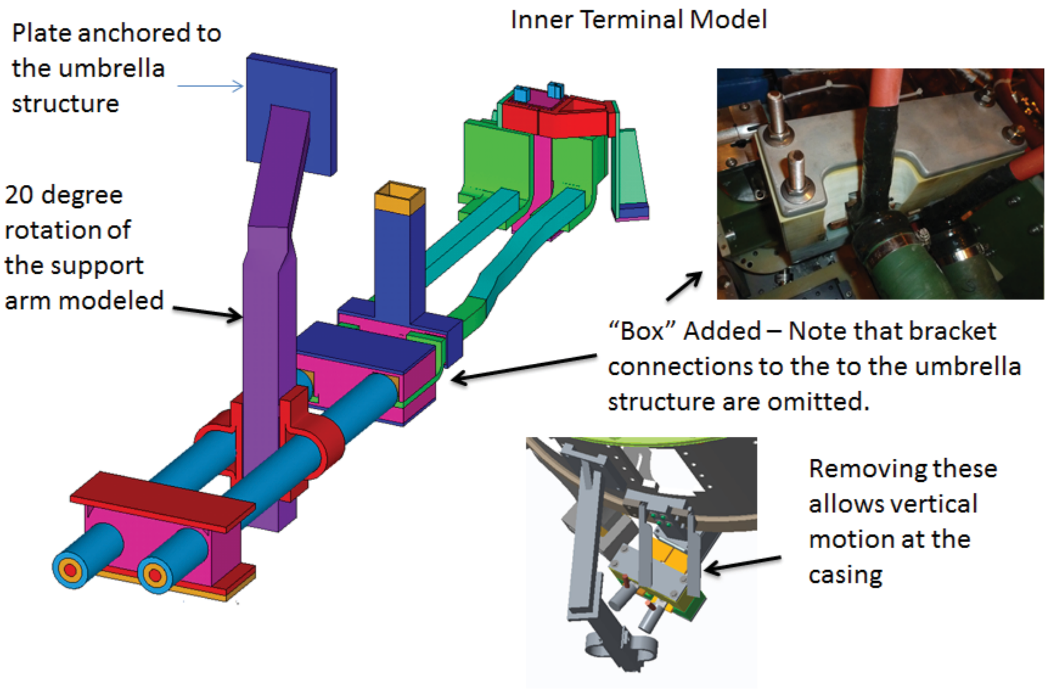

Figure 7.1-2 Model of NSTX PF 2 ,3, 4, 5 Break-Out and Cables Up to the First Support

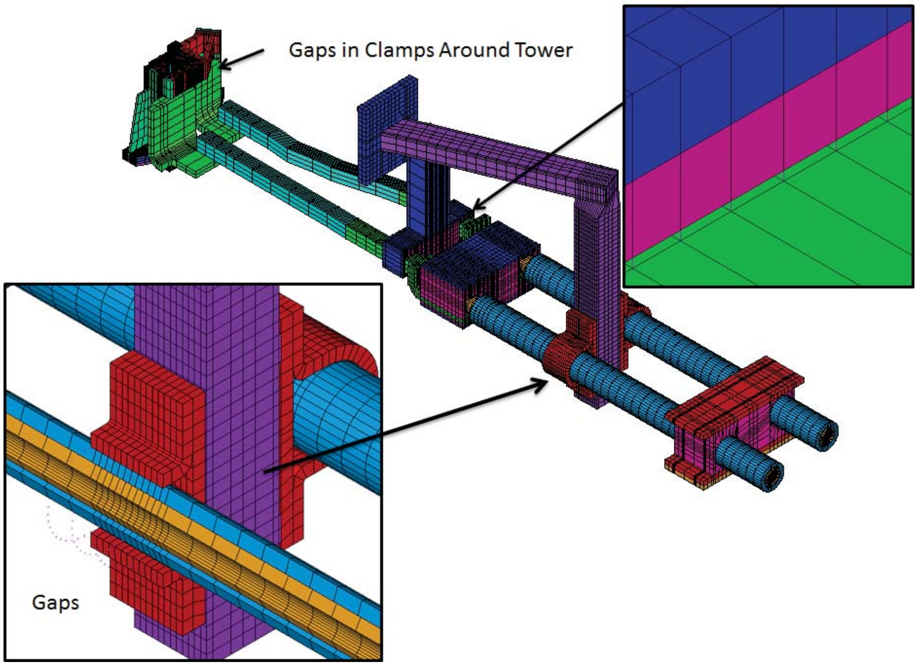

Figure 7.1-3 Location of Gap Elements

The model is multiply non-linear. It has sliding gap elements, elastic-plastic copper properties and a large displacement solution.

7.2 PF1a Lower Model

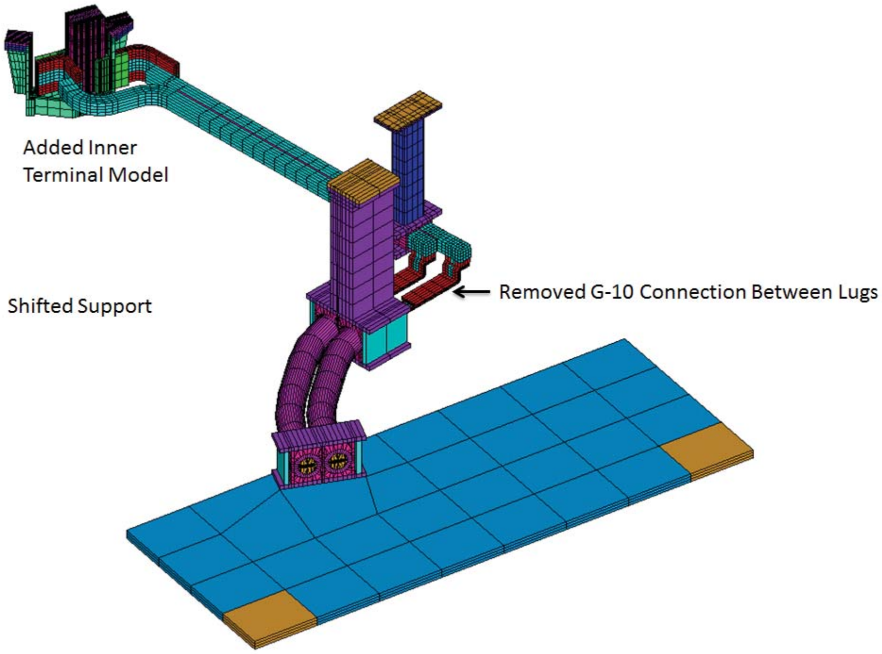

Figure 7.2-1 Model of NSTX PF1a Lower Solid and Flex Bus Supports

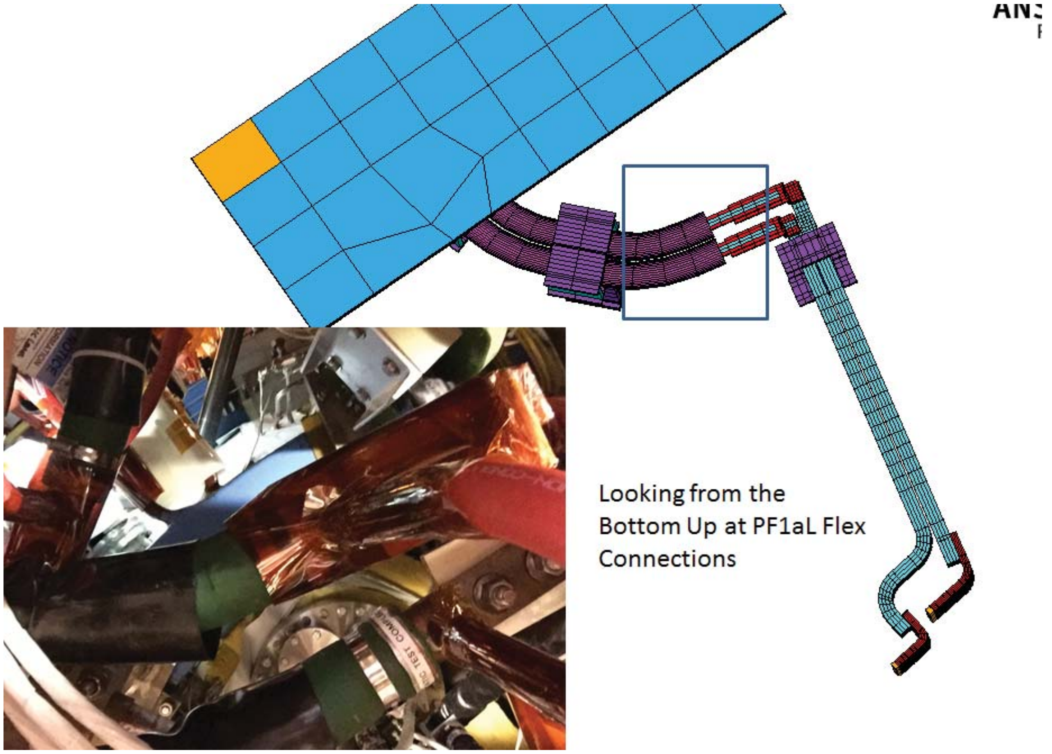

Figure 7.2-2 PF1a Lower Looking Up at the Flex Cables Before the Supports Were Added, along with the Model with from a similar View Angle – Looking up

7.3 Inner Terminal Model

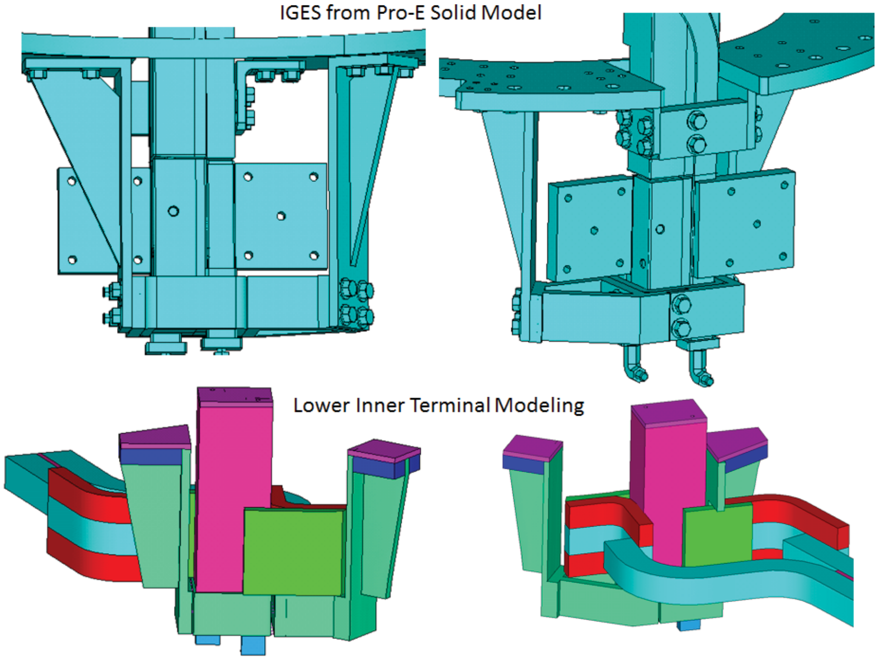

Figure 7.3-1 Model of NSTX PF1a Lower Inner Terminal and Connection to Solid Bus Bar Flags

8.0 Conductor Cooling Calculations

A simple rule of thumb may be used for initial sizing of the bus bar:

Air-cooled Bus Bar	1 kA/in^2
Water cooled Bus Bar	10 kA/in^2

The PF1a peak current is 19 kA which yields a current density of 19000/1.5/1.5 = 8.4 kA/in^2. So the solid bus is not sized for steady state air cooled bus service. The Joule heating of the PF1a solid bus was analyzed in Reference [12] by Andrei Khodak and the temperature distribution is shown in Figure 8.0-1. The flex cables used for PF1a are water cooled and are selected (by others) to meet the joule heating requirements of their currents.

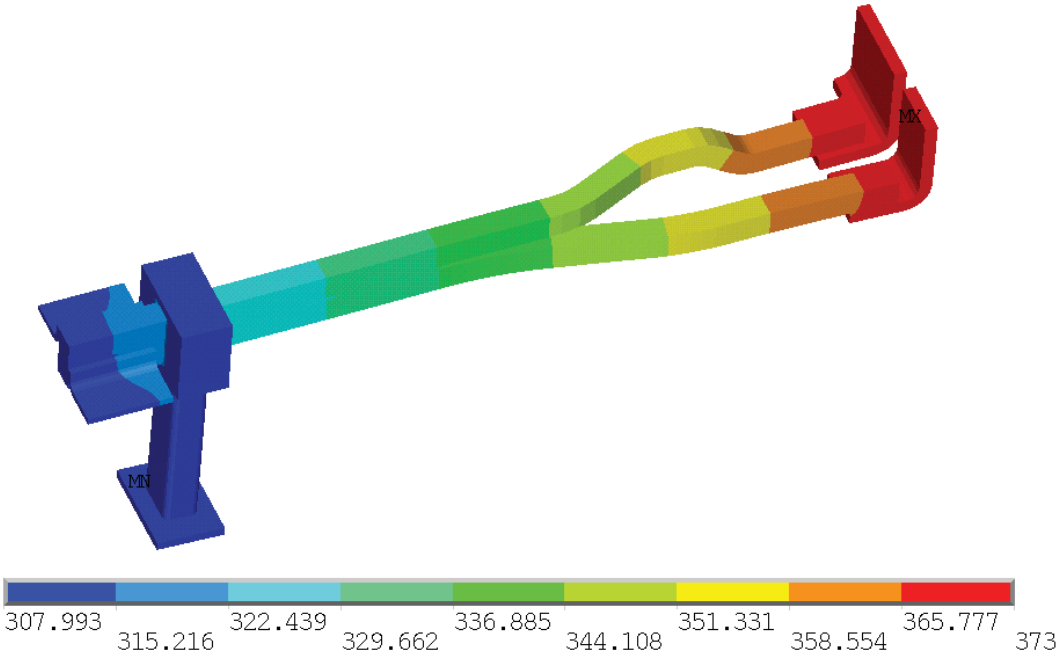

Figure 8.0-1 Temperature Distribution from Joule Heat of PF1a Upper Solid Air Cooled Bus [12]

The temperatures shown in figure 8.0-1 are for PF1a Upper and are before the solid conductor was shortened. The temperature will go down for the shorter bus which puts more of the copper close to the water cooled flexbus. PF1a Lower should be similar to what is shown. For the thermal expansion evaluation, a 50C differential appears representative.

9.0 Fields and Forces

9.1 Max Currents for PF1a Upper and Lower for Lorentz Force Calculations

For many of the NSTX calculations, EQ 79 is used as the most limiting. This results from global torque assessments for which EQ 79 is the largest. It is not clear if that is the worst for the PF1a upper and lower. The worst, or the maximum current from the design point spreadsheet [2], is 19 kA. This was used in developing the Lorentz forces to apply on the structural model. Stress reversals are a concern for the elastic-plastic response of the lugs. In Figure 9.1.1, the 96 equilibria currents are plotted. Some equilibria have negative currents. These are only 7.161 kA vs. the 19 kA that was used in developing the loading on the finite element models. Stefan Gerhardt presented results plotted in figure 9.1-2 that showed no reversal of the PF1a currents in early operation.

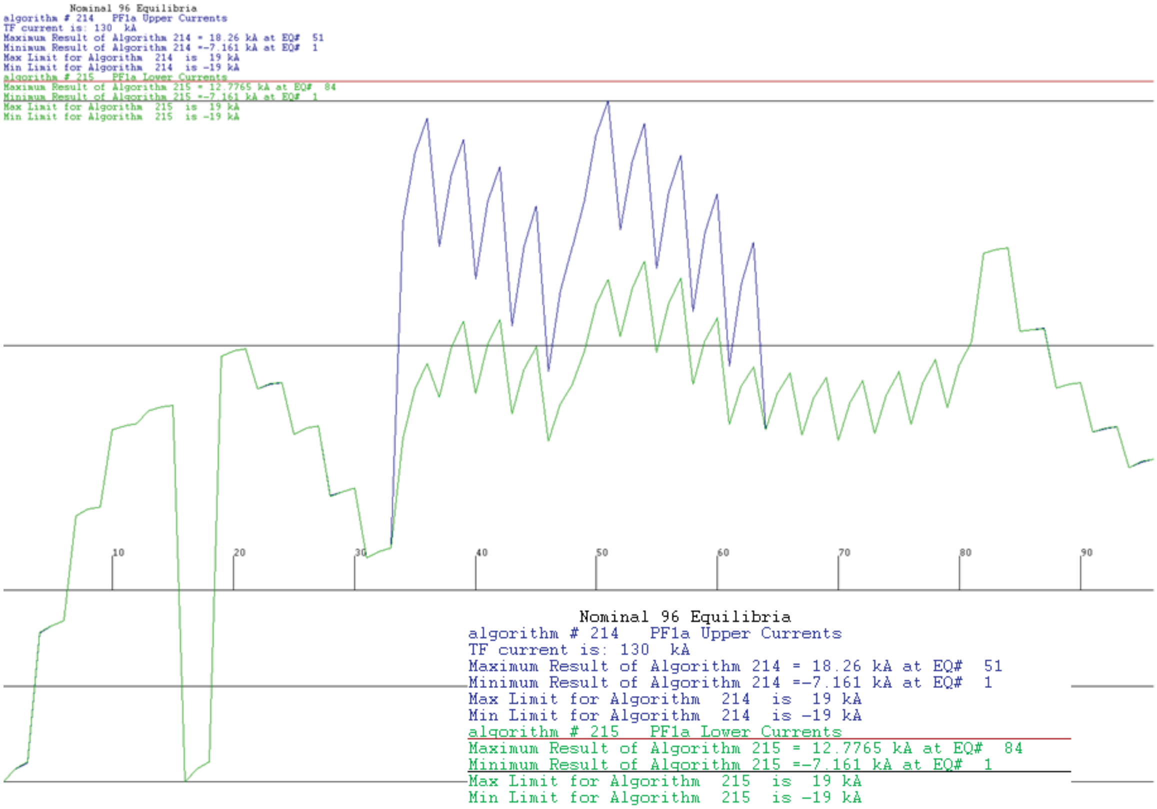

Figure 9.1-1 “DCPS” Algorithm Plotting the 96 Design Equilibrium Currents

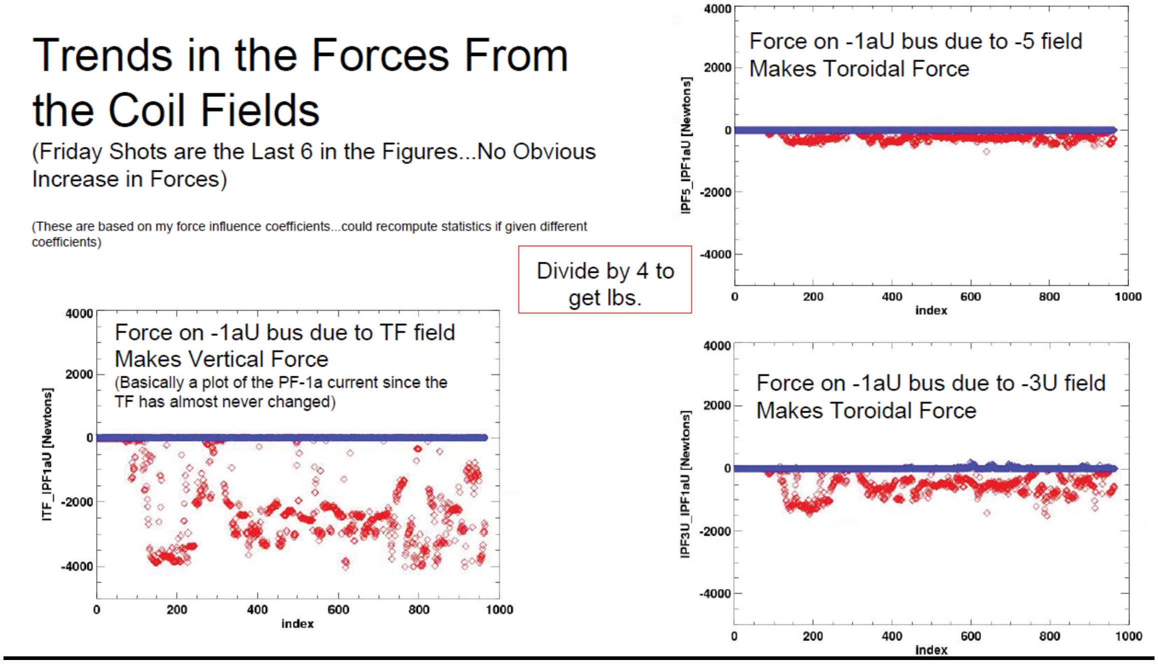

Trends in the Forces From the Coil Fields

(Friday Shots are the Last 6 in the Figures...No Obvious Increase in Forces)

(These are based on my force influence coefficients...could recompute statistics if given different coefficients)

Divide by 4 to get lbs.

Force on -1aU bus due to -5 field Makes Toroidal Force

Force on -1aU bus due to TF field Makes Vertical Force (Basically a plot of the PF-1a current since the TF has almost never changed)

Force on -1aU bus due to -3U field Makes Toroidal Force

Figure 9.1-2 Forces on the PF1a Upper Bus for Recent Operation, Ref [19]

9.2 Max Fields for PF 1a Lorentz Force Calculations

9.2.1 PF1a Max Fields

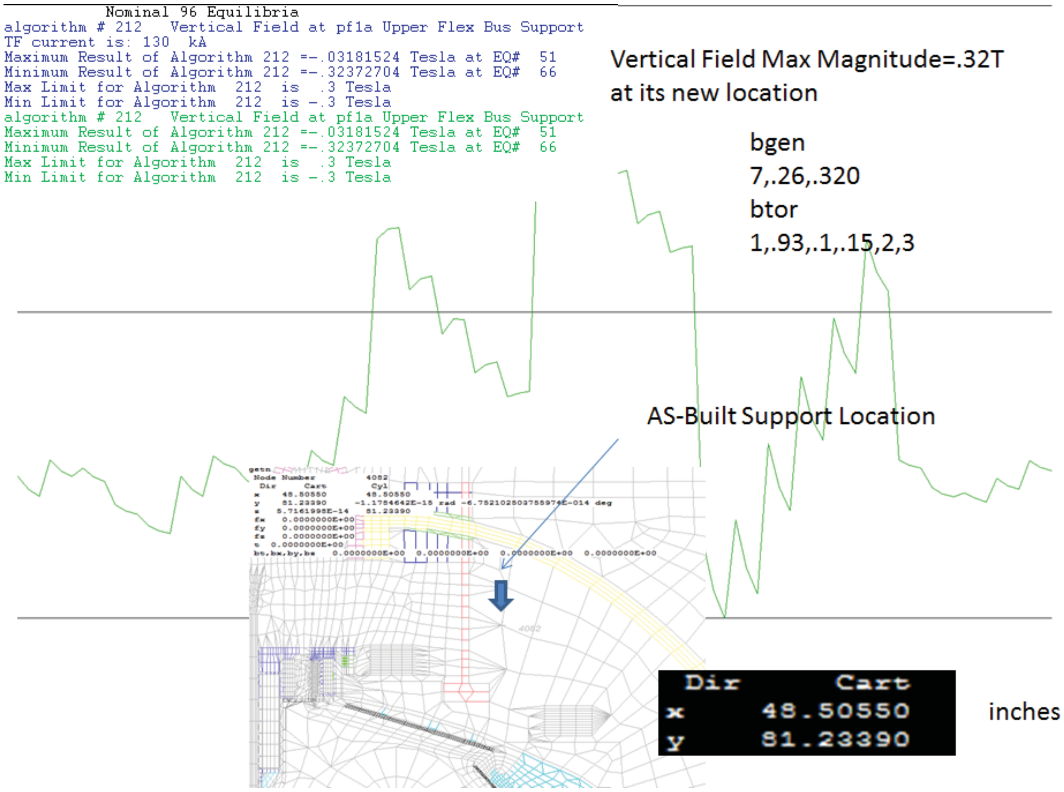

```
            Nominal 96 Equilibria
algorithm # 212   Vertical Field at pf1a Upper Flex Bus Support
TF current is: 130  kA
Maximum Result of Algorithm 212 =-.03181524 Tesla at EQ#  51
Minimum Result of Algorithm 212 =-.32372704 Tesla at EQ#  66
Max Limit for Algorithm  212  is  .3 Tesla
Min Limit for Algorithm  212  is -.3 Tesla
algorithm # 212   Vertical Field at pf1a Upper Flex Bus Support
Maximum Result of Algorithm 212 =-.03181524 Tesla at EQ#  51
Minimum Result of Algorithm 212 =-.32372704 Tesla at EQ#  66
Max Limit for Algorithm  212  is  .3 Tesla
Min Limit for Algorithm  212  is -.3 Tesla
```

Vertical Field Max Magnitude=.32T at its new location

bgen
7,.26,.320
btor
1,.93,.1,.15,2,3

AS-Built Support Location

```
getn
 Node Number          4082
  Dir      Cart        Cyl
 x    48.50550      48.50550
 y    81.23390    -1.1784642E-15 rad -6.752102503755974E-014 deg
 z   5.7161995E-14   81.23390
 fx   0.0000000E+00
 fy   0.0000000E+00
 fz   0.0000000E+00
 t  0.0000000E+00
 bt,bx,by,bz   0.0000000E+00  0.0000000E+00  0.0000000E+00  0.0000000E+00
```

```
Dir      Cart
x    48.50550
y    81.23390
```

inches

Figure 9.2-1 PF1a Vertical Field for all 96 EQ.

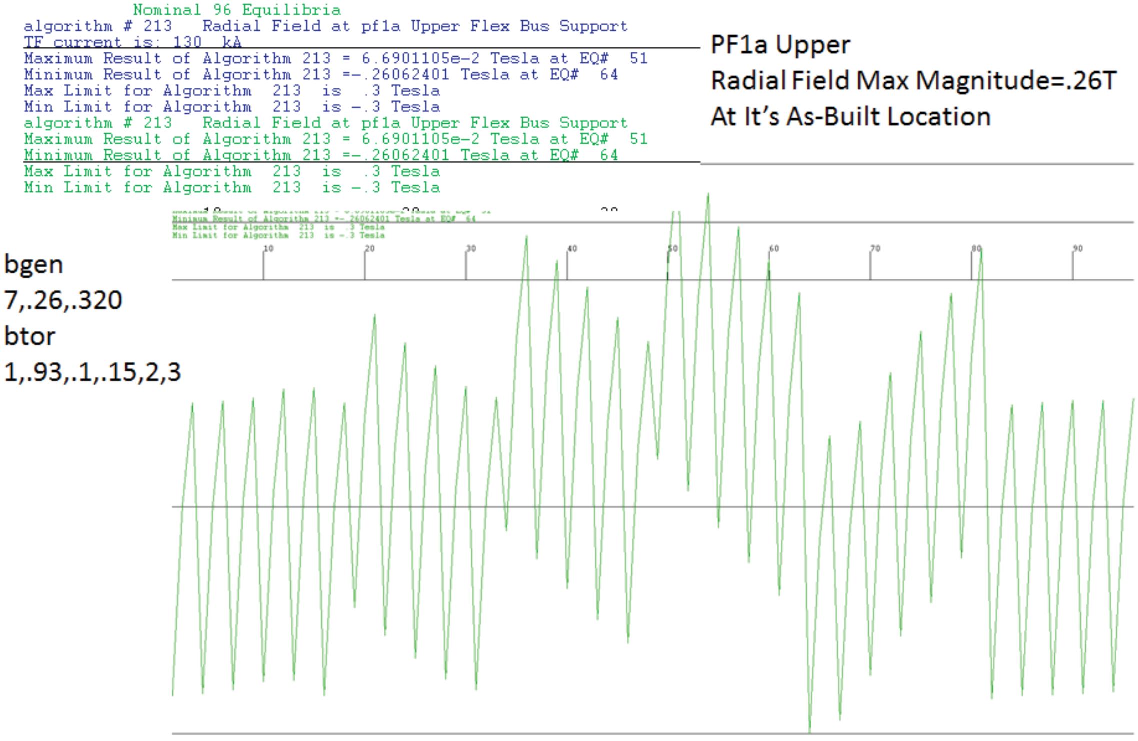

```
               Nominal 96 Equilibria
algorithm # 213   Radial Field at pf1a Upper Flex Bus Support
TF current is: 130  kA
Maximum Result of Algorithm 213 = 6.6901105e-2 Tesla at EQ#  51
Minimum Result of Algorithm 213 =-.26062401 Tesla at EQ#  64
Max Limit for Algorithm  213  is  .3 Tesla
Min Limit for Algorithm  213  is -.3 Tesla
algorithm # 213   Radial Field at pf1a Upper Flex Bus Support
Maximum Result of Algorithm 213 = 6.6901105e-2 Tesla at EQ#  51
Minimum Result of Algorithm 213 =-.26062401 Tesla at EQ#  64
Max Limit for Algorithm  213  is  .3 Tesla
Min Limit for Algorithm  213  is -.3 Tesla
```

Minimum Result of Algorithm 213 =-.26062401 Tesla at EQ# 64
Max Limit for Algorithm 213 is .3 Tesla
Min Limit for Algorithm 213 is -.3 Tesla

PF1a Upper
Radial Field Max Magnitude=.26T
At It's As-Built Location

bgen
7,.26,.320
btor
1,.93,.1,.15,2,3

Figure 9.2-2 PF1a Radial Field for all 96 EQ.

```
let an=212
let algor$(an)="Vertical Field at pf1a Upper Flex Bus Support"
let algunits$(an)="Tesla"
let algaccept(an)=.3
let algNegAccept(an)=-.3
let fine=20
let numpfs=15
let x=1.23
let y=2.06
for j=1 to 96
call sfield(fine,nmax,numpfs,NomCurrents(,),numturns(),j,pfr(),pfz(),pfdr(),pfdz(),nx(),ny(),x,y,bx,by)
let algresults(an,j)= by
next j

let an=213
let algor$(an)="Radial Field at pf1a Upper Flex Bus Support"
let algunits$(an)="Tesla"
let algaccept(an)=.3
let algNegAccept(an)=-.3
let fine=20
let numpfs=15
let x=1.23
let y=2.06
for j=1 to 96
call sfield(fine,nmax,numpfs,NomCurrents(,),numturns(),j,pfr(),pfz(),pfdr(),pfdz(),nx(),ny(),x,y,bx,by)
let algresults(an,j)= bx
next j
```

The Fields applied to the model are:

```
bgen
bgen
1,.26,-.32,0
btor
1,.93,.1,.15,2,3
```

9.3 Max Loading for the 96 Equilibrium

This analysis was used in the initial sizing of the hardware and initially produced loding somewhat below estimates by Stefan Gerhardt. This was because the flex bus was assumed to start where originally intended. In Figure 9.3-1 below, the loading is based on the actial bus location of PF1a Upper and Lower.

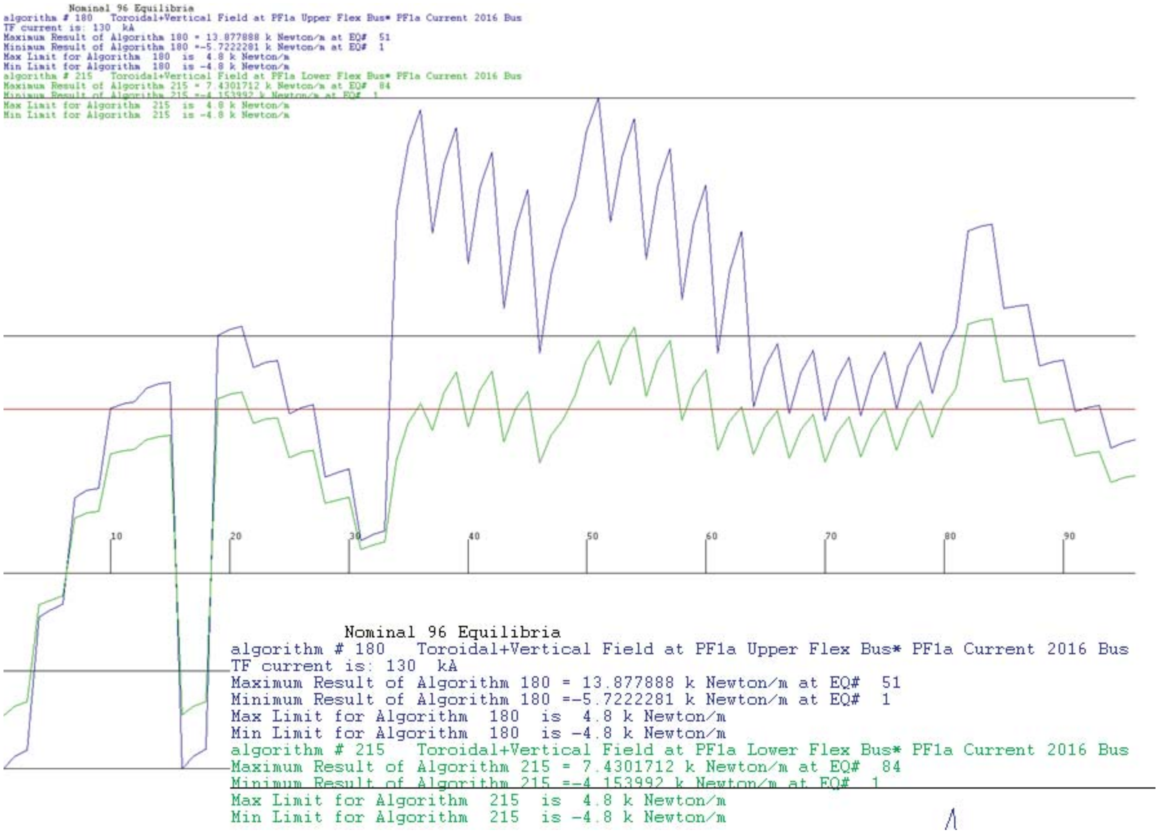

```
            Nominal 96 Equilibria
algorithm # 180   Toroidal+Vertical Field at PF1a Upper Flex Bus* PF1a Current 2016 Bus
TF current is: 130  kA
Maximum Result of Algorithm 180 = 13.877888 k Newton/m at EQ#  51
Minimum Result of Algorithm 180 =-5.7222281 k Newton/m at EQ#  1
Max Limit for Algorithm  180  is  4.8 k Newton/m
Min Limit for Algorithm  180  is -4.8 k Newton/m
algorithm # 215   Toroidal+Vertical Field at PF1a Lower Flex Bus* PF1a Current 2016 Bus
Maximum Result of Algorithm 215 = 7.4301712 k Newton/m at EQ#  84
Minimum Result of Algorithm 215 =-4.153992 k Newton/m at EQ#  1
Max Limit for Algorithm  215  is  4.8 k Newton/m
Min Limit for Algorithm  215  is -4.8 k Newton/m
```

Figure 9.3-1 “DCPS” Algorithm Results for the PF1a Upper and Lower Currents multiplied by the Local Poloidal andf Toroidal Field

Max Inner PF Flex Bus Loads for 96 EQ

PF1a U (2016 Bus)	13.9 kN/m	952 Lb/ft
PF1bU	6.6kN/m	452 Lb/ft
PF1cU	8.07 kN/m	552 Lb/ft
PF1aL	6.5kN/m	445 Lb/ft
PF1bL	7.4 kN/m	507 Lb/ft
PF1cL	8.07kN/m	552 Lb/ft

Figure 9.3-2 Loading Summary for all 6 inner PF Coils

Note that the PF1a Lower loadinng is 445/952 = 47 % of the PF1a Upper loading. This is largely the consequence of the larger TF field at the end of the solid bus.

Figure 9.3-3

9.4 Lorentz Forces Applied to the Finite Element Model

The mesh generation and calculation of the Lorentz forces is done outside of ANSYS using a code written by the author of this report. The mesh generation feature of the code is checked visually and within ANSYS during the PREP7 geometry check. But for the calculation of loads on the terminals and stress analysis of the terminals, a simpler model is used. Background fields are imposed and currents applied and the forces are computed by the cross product.

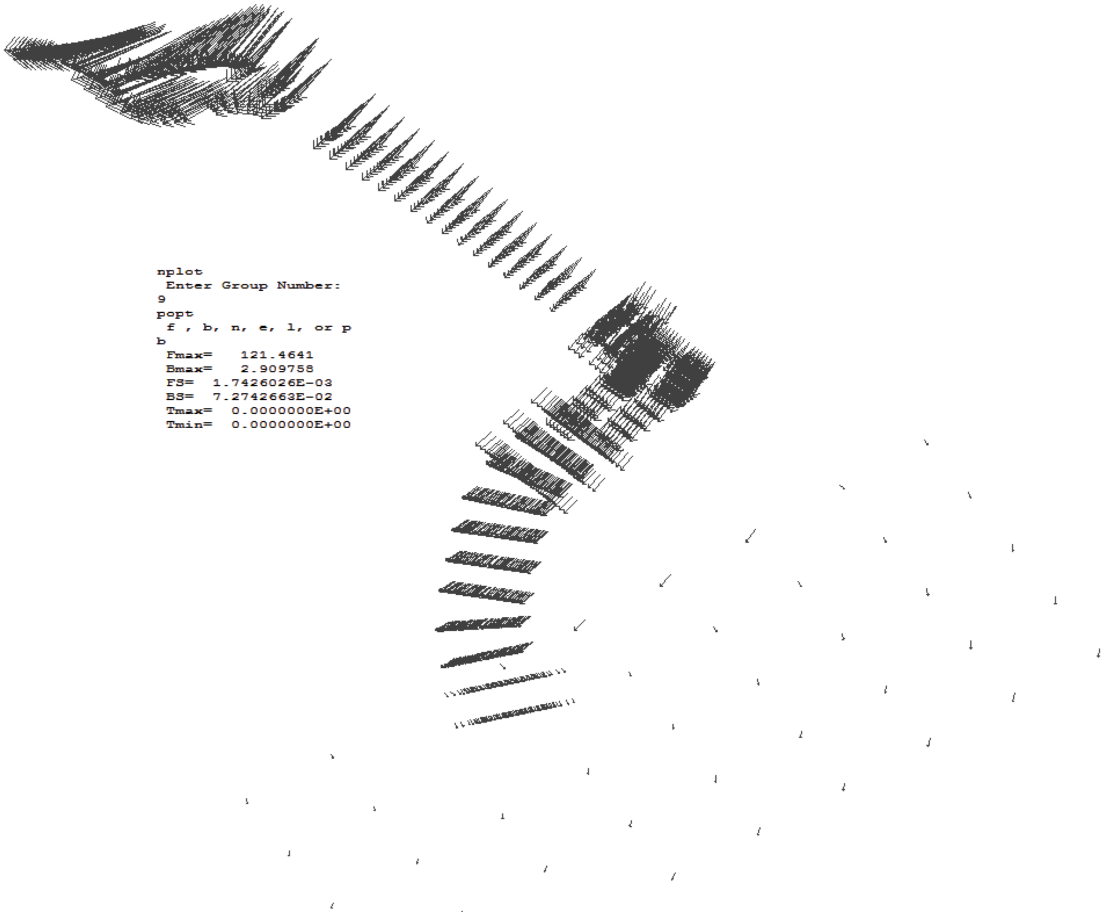

```
nplot
 Enter Group Number:
9
popt
 f , b, n, e, l, or p
b
 Fmax=    121.4641
 Bmax=    2.909758
 FS=  1.7426026E-03
 BS=  7.2742663E-02
 Tmax=  0.0000000E+00
 Tmin=  0.0000000E+00
```

Figure 9.4-1 PF1a Lower Fields on the Model Used to Calculate Lorentz Forces

Fields are applied to the model as background fields with the maximum poloidal fields from the “DCPS” analysis and a 1/r toroidal field distribution which is evident in Figure 9.4-1 above.

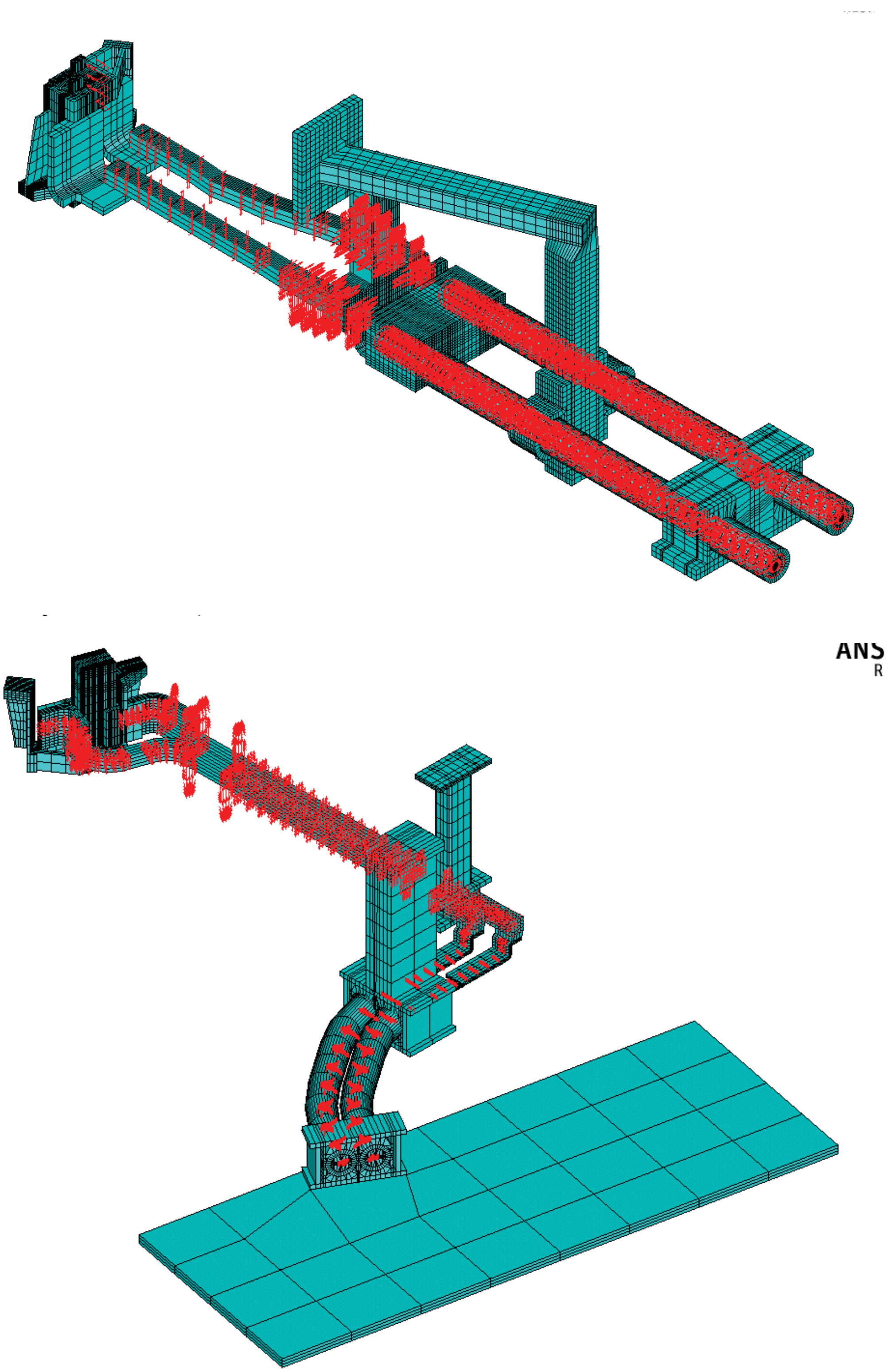

Figure 9.4-2 Lorentz Forces on the PF1a Lower Model

10.0 Simulation of the Flex Motion and Bent Lug Evaluation of Inner Terminal Supports – PF1aU

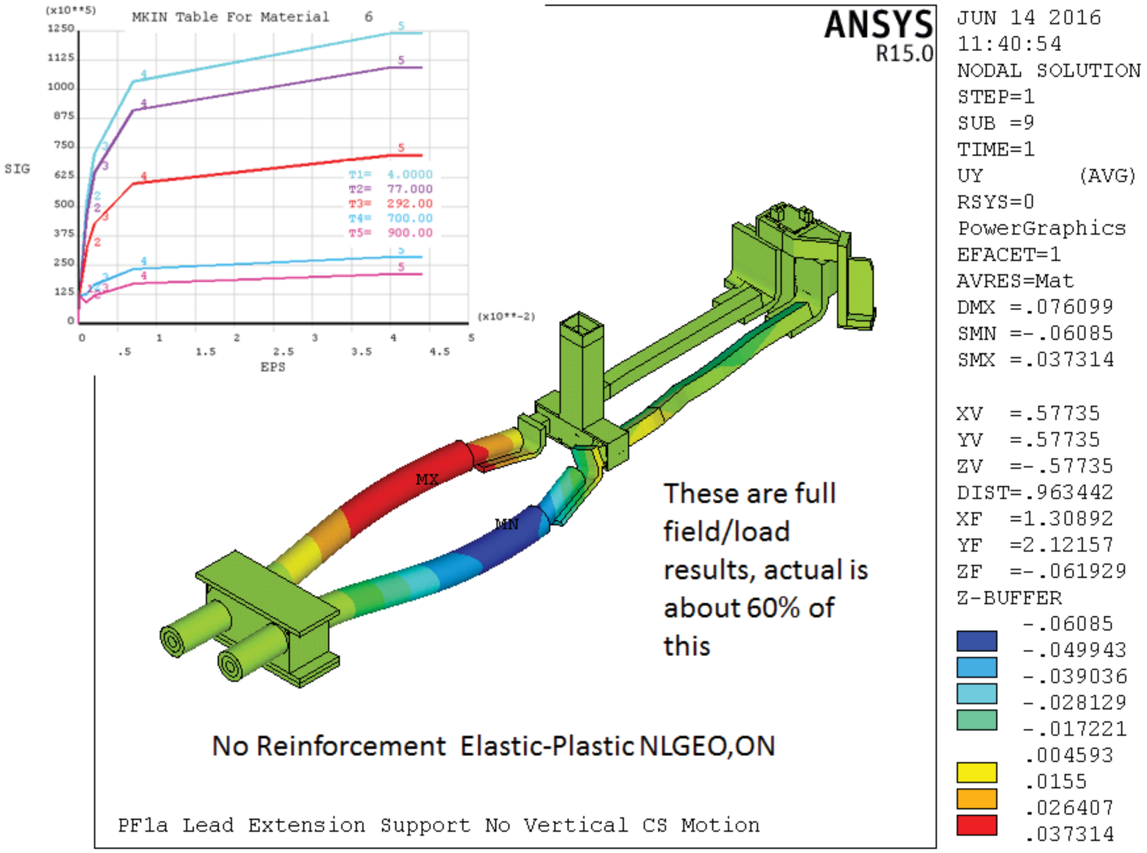

These are full field/load results, actual is about 60% of this

No Reinforcement Elastic-Plastic NLGEO,ON

Figure 10.0-1 Displacement of the Flex Cables without any Support

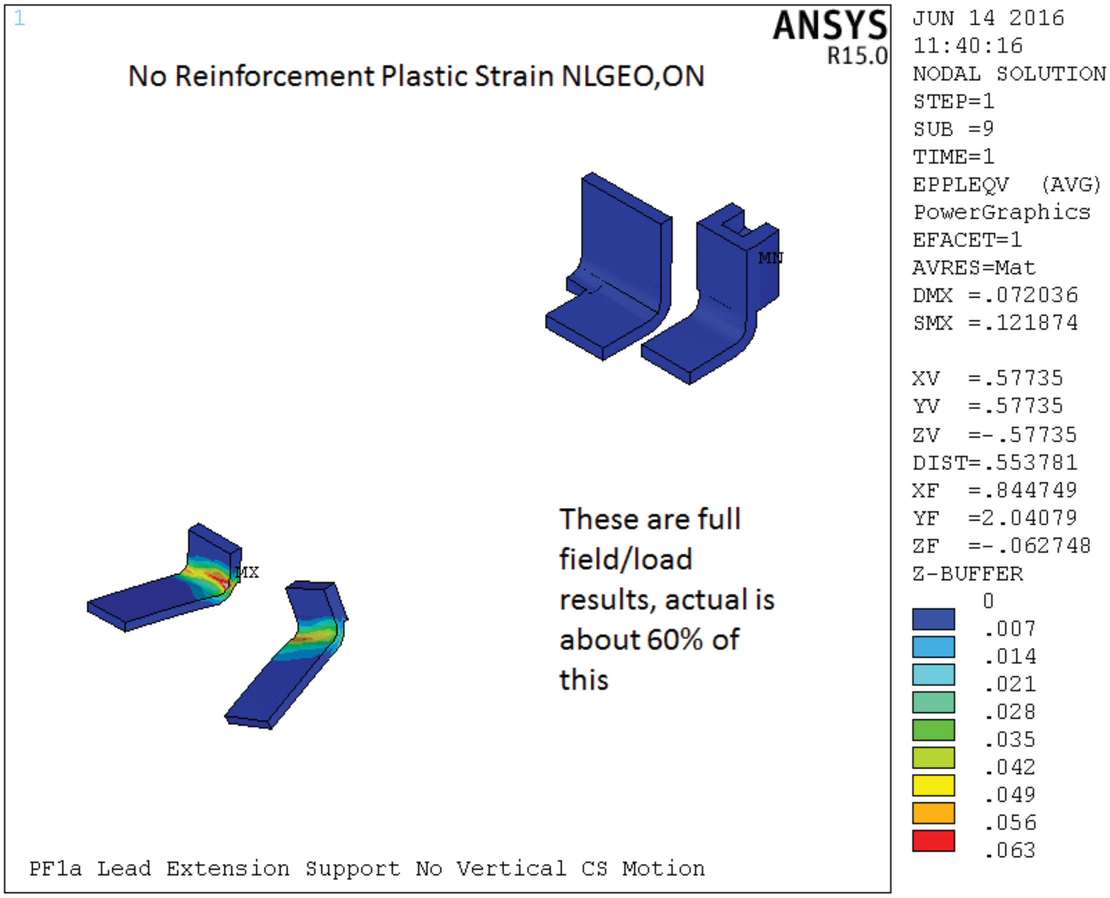

Figure 10.0-2 Plastic Strain in the Lugs

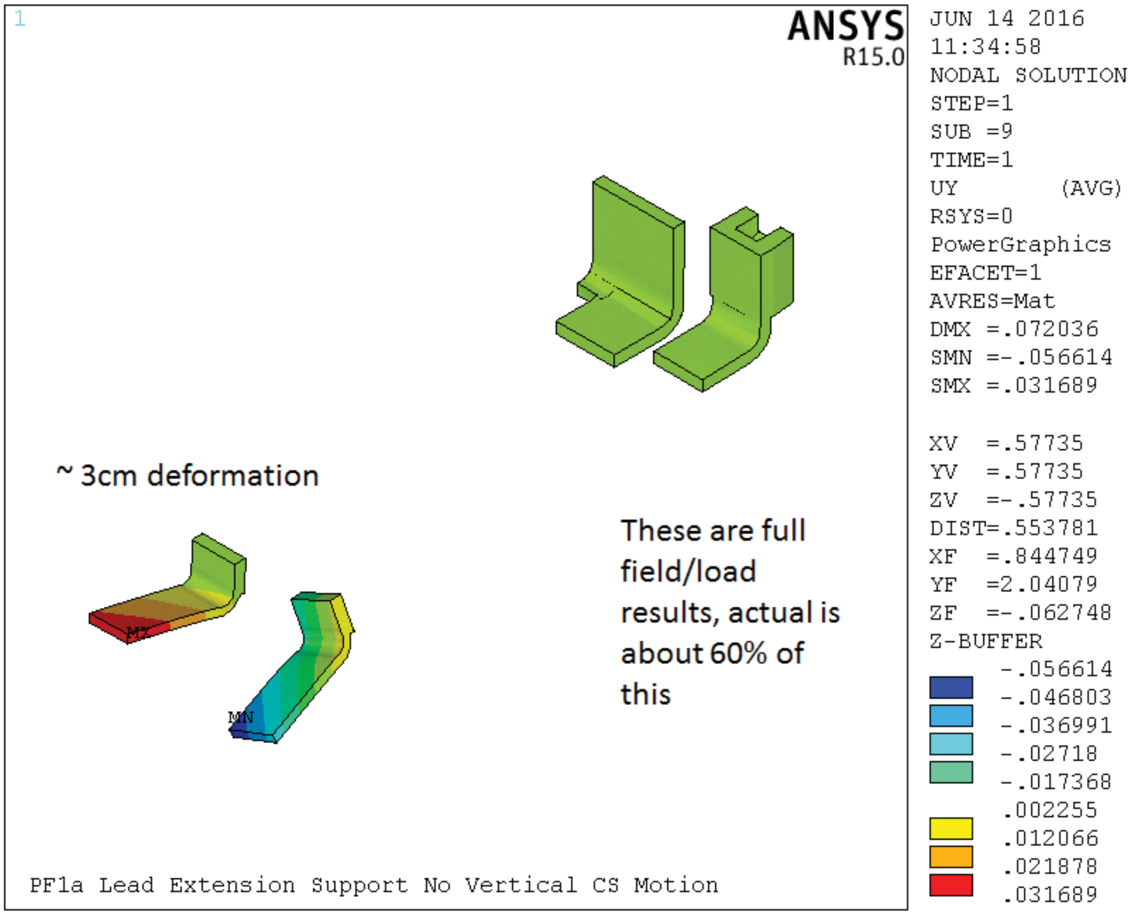

~ 3cm deformation

These are full field/load results, actual is about 60% of this

Figure 10.0-3 Deformation of the hard Bus Lugs

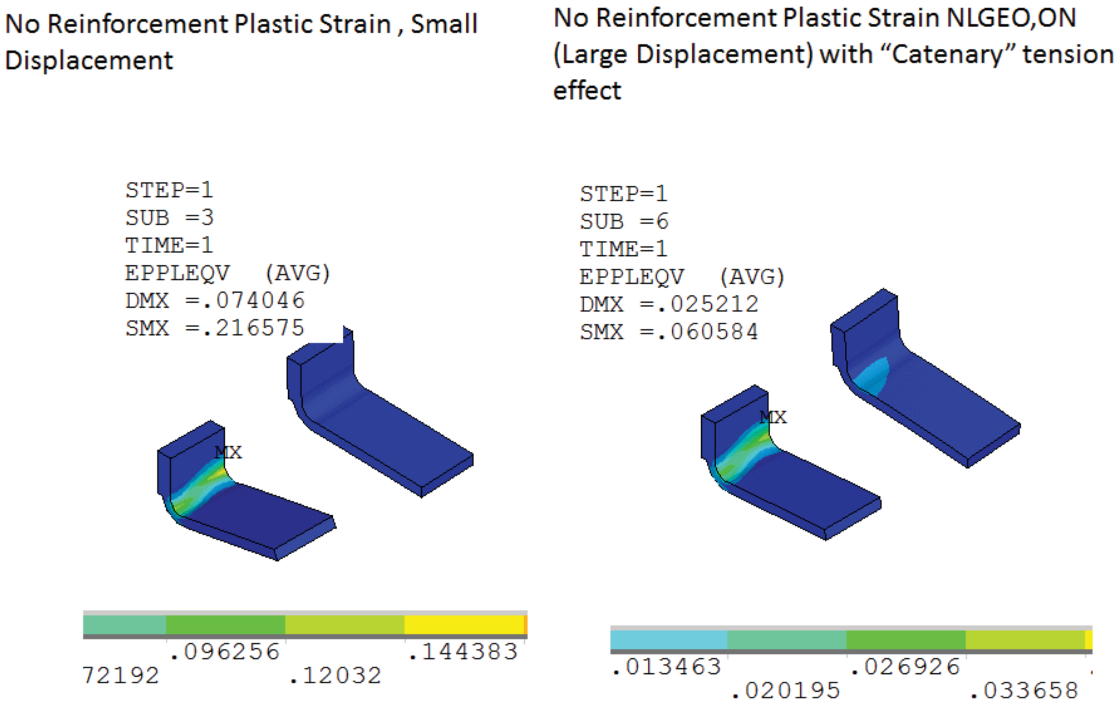
No Reinforcement Plastic Strain , Small Displacement

No Reinforcement Plastic Strain NLGEO,ON (Large Displacement) with “Catenary” tension effect

Figure 10.0-4 Effect of Large Displacement Analysis on the Amount of Plastic Strain

11.0 Evaluation of Inner Terminal Supports – PF1a U &L

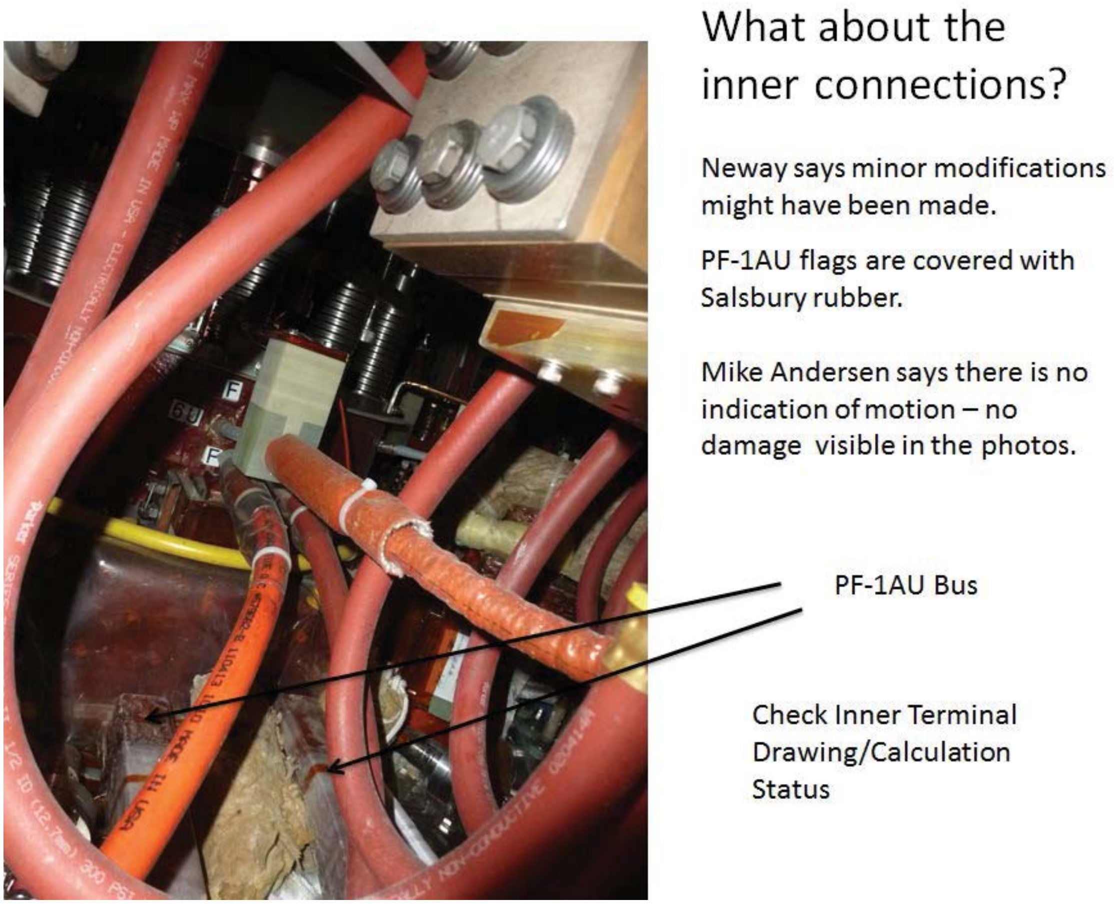

What about the inner connections?

Neway says minor modifications might have been made.

PF-1AU flags are covered with Salsbury rubber.

Mike Andersen says there is no indication of motion – no damage visible in the photos.

PF-1AU Bus

Check Inner Terminal Drawing/Calculation Status

Figure 11.0-1 Best Picture Currently Available of Inner PF1a Connection to the Terminal Tower

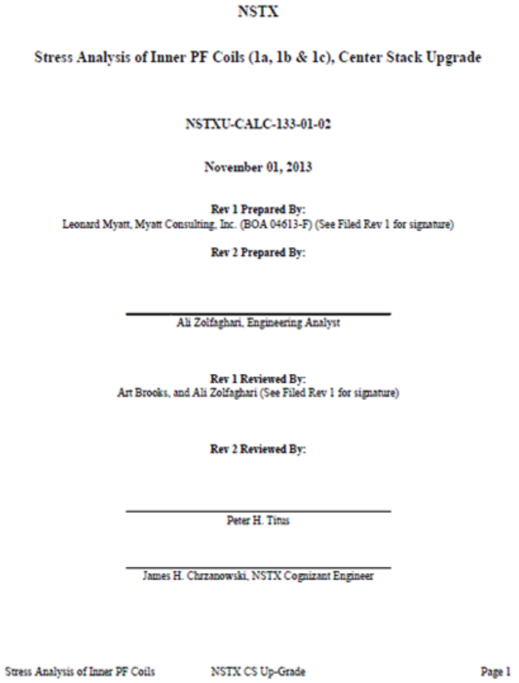

NSTX

Stress Analysis of Inner PF Coils (1a, 1b & 1c), Center Stack Upgrade

NSTXU-CALC-133-01-02

November 01, 2013

Rev 1 Prepared By:
Leonard Myatt, Myatt Consulting, Inc. (BOA 04613-F) (See Filed Rev 1 for signature)

Rev 2 Prepared By:

Ali Zolfaghari, Engineering Analyst

Rev 1 Reviewed By:
Art Brooks, and Ali Zolfaghari (See Filed Rev 1 for signature)

Rev 2 Reviewed By:

Peter H. Titus

James H. Chrzanowski, NSTX Cognizant Engineer

Stress Analysis of Inner PF Coils NSTX CS Up-Grade Page 1

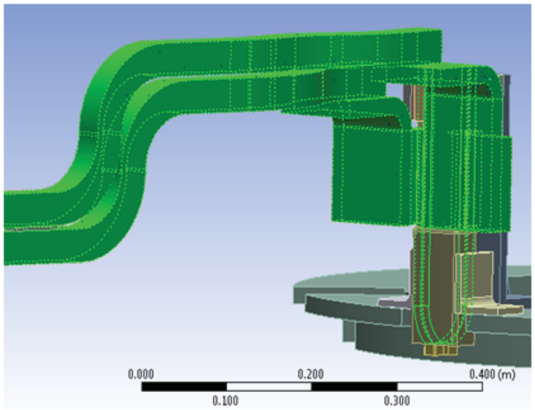

Figure 4.6-3 Geometry highlighting parts on which the EM force density from Maxwell is mapped.

Figure 11.0-2 NSTX Upgrade Calculation of Bus to Terminal Connection [9]

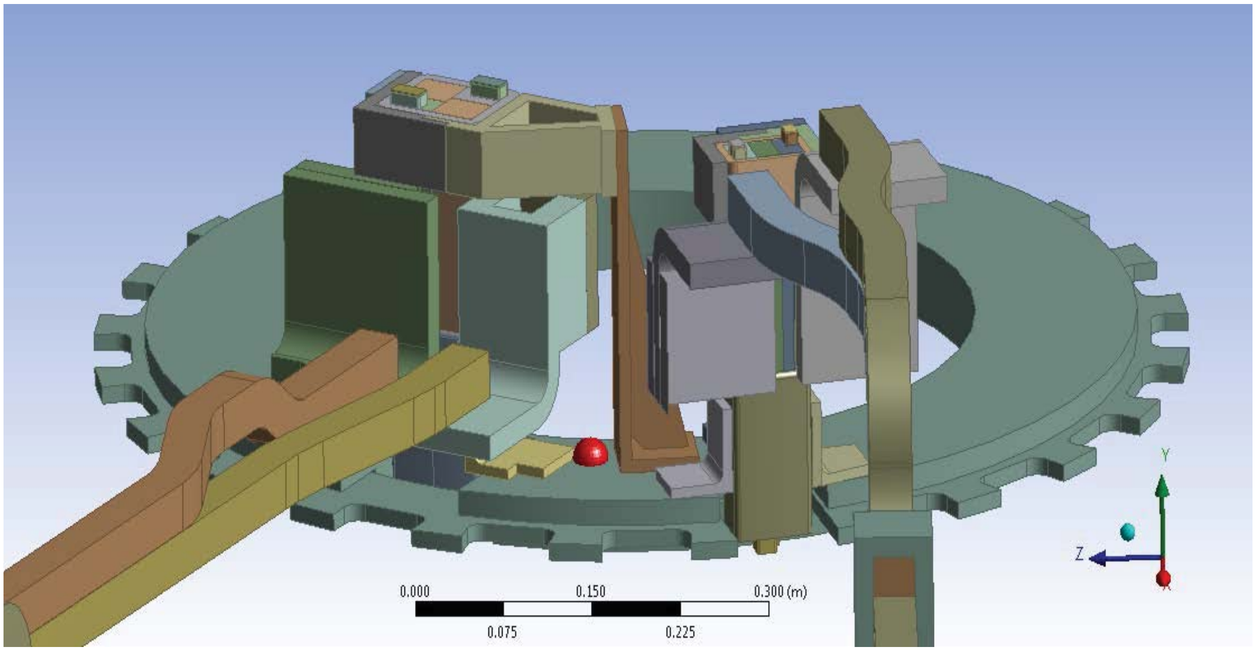

Figure 11.0-3 Solid Model of the Inner Terminal Connections (PF1a at Left) from [9]

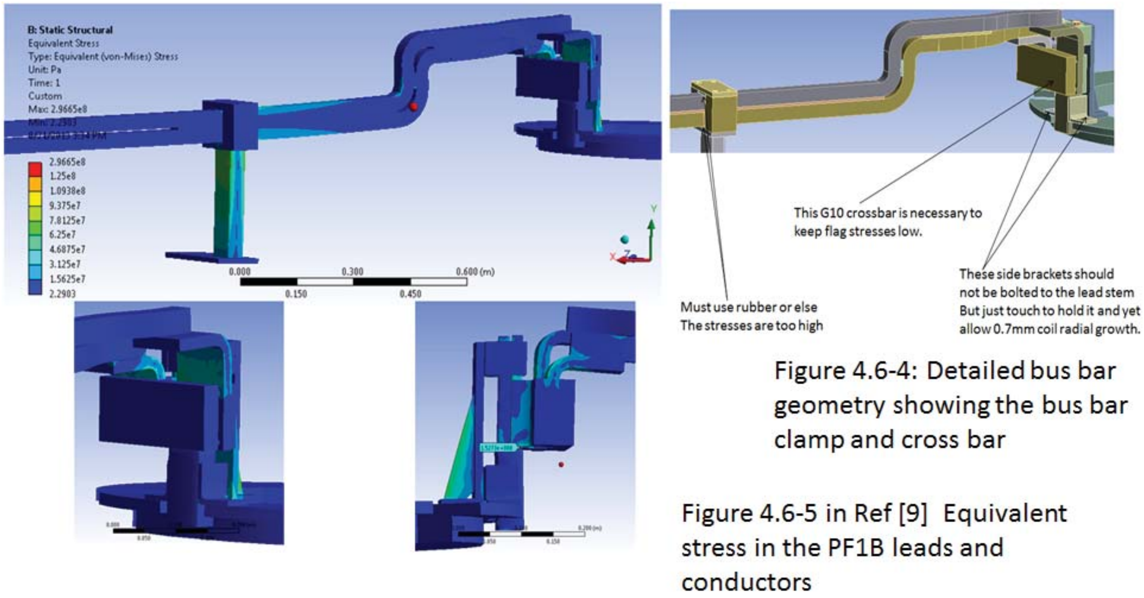

Figure 4.6-4: Detailed bus bar geometry showing the bus bar clamp and cross bar

Figure 4.6-5 in Ref [9] Equivalent stress in the PF1B leads and conductors

Figure 11.0-4 Some Stress Plots from [9]

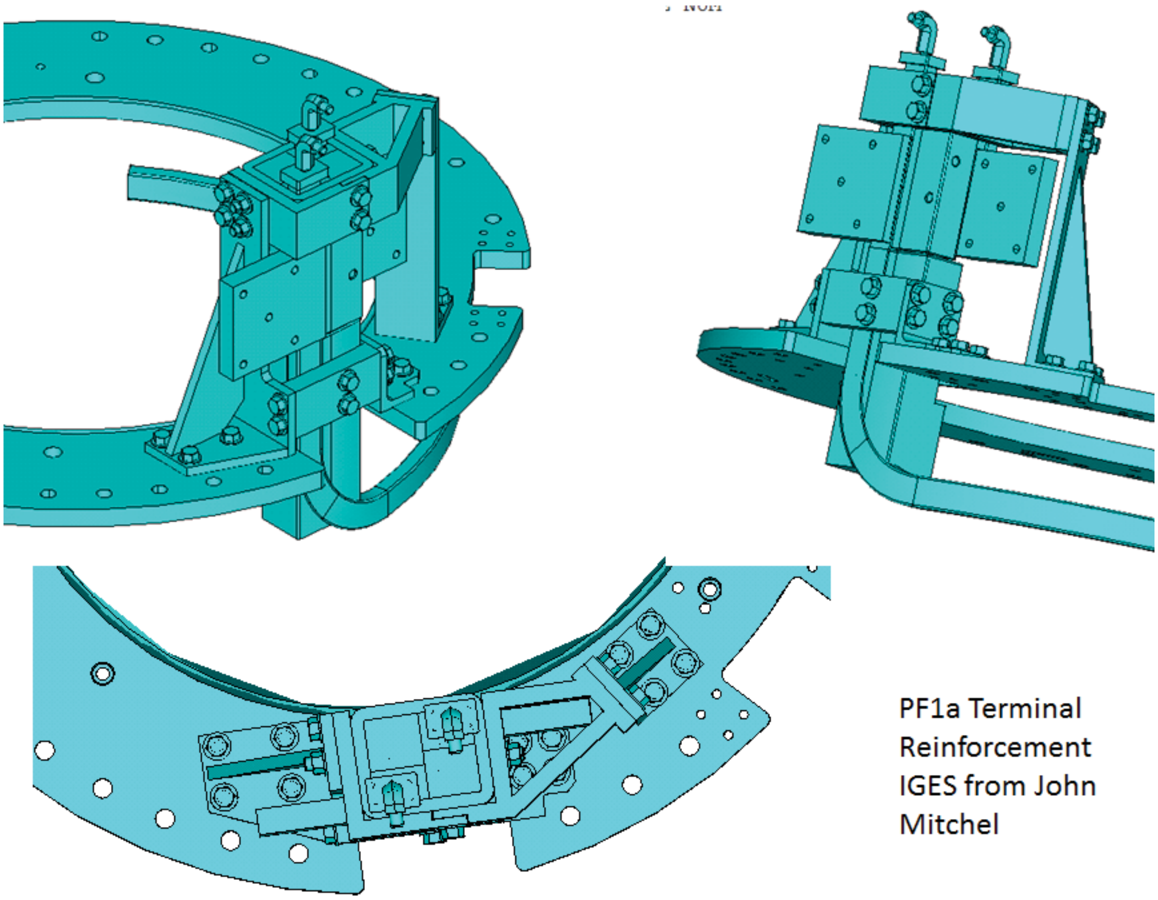

Figure 11.0-5 IGES Model from John Mitchel of the Current (June 2016) Status of the Pro-E Solid Model

The terminal reinforcements were constructed per the drawings and were not part of the field fit-up of the bus connections. The terminal reinforcements are as required by the calculations and are qualified. The modeling used in this calculation is intended to provide an appropriate boundary condition for the bus connections and evaluate centerstack casing expansion and not to substitute for the qualification provided by [9]. Solid Bus connections to the PF1a inner terminal are re-evaluated in this calculation to assess the acceptability of the modified bus and flex cable supports for the full 7 mm vertical expansion of the centerstack casing during high power long pulse shots. – See section 12.2.

12.0 Evaluation of Added Supports for PF1aU

12.1 With Added Supports – Lug Stress and Strain

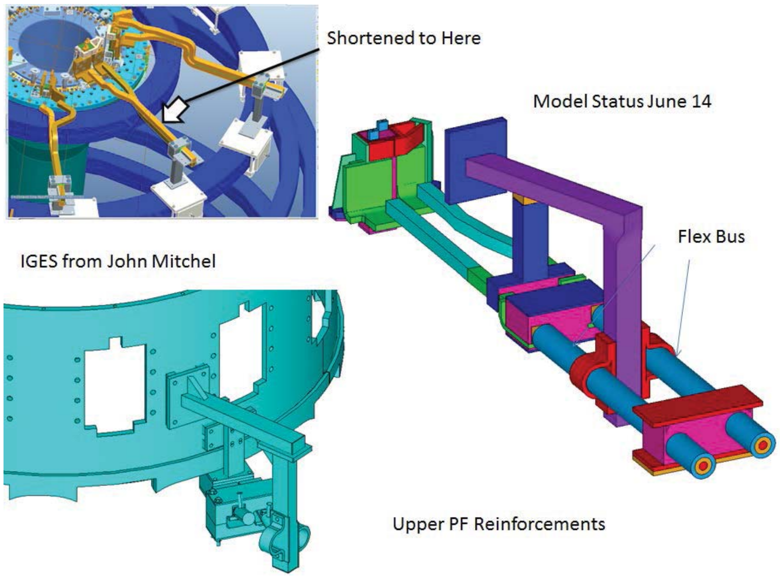

Figure 12.1-1 Model of the PF1a Bus Connection and Flex Bus Support

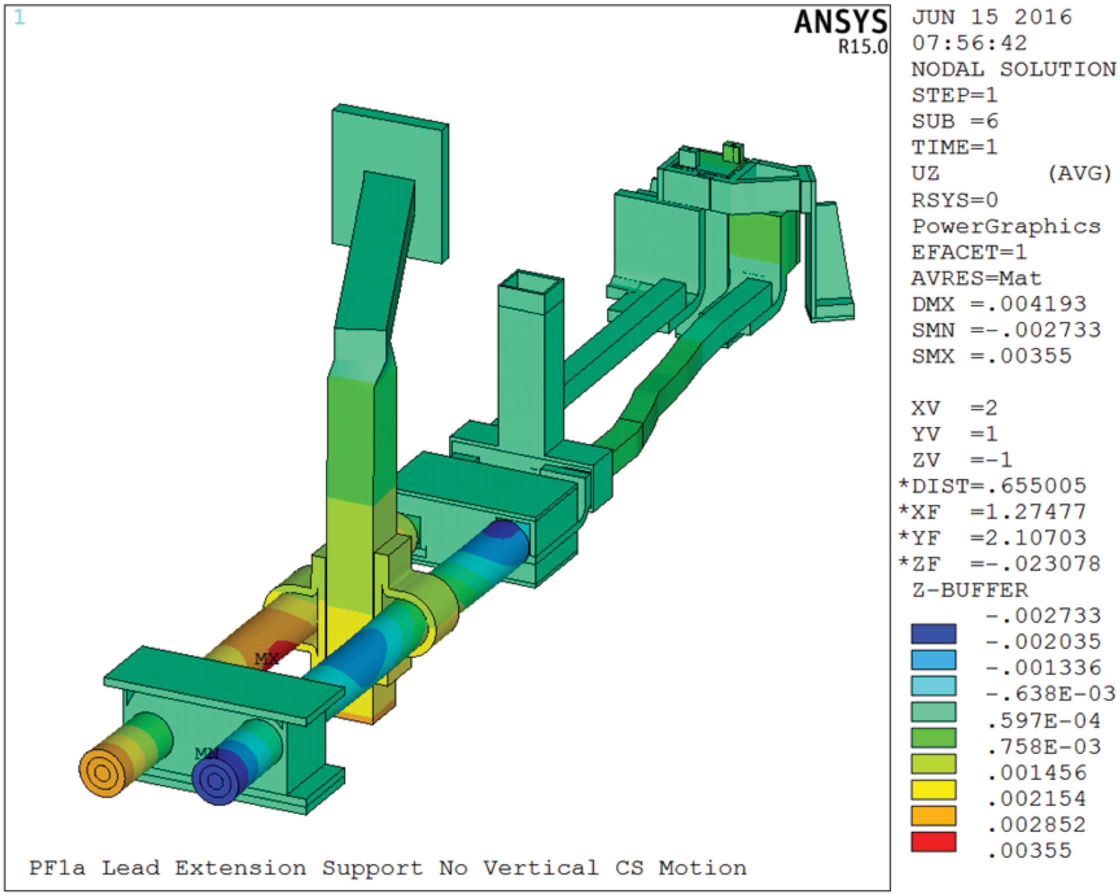

Figure 12.1-2 Displacement Results

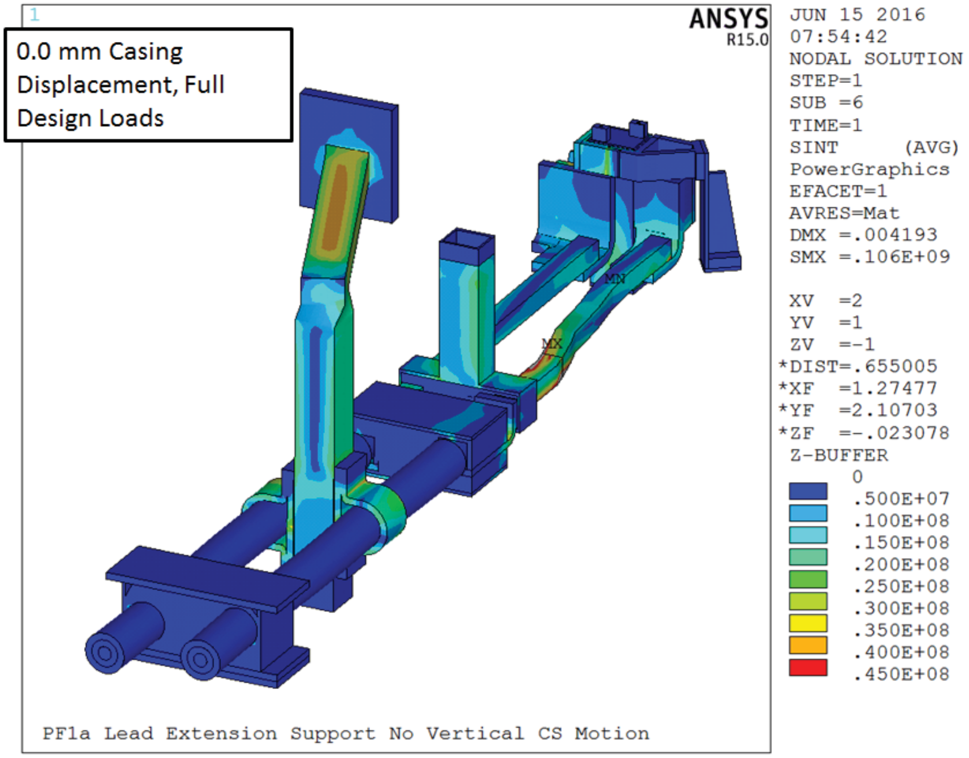

Figure 12.1-3 Stress Result

In the plot in figure 12.1-3, the stress contours are set to 45 MPa –max. This shows that in general the components are modestly stressed.

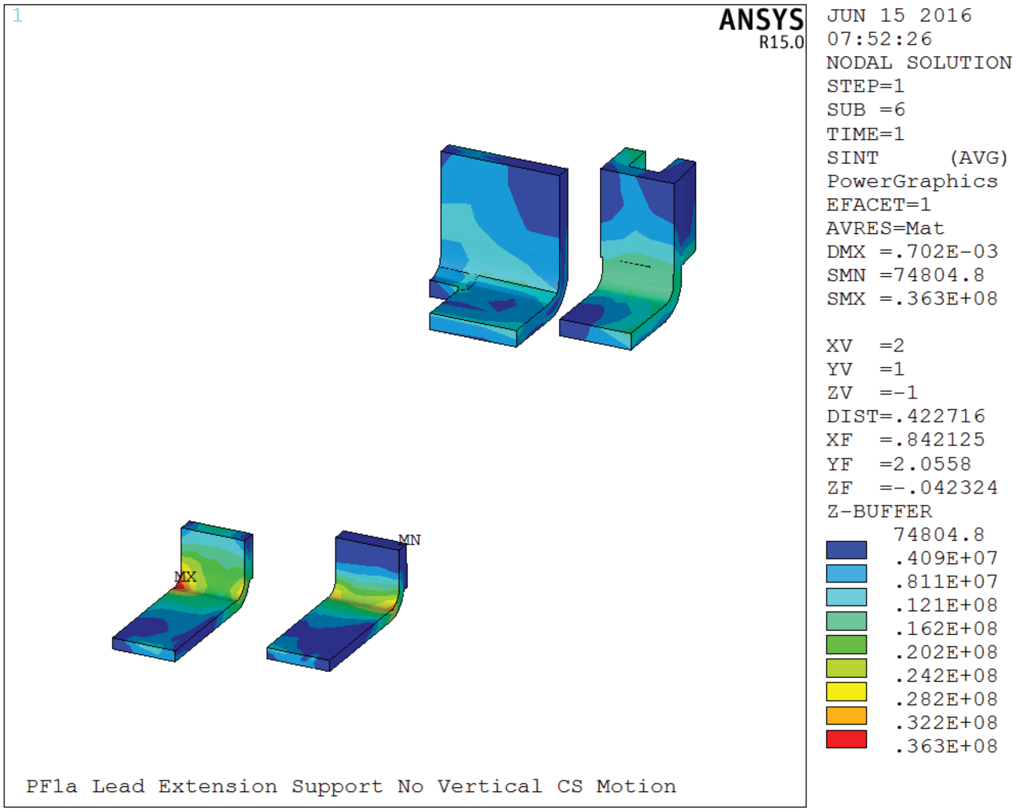

Figure 12.1-4 Tresca Stress in the Lugs

The lug Tresca stress is shown in Figure 12.1-4. The copper properties are modeled as elastic-plastic properties as shown in Section 6.4.1. Figure 12.1-5 shows the plastic strain for the fully loaded case.

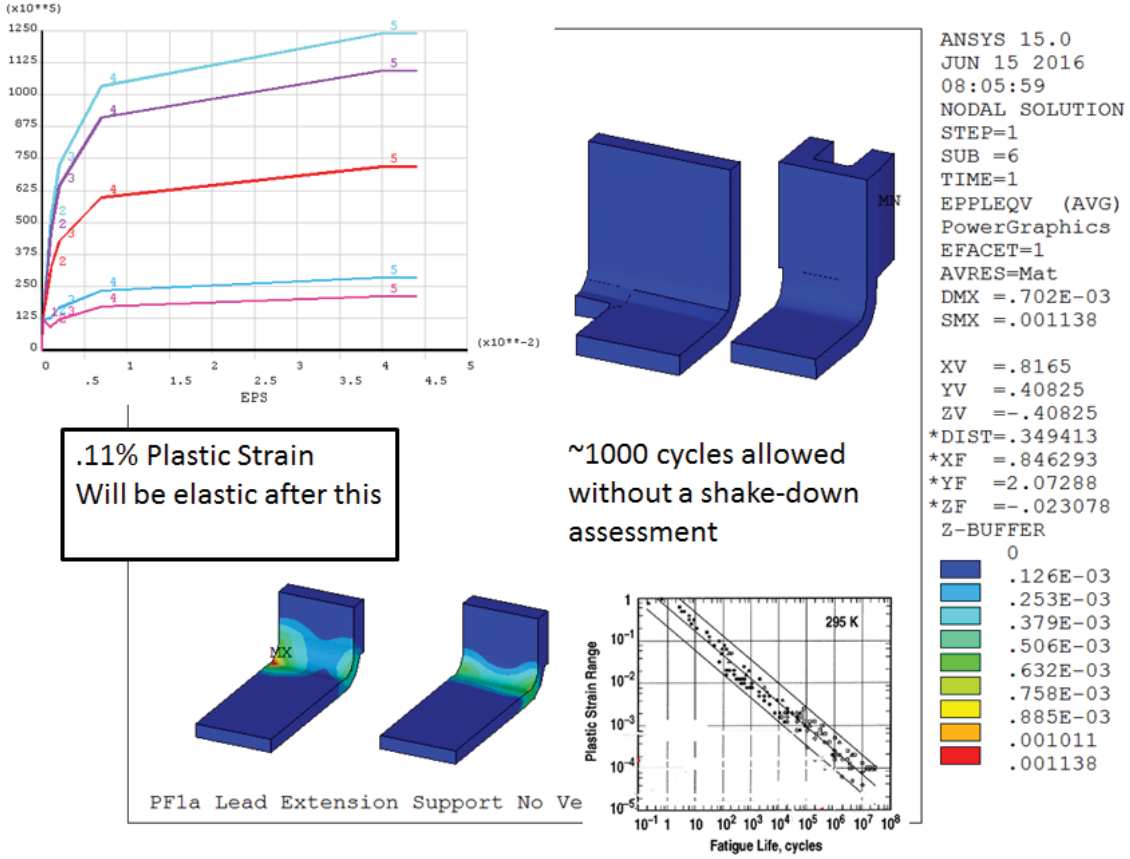

.11% Plastic Strain
Will be elastic after this

~1000 cycles allowed without a shake-down assessment

Figure 12.1.-4 PF1a Upper Lug Plastic Strain

12.2 Evaluation of Centerstack casing Expansion

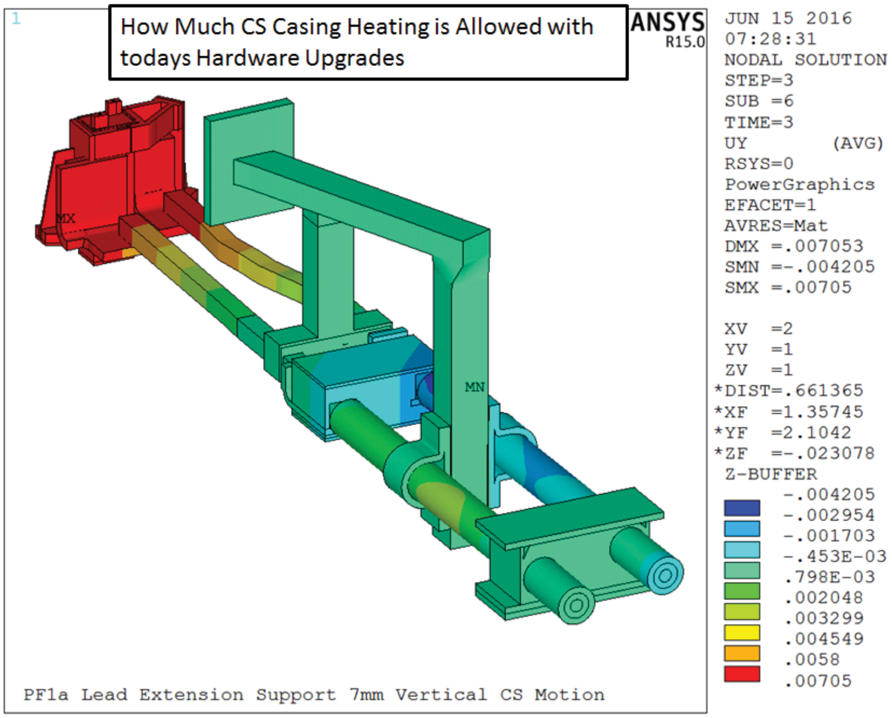

Figure 12.2-1 Vertical Displacement Imposed by the Full 7mm Centerstack Heating Motion

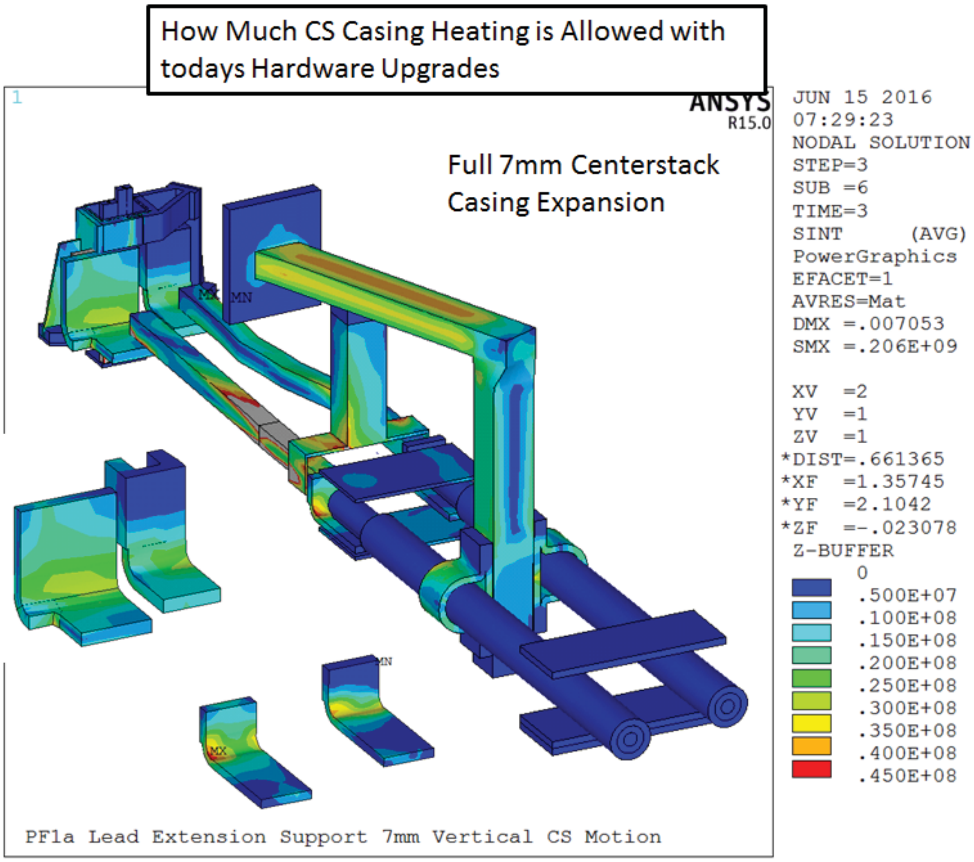

Figure 12.2-2 Stress Imposed by the Centerstack Heating Vertical Motion

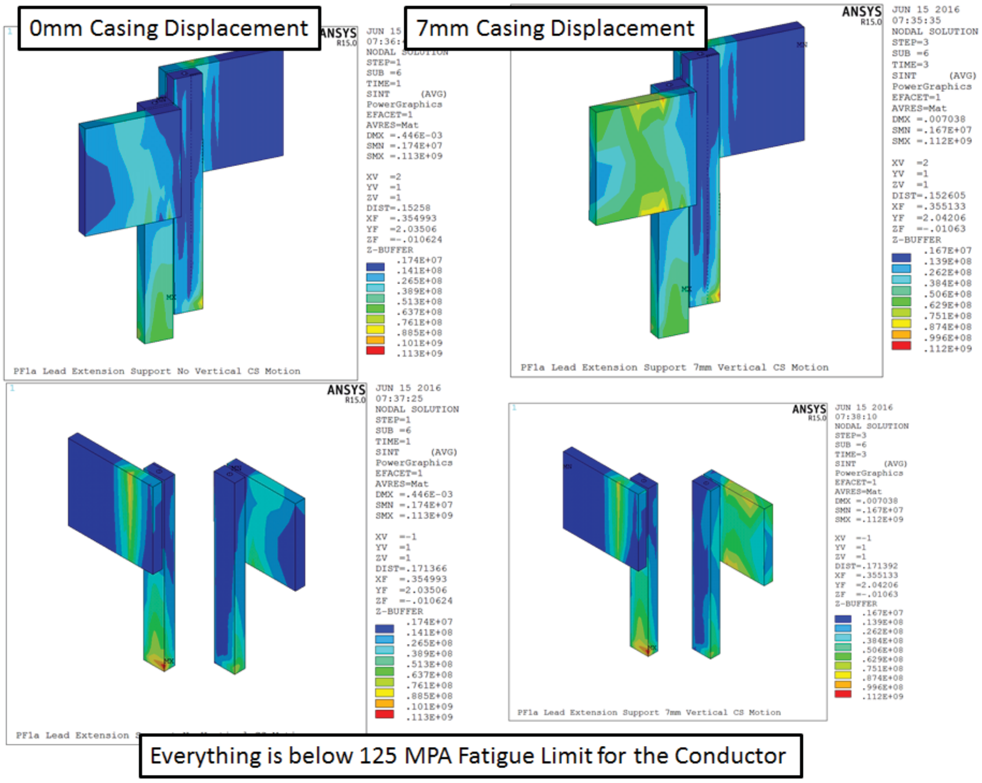

Figure 12.2-3 Inner Terminals and Flag Stress Imposed by the Centerstack Heating

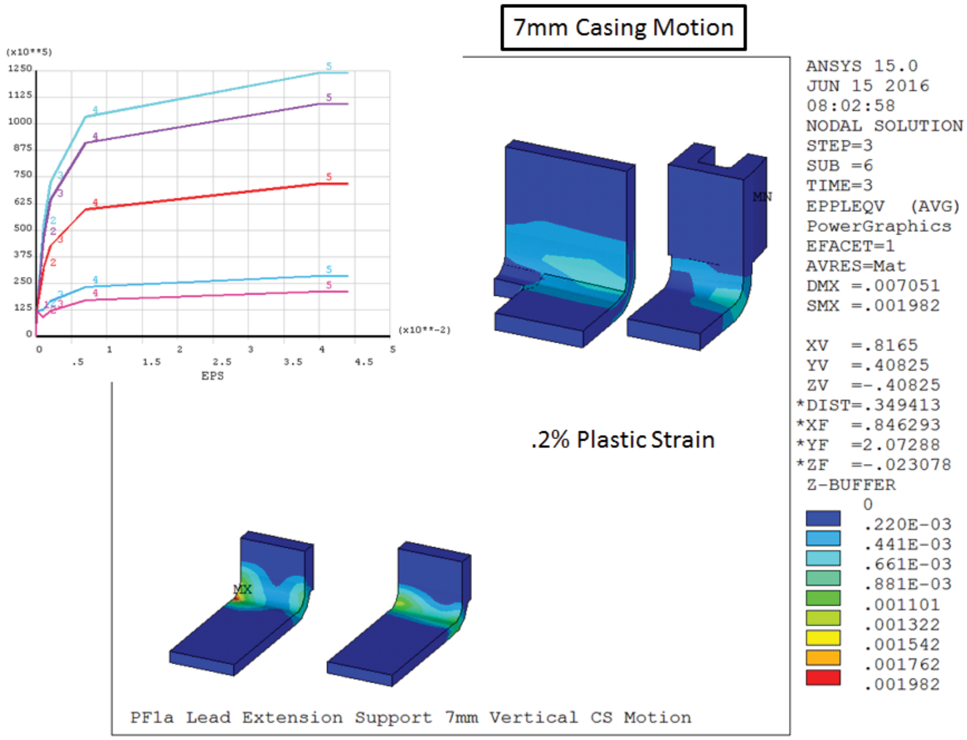

Figure 12.2-4 Inner Terminals and Flag Strain Imposed by the Centerstack Heating 7mm Motion

12.3 Evaluation of Thermal Expansion due to Joule Heat

Allowance for Thermal Expansion due to Joule Heat –Upper, Heating to 50C

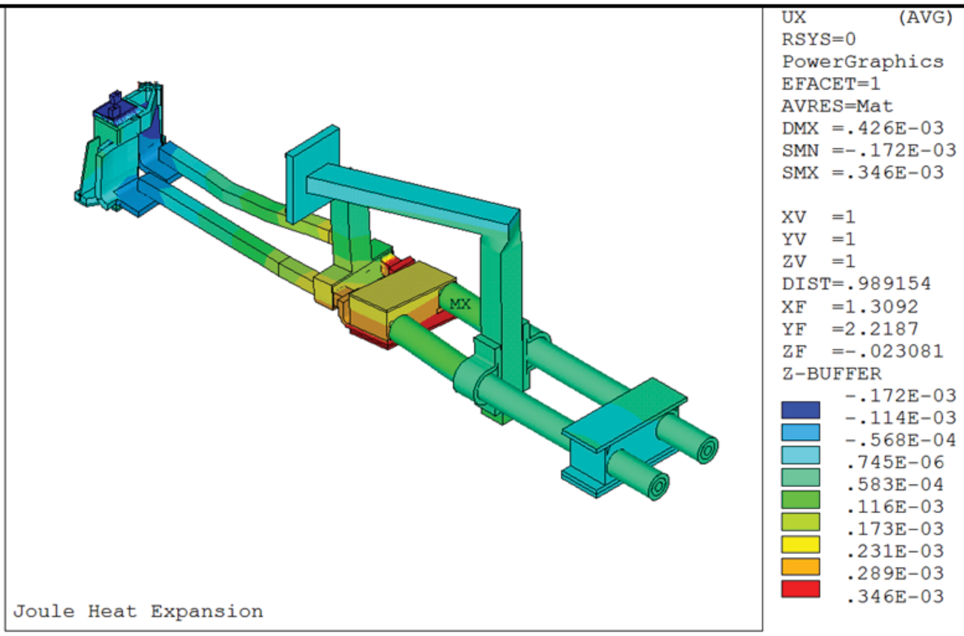

Figure 12.3-1 Radial Motion Due to Expansion of Mostly the Solid Bus

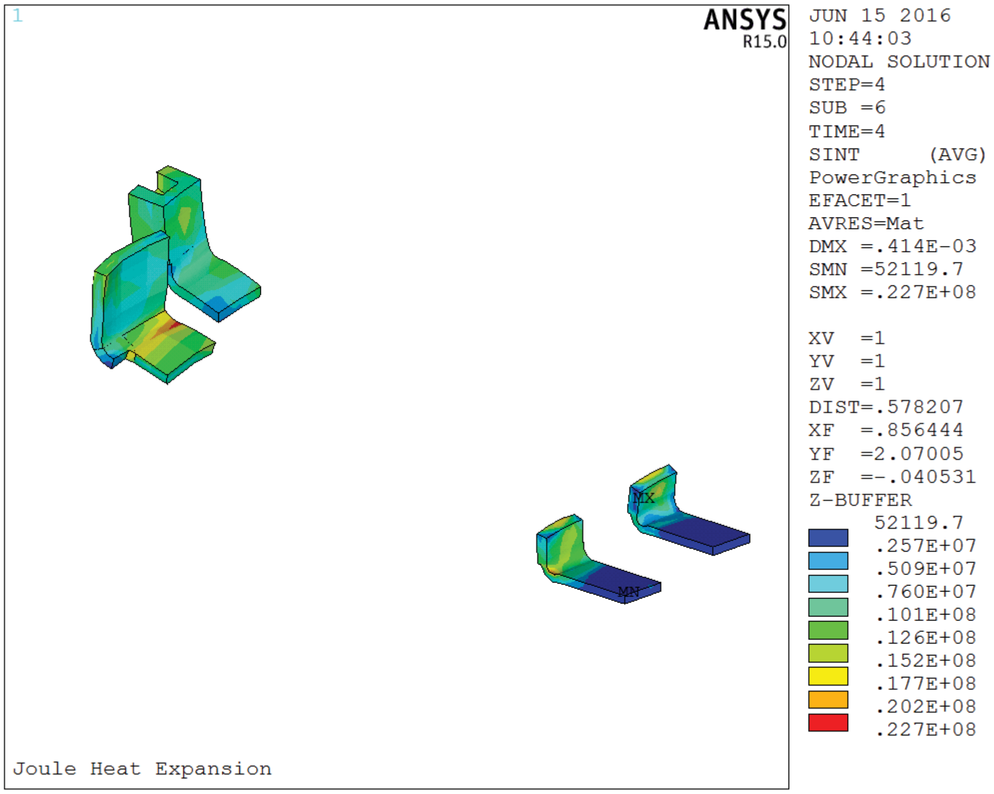

Figure 12.3-2 Lug Stress Due to Joule Heat Expansion of the Bus

13.0 Evaluation of Added Supports for PF1aL

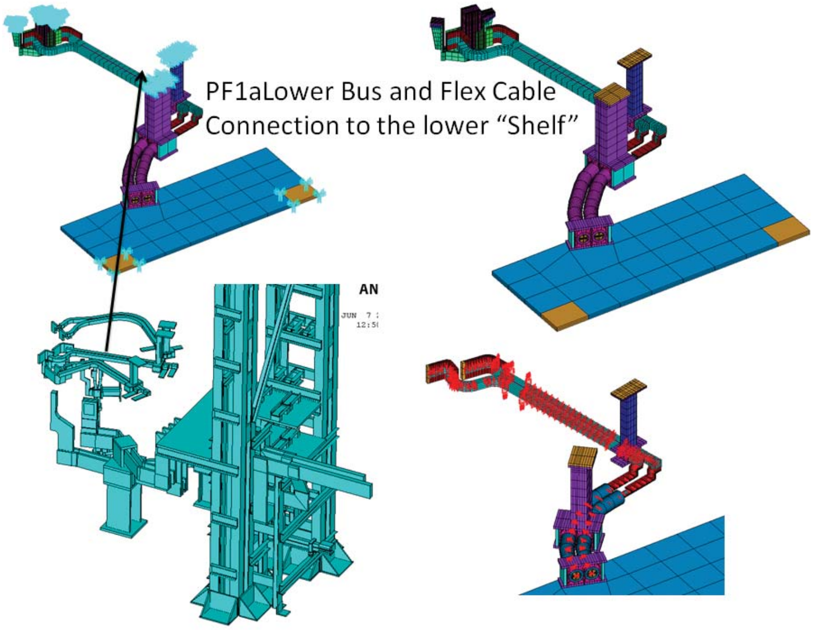

Figure 13.0-1 Analysis Model Used for the PF1a Lower Bus Support Analysis

The Lower Extent of the IGES file for the bus analysis is shown at the Lower left corner of Figure 13.0-1. This was the input to the bus bar calculation –Reference [12]. This IGES model was used to extract some of the details of the PF1a Lower Bus.

13.1 With Added Supports – Lug Stress and Strain

There were a few intermediate attempts to fit supports around existing components. One earlier attempt is shown in Figure 13.1-1. The lugs were interconnected with a G-10 plate. This was found to be very difficult to install, and had to be deleted.

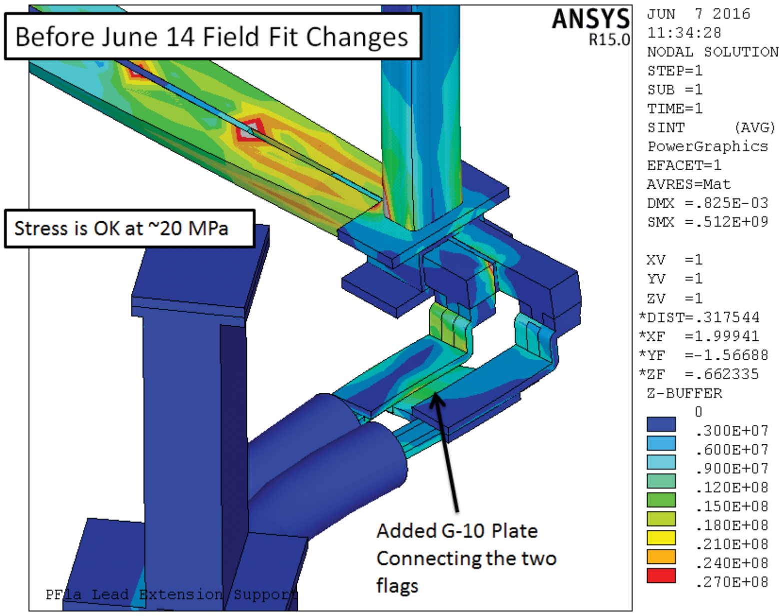

Figure 13.1-1 Stress for an Earlier Support Concept

The flex cable support also had to be moved closer to the lugs. This provided support to the lugs but the lug stress still went up.

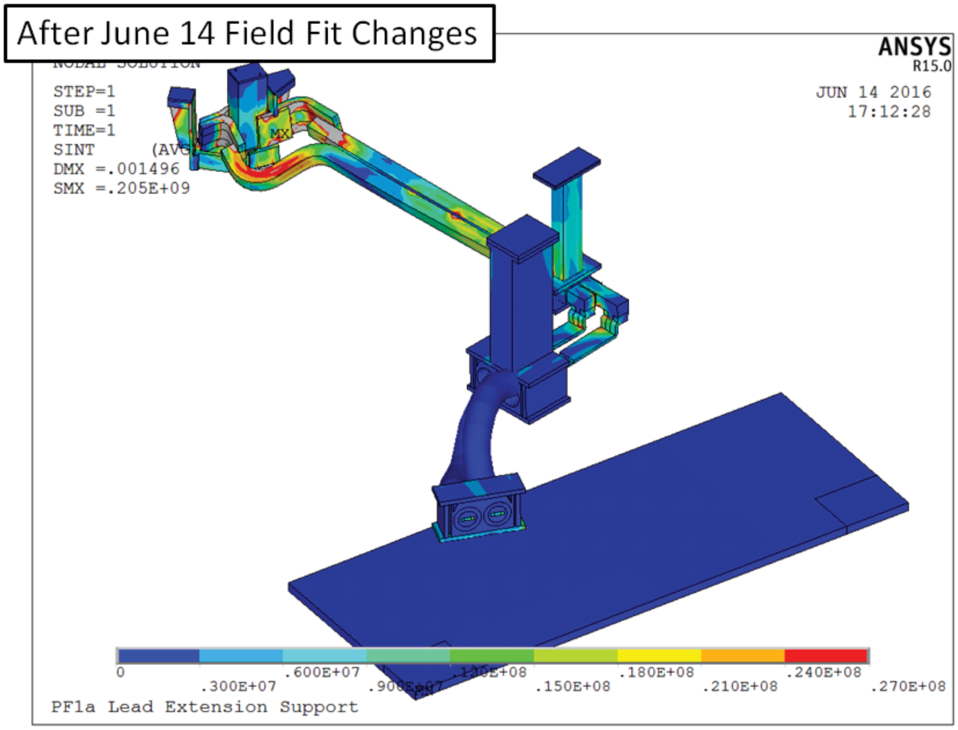

Figure 13.1-2 Stresses After Final Shift of the Support and Removal of the G-10 Plate Connecting the Two Lugs

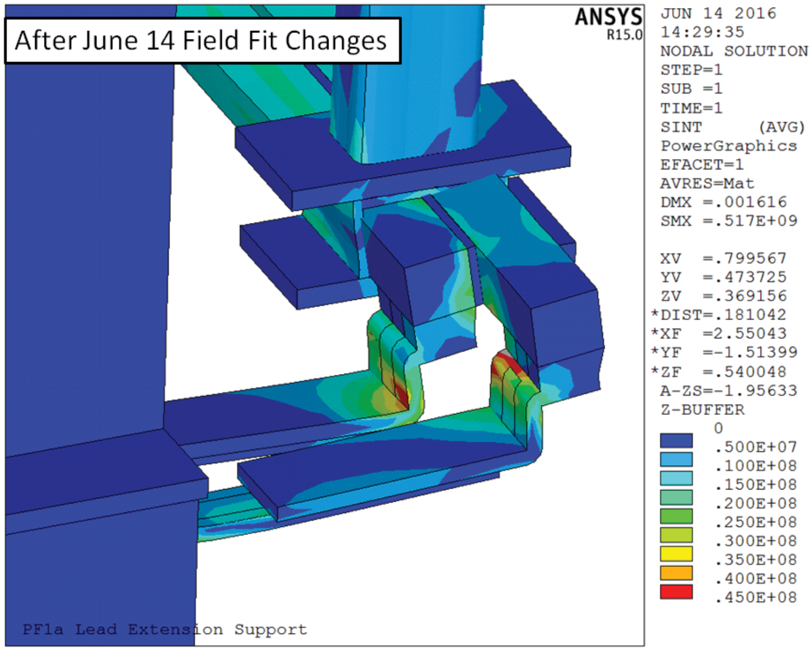

Figure 13.1-3 Lug Stresses After Final Shift of the Support and Removal of the G-10 Plate Connecting the Two Lugs

Stresses in the lugs are at 45 MPa which is at the stress limit for the annealed copper.

13.2 Evaluation of Thermal Expansion due to Joule Heat

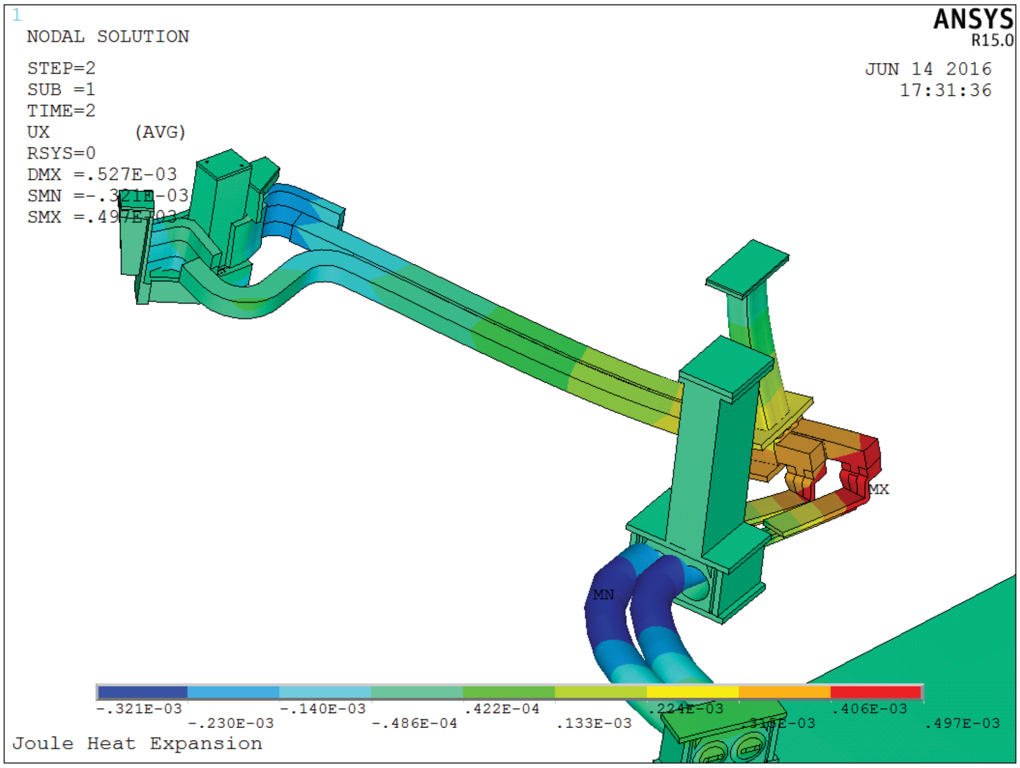

Figure 13.2-1 Thermal Expansion Due to Joule Heat

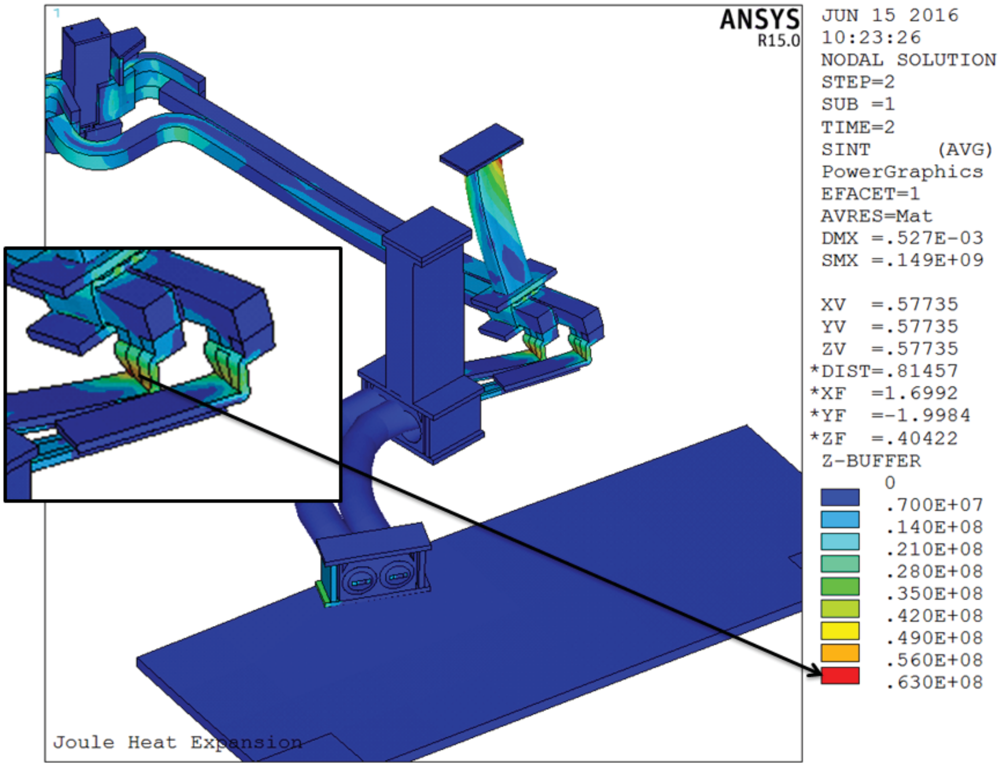

Figure 13.2-2 Thermal Expansion Stress Due to Joule Heat

The supports for the PF1a lower flex clamps are acceptable as installed (June 14). They may need to be modified in order to provide some strain relief for operation in which the lower bus bar heats substantially.

Appendix A
Input file for the NTFTM Terminal Load Calculation, ter9.txt

```
zero
read
ter9
gtrans
0,-47.748,0,0   !shift from PF5 radius to PF2
0,-20,0,0,      !shift from PF5 radius to PF3
0,0,0,0,0       !Remain at PF5 Radius

tera
smat
10,10
snal
1
merge
1,.000001
chke
gerase
99
redu
conv
1,1
redu

bgen
1,.168,-.59,0
1,.3,-.5,.43
btor
1,.93,.1,.15,2,3
seal
1
smat
17,17
grprel
17,17
r
17,1,1846     !14770/8

mfor
17,1,2,3,4,5,6,7,8
tmsa
ter9,2
exit
```

Appendix B
Input file for the ANSYS Stress Analysis of the Small Terminal and Cable Model

```
/batch
/prep7
et,1,45
*do,imat,1,100
ex,imat,117e9
r,imat,.1
```

```
ex,5,20e9
ex,10,185e9
ex,11,1e6
*enddo
/input,conn,mod
nummer,node,.0001
esel,mat,40
nelem
d,all,all,0,0
nall
eall
save
fini
/solu
/title, Max fields 14 kA in PF2
solve
save
fini
/exit
```

Appendix C
Biot Savart Beam=-Stick Model (ch66.txt)

Appendix D
Memo from M. Mardenfeld on Fatigue Damage from First Load Application

M. Mardenfeld
Estimation of Fatigue Life Usage During Elastic-Plastic Deflection of PF1AL Lead Flag Tab
10 June 2016

Summary: The impact of Elastic-Plastic Deformation on the long term fatigue performance of PF1A Lower Lead Tab was estimated. Each plastic load cycle reduced the fatigue life by 1%, as calculated without safety factor. Considering the typical safety factor of 20x life, one fifth of the total usable life has been consumed. **This is based on the assumption that the load direction never reversed.**

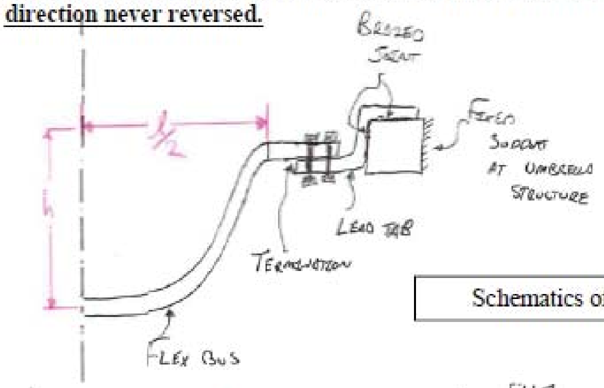

Schematics of Region of Interest

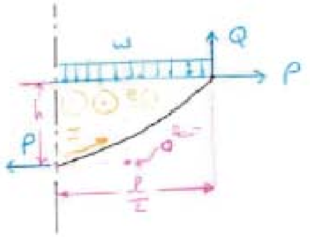

Free-body Diagram of Flex Bus

$$w = Bc \quad \left[\frac{N}{m}\right]$$

$$\uparrow \sum F_y = 0 = +Q - w\frac{l}{2}$$

$$\hookrightarrow Q = w\frac{l}{2} = \frac{Bcl}{2} \quad \left[\left(\frac{N}{m}\right)m\right]$$

$$\circlearrowleft \sum M_{\text{Point } O} = 0 = +\frac{Ql}{4} - Ph$$

$$\hookrightarrow P = \frac{Ql}{4h} = \frac{Bc\,l^2}{8h} \quad \left[\frac{\frac{N}{m}m^2}{m}\right]$$

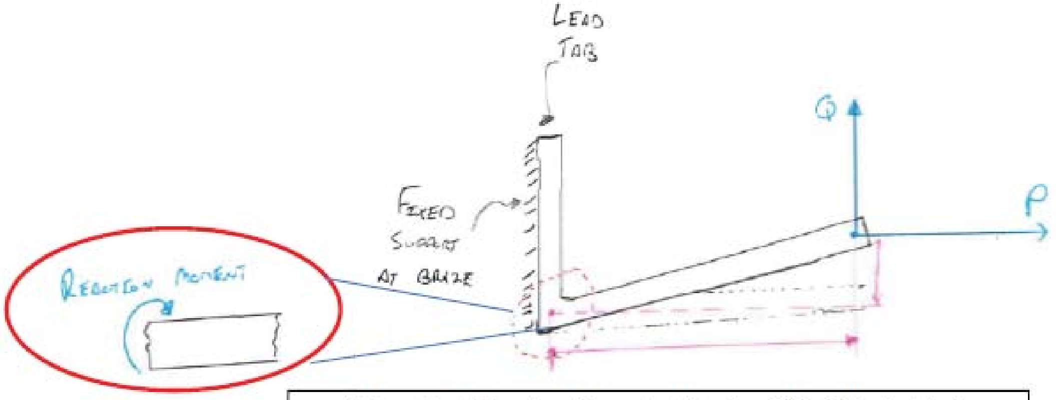

Schematic of Reaction Moment at Region of Peak Plastic Strain

Note that as the ratio $\frac{h}{l}$ decreases the force multiplication $\frac{P}{Q}$ increases.

However, where force Q tends to increase the Reaction Moment, P tends to reduce the Reaction Moment. So in some sense, the bending moment is self-limiting. It is likely that the lead tab deflected until it was aligned tangent to the cable, at which point the force was reacted solely by tension.

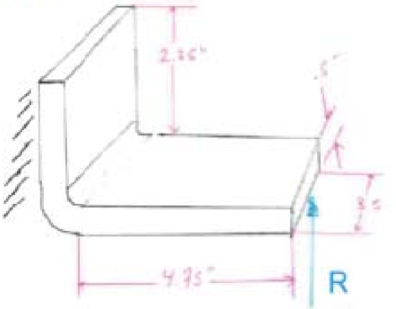

Schematic of Simplified Analysis

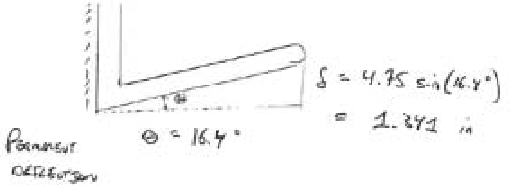

Desired Deformed Shape

Since the loading was **applied unidirectionally** the fatigue life degradation depends only on the magnitude of the peak plastic strain.

To determine the peak plastic strain we can apply a fictitious load R which produces the same net bending moment at the region of interest as the actual (competing) loads Q and P. The calculation proceeded as follows:

A. During load step 1 a fictitious load R was applied to a sub model of the lead tab which had large deformations and plasticity enabled.
B. During load step 2 the load R was removed and the permanent tip deflection in the unloaded position was probed.
C. This was iterated through trial and error until it was found that the correct value for the fictitious load R to recreate the actually observed and measured deflection is approximately 685 pounds.

1. The model was rerun with multiple cycles (4x) of unidirectional loading and unloading to confirm that after the first load cycle strains remained elastic (i.e. no plastic ratcheting).

2. The peak plastic strain was compared to low cycle fatigue curve to demonstrate that ample fatigue life remains.

Material Properties:

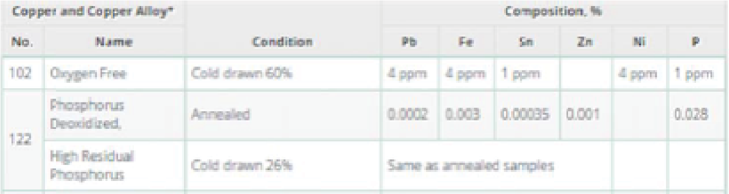

Copper and Copper Alloy*		Condition	Composition, %					
No.	Name		Pb	Fe	Sn	Zn	Ni	P
102	Oxygen Free	Cold drawn 60%	4 ppm	4 ppm	1 ppm		4 ppm	1 ppm
122	Phosphorus Deoxidized,	Annealed	0.0002	0.003	0.00035	0.001		0.028
	High Residual Phosphorus	Cold drawn 26%	Same as annealed samples					

Copper #122 is very similar to OFHC
Source: http://www.copper.org/resources/properties/144_8/

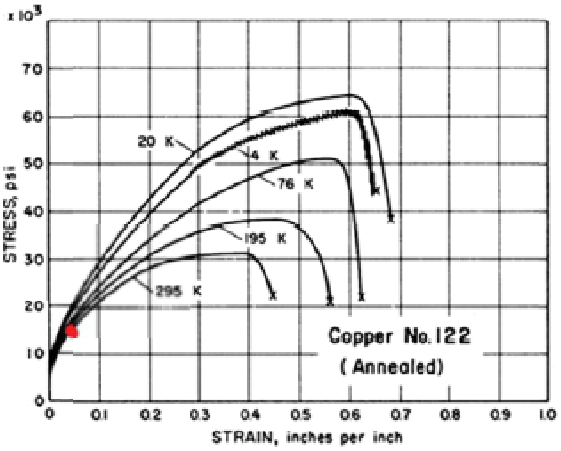

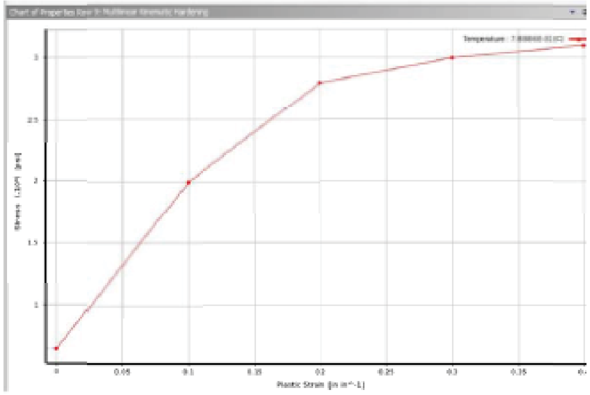

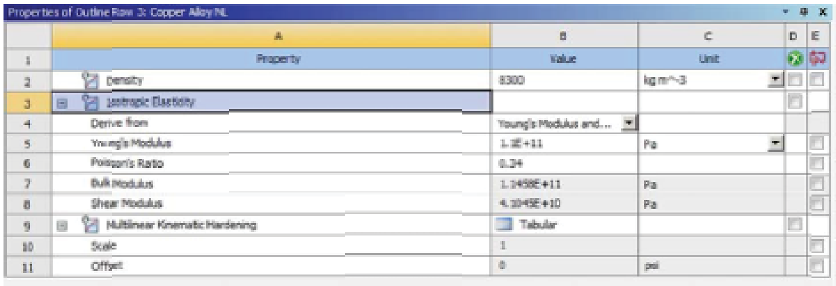

	A	B	C	D	E
1	Property	Value	Unit		
2	Density	8300	kg m^-3	☐	☐
3	Isotropic Elasticity			☐	
4	Derive from	Young's Modulus and...			
5	Young's Modulus	1.1E+11	Pa		☐
6	Poisson's Ratio	0.34			☐
7	Bulk Modulus	1.1458E+11	Pa		☐
8	Shear Modulus	4.1045E+10	Pa		☐
9	Multilinear Kinematic Hardening	Tabular		☐	
10	Scale	1			☐
11	Offset	0	psi		☐

Implemented Multilinear Kinematic Hardening for Cu #122 at 295K, Annealed
Source: http://www.copper.org/resources/properties/144_8/

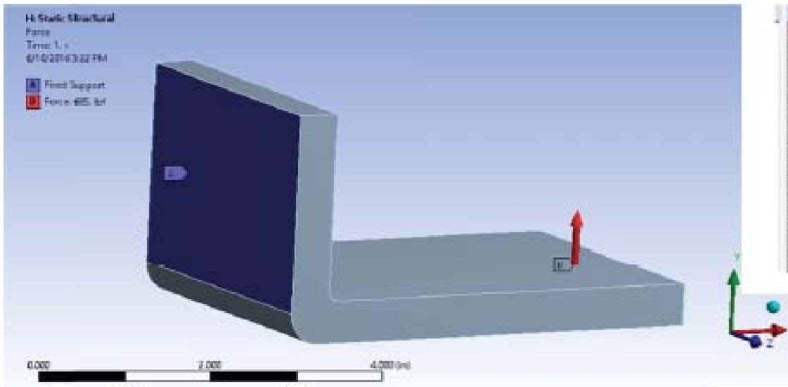

Boundary Conditions and Loads

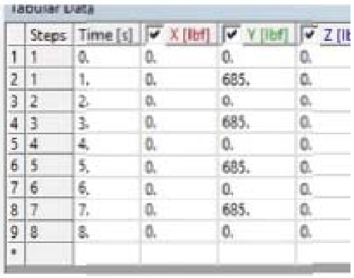

	Steps	Time [s]	☑ X [lbf]	☑ Y [lbf]	☑ Z [lb
1	1	0.	0.	0.	0.
2	1	1.	0.	685.	0.
3	2	2.	0.	0.	0.
4	3	3.	0.	685.	0.
5	4	4.	0.	0.	0.
6	5	5.	0.	685.	0.
7	6	6.	0.	0.	0.
8	7	7.	0.	685.	0.
9	8	8.	0.	0.	0.
*					

4x Cycles Unidirectional
with R= 685 lnf

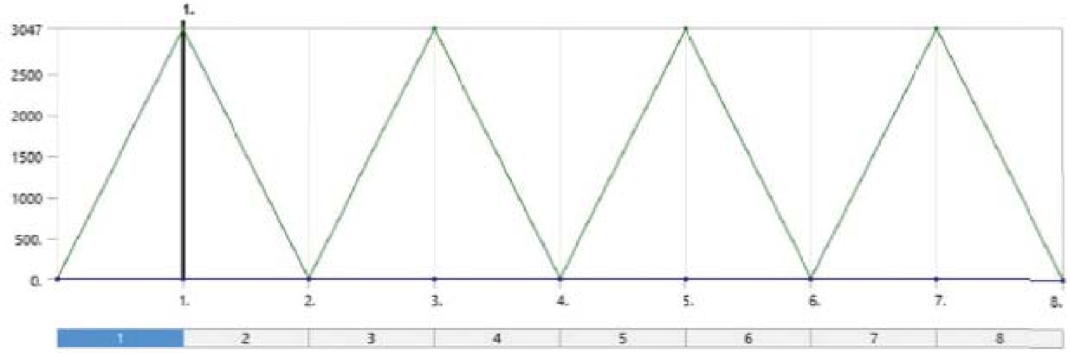

Load Application vs Load Step

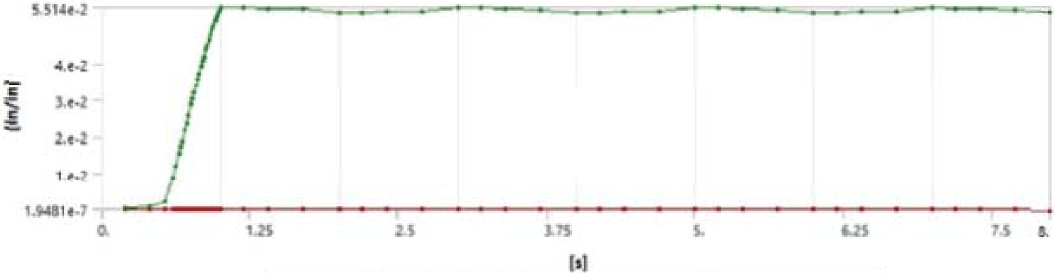

Min and Max Equivalent Strain vs Load Step

Note that plastic strain is essentially constant after first load cycle – there is no plastic ratcheting.

MARDENFELD 13 June 2016 4 of 7

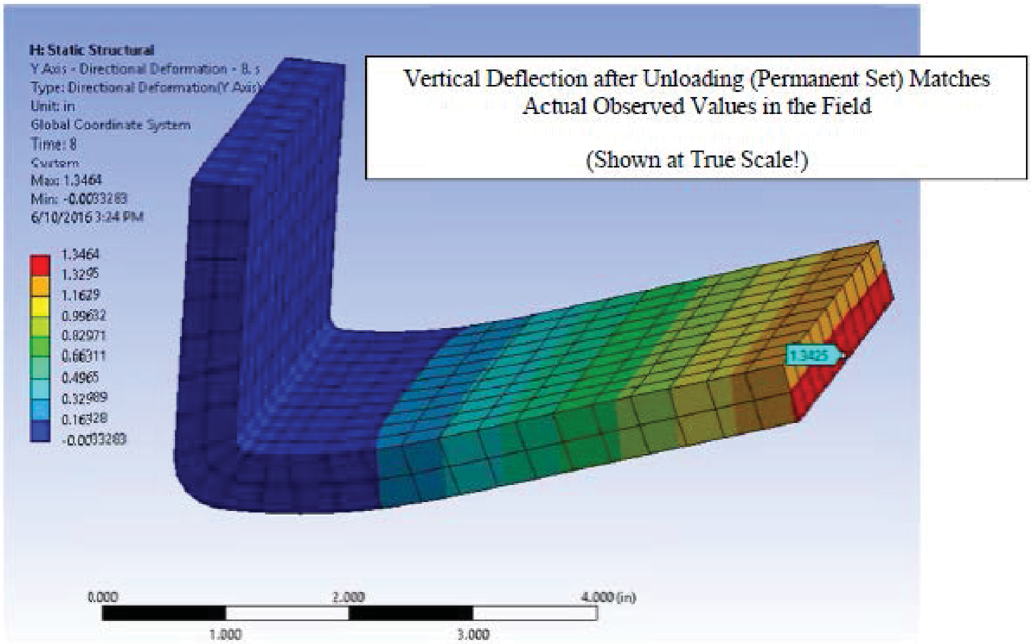

Vertical Deflection after Unloading (Permanent Set) Matches Actual Observed Values in the Field

(Shown at True Scale!)

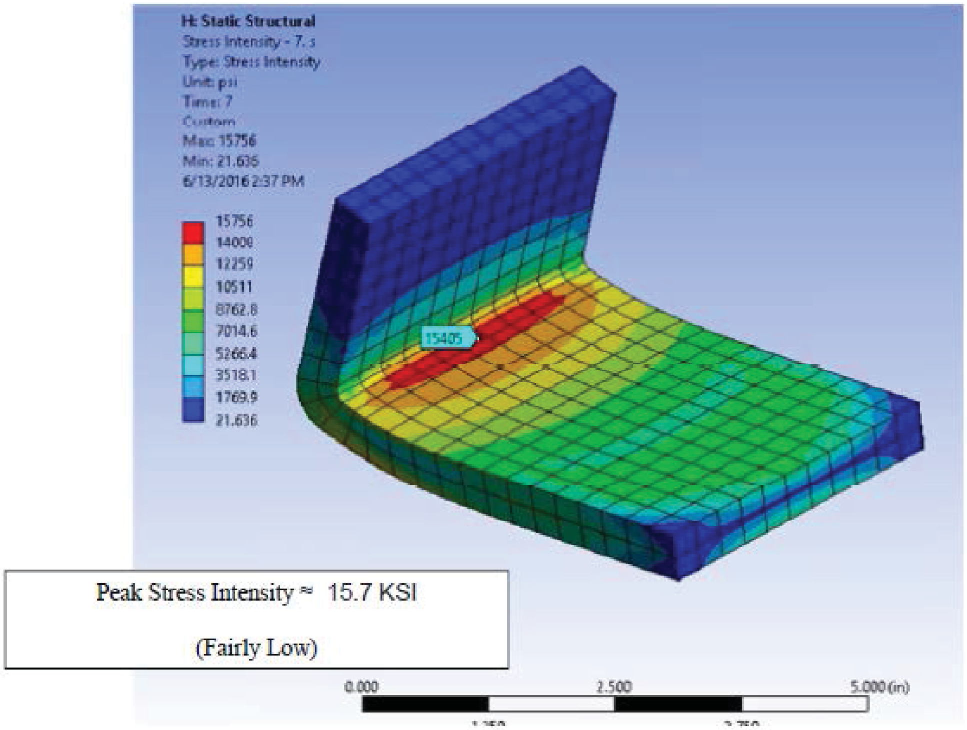

Peak Stress Intensity ≈ 15.7 KSI

(Fairly Low)

MARDENFELD 13 June 2016 5 of 7

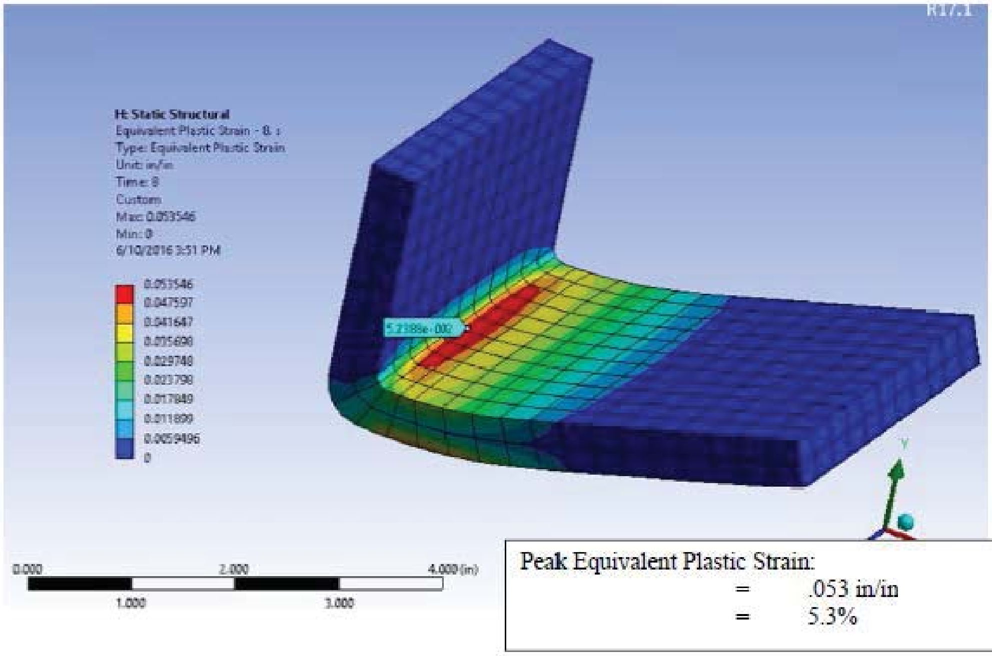

Peak Equivalent Plastic Strain:
= .053 in/in
= 5.3%

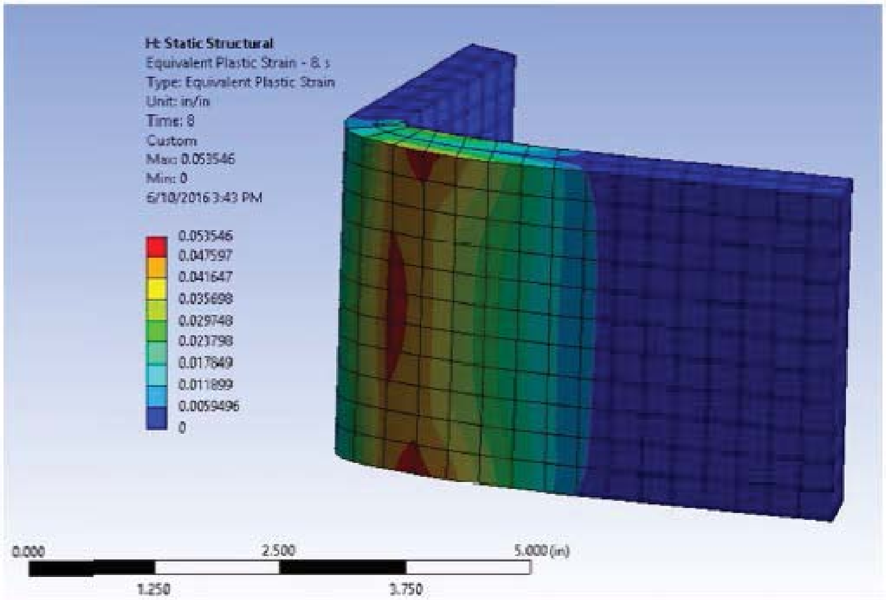

Note that 5% Plastic Strain is marked on the Stress-Strain Curve on page 3.

The local cold work from bending is approximately equal to that seen in 1/8 hard OFHC.

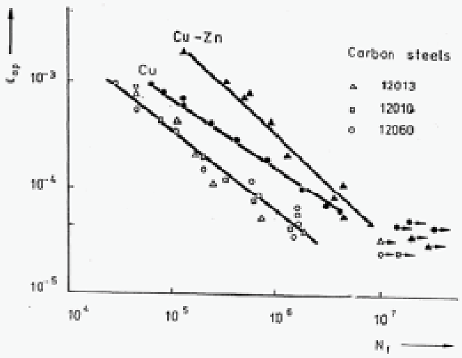

Figure 2. Mason-Coffin curves for copper, α-brass, and three steels [1].

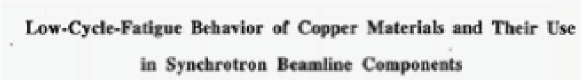

Low-Cycle-Fatigue Behavior of Copper Materials and Their Use in Synchrotron Beamline Components

Zhibi Wang, Tom Nian, David Ryding, and Tuncer M. Kuzay

Strain Life Curve for Copper, Available:
http://www.osti.gov/scitech/servlets/purl/10182875/

Although 0.053 in/in strain is off the scale of the strain life curve shown above, the data was extracted digitally using a web applet (http://arohatgi.info/WebPlotDigitizer/), and fit the curve below with R^2=.9992

$$\epsilon = (10^{-.0042})(N_f^{-.6359})$$

Cycles to Failure	Strain (in/in)
1.00E+07	3.50E-05
1.00E+06	1.51E-04
1.00E+05	6.55E-04
1.00E+03	1.22E-02
100	0.0530
35	0.106

Calculated Strain

2x Calculated Strain

Using a Miner's Rule correlation, and the assumption that the electromagnetic force was never reversed, we can conclude that the plastic deformation consumed approximately 1/100, or about 1% of the total fatigue life. This is without any safety factor added.

Typical practice for safety factor is to use the more severe of either 20x life or 2x strain. With the 20x life safety factor included, the allowable cycles would 5 cycles, and therefore 20% of the allowable fatigue life was consumed during this single plastic deformation.

Due to the logarithmic nature of the Strain-Life curve we can neglect any subsequent cycles which remained fully elastic, provided the load direction never reversed.

Extrapolation this far beyond the measured cyclic data is not terribly accurate, it serves to illustrate that although this event was severe, even with stringent safety factors, the majority of the lead tab's estimated fatigue life is still available for future use.

Appendix E

Photos of Installed Cable Supports [15]

Appendix F
Flex Cable Catalog

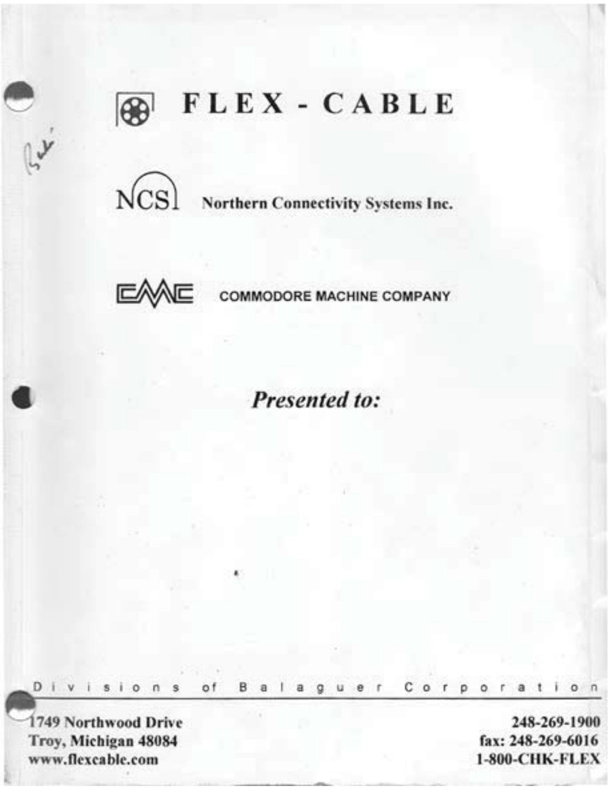

FLEX-CABLE

NCS Northern Connectivity Systems Inc.

CMC COMMODORE MACHINE COMPANY

Presented to:

Divisions of Balaguer Corporation

1749 Northwood Drive
Troy, Michigan 48084
www.flexcable.com

248-269-1900
fax: 248-269-6016
1-800-CHK-FLEX

Applications Our standard cable.
Suitable for both manual and robotic applications.

Technical Data

MCM Ratings	350	400	500	600	700	10
Min. Bend Radius	2"	2"	3"	3"	4"	4"
Hose OD	1.45	1.56	1.69	1.81	1.93	2.2
Color Code	Black with White Identifying Stripe					
Jacket Material	SBR					
Reinforcement	Polyester Tire Cord					
Working Pressure	150psi					
Voltage Rating	100V					
Temperature Rating	180°F					
Torsional Flexibility Factor	4.2					
Bend Flexibility Factor	7.4					
Abrasion Resistance Factor	3.0					

Very-Flex™

Applications Very-Flex has an extra reinforcing spiral which provides abrasion and impact resistance along the entire length of the cable. Recommended for tough robotics applications.

Technical Data

MCM Ratings	350	400	500	600	700	
Min. Bend Radius	2"	2"	3"	3"	4"	4"
Hose O.D.	1.59	1.65	1.78	2.00	2.19	2
Color Code	Yellow with Black Stripe					
Jacket Material	SBR with Rope Impression					
Reinforcement	Polyester Tire Cord					
Working Pressure	150psi					
Voltage Rating	100V					
Temperature Rating	180°F					
Torsional Flexibility Factor	3.6					
Bend Flexibility Factor	6.8					
Abrasion Resistance Factor	5.1					